UNIVERSIDADE DA BEIRA INTERIOR
Faculdade de Ciências

A Microwave Assisted Optimization of New Spiroindolin-3-one(thio)barbiturates
Synthesis, biological and computational evaluation

Pedro António Fantini Soeiro

Dissertação para obtenção do Grau de Mestre em
Química Medicinal
(2º ciclo de estudos)

Orientador: Prof. Doutor Renato Emanuel Félix Boto
Coorientador: Prof. Doutor Paulo Jorge da Silva Almeida

Covilhã, outubro de 2018

Aos meus pais e irmãs

Acknowledgments

Em primeiro lugar, quero agradecer ao meu orientador, o Professor Doutor Renato Boto, e ao meu coorientador, o Professor Doutor Paulo Almeida, pela disponibilidade e orientação ao longo desta dissertação. Sinto-me privilegiado por todo o conhecimento, esforço e dedicação que me transmitiram neste último ano.

De igual modo, quero agradecer ao Professor Doutor Samuel Silvestre, pelo apoio, conselhos e sugestões partilhadas, principalmente nos estudos de avaliação biológica.

Ao João e à Joana, obrigado pela vossa presença e auxílio no laboratório. Foram sem dúvida indispensáveis para este trabalho.

Ao pessoal do CICS, principalmente ao Octávio, obrigado por me terem recebido de mãos abertas e por toda a ajuda demonstrada.

À D. Ana, D. Dulce e ao Sr. João, um obrigado pela paciência e disponibilidade demonstradas sempre que possível.

Quero agradecer também ao Carlos e à Rita, por confiarem em mim e por tudo o que partilhamos nestes últimos anos.

Um especial obrigado à Melani e à Marta, pela vossa amizade e paciência. Pela vossa cumplicidade e por estarem sempre ao meu lado. Foram a melhor companhia que pude escolher neste percurso.

Por fim quero agradecer aos meus pais e as minhas irmãs, por acreditarem em mim e no meu trabalho. Pelo apoio incondicional que me deram, pois sem vocês não estaria aqui. Obrigado por esta oportunidade.

Resumo Alargado

A Química Medicinal é uma área científica que se dedica à descoberta e desenvolvimento de novos compostos químicos, com o objetivo de identificar a sua atividade biológica, efeitos secundários, metabolismo e interpretação das relações estrutura-atividade com os seus recetores. A descoberta e desenvolvimento de fármacos pode ser dividida em duas fases distintas: uma primeira fase de estudos pré-clínicos onde é desenvolvido um candidato a fármaco, e uma segunda fase de estudos clínicos onde este candidato é avaliado ao nível da sua tolerância, eficácia e segurança em seres humanos, antes de ser comercializado.

Os barbituratos pertencem a uma classe relevante de compostos químicos devido à sua, já conhecida, ampla gama de atividades biológicas. Estes compostos têm sido utilizados como depressores do sistema nervoso central, podendo atuar como ansiolíticos, sedativos, hipnóticos, anestésicos e anticonvulsivantes, mas também podem ser utilizados como agentes antibacterianos, anticancerígenos, antiangiogénicos, imunomoduladores, antifúngicos e antioxidantes. O ácido barbitúrico, por si só, não apresenta atividade biológica relevante, mas, alterações na sua estrutura, principalmente na posição C5, podem potenciar um efeito farmacológico mais promissor. Face a isso, nos últimos anos, testemunhou-se um elevado interesse na síntese de barbituratos substituídos nessa mesma posição, com diversas atividades biológicas. De entre os inúmeros exemplos, são de destacar os 5-(benzisoxazol-3-ilideno)(tio)barbituratos, com atividade inibitória da produção de ácido úrico, inibindo a enzima xantina oxidase. Estes 5-(benzisoxazol-3-ilideno)(tio)barbituratos, têm na sua constituição um ácido (tio)barbitúrico substituído em C5 por um anel 2,1-benzisoxazole. Os 2,1-benzisoxazois são heterocíclicos aromáticos constituídos por um isoxazole fundido com um anel de benzeno, sendo conhecidos como precursores de outras moléculas bioativas, nomeadamente quinolinas, acridinas, quinazolinas e benzodiazepinas. Este interesse sintético deve-se principalmente à facilidade de clivagem térmica da ligação N-O do núcleo isoxazole, tendo sido descrita a formação de compostos espiros como intermediários, mais precisamente de uma espiroindolin-3-ona. Neste contexto, é de referir que compostos espiro são constituídos por duas ou mais estruturas cíclicas fundidas num único átomo de carbono. A natureza tetraédrica desse carbono permite a formação de um ângulo perpendicular entre os anéis, o que leva a uma conformação rígida e tridimensional única para estes compostos, podendo apresentar diferentes propriedades farmacológicas.

No presente trabalho, foram desenvolvidos novos espiroindolin-3-ona(tio)barbituratos, utilizando como precursores (tio)ureias 1,3-dissubstituídas e, sequencialmente, os seus respetivos ácidos (tio)barbitúricos 1,3-dissubstituídos, 5-(2-nitrobenzilideno)pirimidinas e 5-(benzisoxazol-3-ilideno)pirimidinas. A síntese dos espiroindolin-3-ona(tio)barbituratos foi sujeita a um processo de otimização das condições reacionais, fazendo-se variar a temperatura

e o solvente utilizado, e utilizando-se diferentes tipos de aquecimento (banho de óleo, mufla, lâmpada de aquecimento e micro-ondas). Todos os compostos obtidos foram devidamente caracterizados por determinação dos seus pontos de fusão, espectroscopia de infravermelho e de ressonância magnética nuclear de protão e carbono.

Todos os espiroindolin-3-ona(tio)barbituratos simétricos sintetizados foram avaliados biologicamente, analisando os seus efeitos na viabilidade celular, tendo sido também determinada a sua atividade inibitória para com a xantina oxidase. Os estudos de viabilidade celular foram realizados em fibroblastos normais da derme humana e em células de cancro da mama. Num *screening* inicial, as células foram expostas aos compostos sintetizados, numa concentração de 30 μM durante 72 horas, tendo sido utilizado o 5-fluorouracilo como controlo positivo. A determinação da proliferação celular foi realizada mediante ensaio do brometo de 3-(4,5-dimetiltiazol-2-il)-2,5-difenil-tetrazólio. Para os compostos que apresentaram a maior ação antiproliferativa nos fibroblastos normais da derme humana, procederam-se a ensaios para determinar a curva concentração-resposta. Para tal, os compostos foram incubados com as células, em seis concentrações distintas (0,1, 1, 10, 30, 50 e 100 μM) no mesmo período de 72 horas, e os valores de IC_{50} foram calculados por um ajuste sigmoidal, considerando-se um intervalo de confiança de 95%. A atividade inibitória na xantina oxidase para com os espiroindolin-3-ona(tio)barbituratos sintetizados foi determinada espectrofotometricamente quantificando-se a quantidade de ácido úrico formado a partir da xantina ao longo do tempo. Utilizando o alopurinol como controlo positivo, realizou-se igualmente um *screening* dos espiroindolin-3-ona(tio)barbituratos, utilizando-se uma suspensão de xantina oxidase. A reação enzimática foi iniciada após a adição de xantina e posterior incubação a 37°C durante 10 minutos, e as leituras das absorvâncias foram realizadas a 295 nm ao fim de cada minuto. Para os compostos que demonstraram uma maior ação inibitória, procederam-se a ensaios para determinar a curva concentração-resposta. Para tal, incubaram-se novamente os compostos com a enzima em seis concentrações distintas (0,01, 0,1, 1, 7,5, 15 and 30 μM) e os valores de IC_{50} foram calculados por um ajuste sigmoidal dos resultados obtidos, considerando-se um intervalo de confiança de 95%.

Adicionalmente, estudos de *docking* molecular foram realizados de modo a obter informação relativa à orientação espacial dos ligandos na enzima, permitindo assim uma melhor perceção dos resultados obtidos *in vitro*. Foram também realizadas previsões das propriedades farmacocinéticas e de toxicidade dos espiroindolin-3-ona(tio)barbituratos sintetizados, a partir do software online pkCSM.

A nível da síntese química, todos os compostos obtidos foram sintetizados com rendimentos globais razoáveis. Com a otimização da síntese dos espiroindolin-3-ona(tio)barbituratos, foi possível obtê-los mediante irradiação micro-ondas em dimetilformamida a 100ºC, com rendimentos entre 70-85%.

Neste trabalho foram igualmente avaliadas as atividades dos espiroindolin-3-ona(tio)barbituratos como agentes antiproliferativos e inibidores da xantina oxidase. Quanto à viabilidade celular, nenhum dos compostos apresentou citotoxicidade significativa nas linhas celulares estudadas. No estudo da inibição da xantina oxidase, o 1',3'-diphenyl-2'-thioxo-2',3'-dihydro-4'H-spiro[indoline-2,5'-pyrimidine]-3,4',6'(1'H)-trione foi o composto que demonstrou maior atividade mas, contudo, esta foi inferior ao controlo positivo do alopurinol.

Nos resultados obtidos para o *docking* molecular é de realçar que, alguns dos espiroindolin-3-ona(tio)barbituratos, mostraram afinidades muito próximas às do alopurinol com a xantina oxidase, contudo esses resultados não se refletiram nos resultados obtidos *in vitro*. Em relação às previsões de propriedades farmacocinéticas e de toxicidade, todos os compostos cumpriram as regras de Lipinski, bem como a maioria dos critérios farmacocinéticos e de toxicidade previstos.

Como trabalho futuro, propõe-se estudos para melhorar não só a potência e seletividade dos espiroindolin-3-ona(tio)barbituratos como também a sua farmacocinética. Será de igual forma importante continuar a síntese de mais derivados destes compostos, variando os substituintes no seu esqueleto molecular de modo a otimizar os resultados biológicos obtidos e a sua relação estrutura-atividade. Também é de grande importância continuar a síntese de novos espiroindolin-3-ona(tio)barbituratos assimétricos, bem como a separação de seus enantiómeros para determinar a atividade biológica individual de cada um.

Palavras-chave

Espiroindolin-3-ona(tio)barbituratos, Síntese por Micro-ondas, Caraterização Estrutural, Avaliação Biológica, Estudos Computacionais.

Abstract

Medicinal Chemistry is a scientific area centered in the discovery and development of new bioactivated chemical entities. In recent years, a high interest in the synthesis of C5-substituted barbiturates, with various biological activities, has been shown. 5-(Benzisoxazol-3-ylidene) (thio)barbiturates, owning a 2,1-benzisoxazole, are one of these examples. 2,1-Benzisoxazoles are a class of compounds mainly known as precursors of other bioactive molecules such as quinolines, acridines, quinazolines and benzodiazepines. These transformations may be due to thermal cleavage of the N-O bond of the isoxazole nucleus, where the formation of a spiro, more precisely a spiroindolin-3-one, was postulated as an intermediate. Spiro compounds are composed of two or more cyclic structures fused to a single carbon. The tetrahedral nature of this carbon allows the formation of a perpendicular angle between the rings, which provides a unique rigid and three-dimensional conformation for these compounds, presenting different implications in various biological activities.

In the present work, novel spiroindolin-3-one(thio)barbiturates have been developed. Their synthesis was subjected to an optimization of reactional conditions, varying the temperature and the solvent used, and using different methods of heating (oil bath, muffle, heating lamp and microwave). All compounds were synthetized with very good yields (70-85%) and were structurally characterized by nuclear magnetic resonance and infrared spectroscopy. Additionally, their effect in cell viability and xanthine oxidase inhibitory activity was evaluated, and, for a better understanding of the *in vitro* results, *in silico* studies were also realized.

Generally, none spiroindolin-3-one(thio)barbiturates showed relevant cytotoxicity in the studied cell lines nor any relevant xanthine oxidase inhibitory activity. Further synthesis of new analogues is highly important for an optimization of the biological results, and for a better understanding of their respective structure-activity relationship. It is also of great importance the synthesis of new asymmetric spiroindolin-3-one(thio)barbiturates, as well as the separation of their enantiomers, to determine the individual biological activity of each one.

Keywords

Spiroindolin-3-one(thio)barbiturates, Microwave Synthesis, Structural Characterization, Biological Evaluation, Computational Studies.

Index

Chapter 1 - Introduction 1

1.1. Medicinal Chemistry - Drug discovery and development 2

1.1.1. *In silico* studies 4

1.1.2. Chemical synthesis 6

1.1.3. Biological activity evaluation 7

1.2. Barbiturates 9

1.3. Benzisoxazoles 12

1.3.1. Synthesis of 2,1-benzisoxazoles 13

1.3.2. 2,1-Benzisoxazoles transformations 14

1.4. Spiro compounds - spiroindolinones 16

1.4.1. Synthesis of spiroindolin-3-ones 17

1.4.1.1. Spiro formation with an indole scaffold in the starting material 18

1.4.1.2. Spiro formation without an indole scaffold in the starting material 19

Chapter 2 - Objectives 22

Chapter 3 - Results and Discussion 24

3.1. Synthesis 25

3.1.1. Synthesis of 1,3-disubstituted(thio)ureas 25

3.1.2. Synthesis of 1,3-disubstituted(thio)barbituric acids 28

3.1.3. Synthesis of 5-(2-nitrobenzylidene)pyrimidines 31

3.1.4. Synthesis of 5-(benzisoxazol-3-ylidene)pyrimidines 35

3.1.5. Synthesis of spiroindolin-3-one(thio)barbiturates 38

3.2. Evaluation of Biological Activity 44

3.2.1. Cell viability assays 44

3.2.2. Xanthine Oxidase inhibitory activity assay 46

3.2.3. Structure-Activity Relationship 48

3.3. *In silico* studies 49

3.3.1. Molecular docking 49

3.3.2. Pharmacokinetics and toxicity properties prediction 51

Chapter 4 - Conclusions 54

Chapter 5 - Experimental Section 56
5.1. Synthesis and Structural characterization 57
5.1.1. Synthesis of precursors 58
5.1.1.1. 1,3-Disubstituted(thio)ureas 58
5.1.1.2. 1,3-Disubstituted(thio)barbituric acids 63
5.1.1.3. 5-(2-Nitrobenzylidene)pyrimidines 65
5.1.1.4. 5-(Benzisoxazol-3-ylidene)pyrimidines 69
5.1.2. Spiroindolin-3-one(thio)barbiturates 74
5.1.2. Nitrene trapping – Aziridines derivatives 78
5.2. Biological evaluation 80
5.2.1. Cell viability assays 80
5.2.1.1. Cells cultures 80
5.2.1.2. Preparation of samples solutions 80
5.2.1.3. MTT assay 81
5.2.2. Xanthine Oxidase inhibitory activity assay 81
5.2.1.1. Preparation of samples solutions 81
5.2.1.2. Experimental procedure 82
5.2.3. Statistics 82
5.3. *In silico* studies 82
5.3.1. Molecular docking 82
5.3.2. ADMET properties predictions 83
Chapter 6 - References 84
Chapter 7 – Publications 93
Oral communication fulfilled within this dissertation 94
Panel communication fulfilled within this dissertation 94
Scientific articles in international journals peer-reviewed referred in Journal Citation Reports (JCR) of ISI Wed of Knowledge and/or SciVerse Scopus 94
Chapter 8 – Attachments 95
Attachment 1 - "AD4_Parameters.dat" file 96
Attachment 2 – Abstract of oral communication fulfilled within this dissertation 100
Attachment 3 – Abstract of panel communication fulfilled within this dissertation 102

Attachment 4 – Scientific articles in international journals peer-reviewed referred in Journal Citation Reports (JCR) of ISI Wed of Knowledge and/or SciVerse Scopus 104

List of Figures

Figure 1.1 - Chemical structures of Morphine and its analogues codeine and heroine.[4].....2

Figure 1.2 - Stages in the drug discovery process. Adapted from Lombardino *et al.*[1].....3

Figure 1.3 - Purine and nonpurine inhibitors of xanthine oxidase.[24].....9

Figure 1.4 – Examples of bioactive barbiturate derivatives.[32] 10

Figure 1.5 – Molecular structures of 1,2-benzisoxazole (indoxazene) and 2,1-benzisoxazole (anthranil).[37]..... 12

Figure 1.6 - Examples of drugs with a 1,2-benzisoxazole in their molecular structures.[44] 12

Figure 1.7 – Example of drugs with a spiro scaffold.[54] 16

Figure 1.8 - Molecular structures of C3-spiroindolin-2-one and C2-spiroindolin-3-one.[55]..... 17

Figure 1.9 - Examples of drugs containing C3- and C2-spiroindolinone core structure.[55, 59]... 17

Figure 3.1 - Percentage of relative cell proliferation of NHDF cells after 72 hours exposure to 5-FU and compounds **8a, 8b, 8c, 8d, 8e** and **8f** at a concentration of 30 μM. The data are presented as average values with their SEM and are representatives of the two independent experiments performed. * $p < 0.05$ versus the control (Student's *t*-test)..... 45

Figure 3.2 - Percentage of relative cell proliferation of MCF-7 cells after 72 hours exposure to 5-FU and compounds **8a, 8b, 8c, 8d, 8e** and **8f** at a concentration of 30 μM. The data are presented as average values with their SEM and are representatives of one independent experiment performed. * $p < 0.05$ versus the control (Student's *t*-test)..... 46

Figure 3.3 - Calibration curve for uric acid at 295 nm, with respective equation of line and r^2. 47

Figure 3.4 - Inhibition of XO activity, at 5 minutes of incubation, of ALO and compounds **8a, 8b, 8c, 8d, 8e** and **8f** at a concentration of 30 μM. The data are presented as average values with their SEM and are representative of the two independent experiments performed. * $p < 0.05$ versus the control (Student's *t*-test). 47

Figure 3.5 - Over time inhibition of XO activity for ALO and spiroindolin-3-onethiobarbiturate **8c,** at a concentration of 30μM. 48

Figure 3.6 – SAR of spiroindolin-3-one(thio)barbiturates **8a-f** for cell cytotoxicity in NHDF and MCF-7 and XO inhibition. 49

Figure 3.7 – Interactions of Y-700, ALO, **8a** and **8b** with XO. Green dashes – Hydrogen bonds; Light green dashes – van der Waals interactions; Purple dashes – Pi-Sigma interactions; Yellow – Pi-Sulfur interactions; Pink – Pi-Pi Stacked interactions; Light pink dashes – Pi-Alkyl interactions; Red dashes – Unfavorable Acceptor-Acceptor interactions. 51

List of Schemes

Scheme 1.1 - Overall steps involved in molecular dockings. Adapted from Gupta *et al.*[7].....5

Scheme 1.2 – Reduction of MTT to formazan. Adapted from Mosmann *et al.*[22].....8

Scheme 1.3 - Oxidative hydroxylation of hypoxanthine through xanthine to uric acid, and formation of ROS. Adapted from Šmelcerović *et al.*[23] 8

Scheme 1.4 - Synthesis of barbituric acid.[29] 9

Scheme 1.5 - Chemical synthesis of barbiturates functionalized in C5. Adapted from Figueiredo *et al.*[27] and Serrano *et al.*[37] 11

Scheme 1.6 – Methods of C-O bond formation to prepare 2,1-benzisoxazole. Blue bond – New C-O bond formed. Adapted from Serrano *et al.*[37] 13

Scheme 1.7 - Methods of N-O bond formation to prepare 2,1-benzisoxazole. Blue bond – New N-O bond formed. Adapted from Serrano *et al.*[37] 14

Scheme 1.8 – Simultaneous C-O and C-N bond formation to prepare 2,1-benzisoxazole. Red bonds – New C-O and C-N bonds formed. Adapted from Serrano *et al.*[37] 14

Scheme 1.9 - Obtention of biological active compounds via 2,1-benzisoxazoles. Adapted from Więcław *et al.*[48] 15

Scheme 1.10 – Cleavage of the N-O bond of the 2,1-benzisoxazole in the formation of I,2,3,4-tetrafluoroacridone. Adapted from Coe *et al.*[50] 15

Scheme 1.11 – Spiro formation from a nitrene intermediate in the synthesis of acridones. Adapted from Hawkins *et al.*[51] 16

Scheme 1.12 - Synthesis of C2-spiroindolin-3-one by [3+2] annulation of α,β-unsaturated aldehydes with indolin-3-ones. Adapted from Guo *et al.*[61] 18

Scheme 1.13 - Synthesis of C2-spiroindolin-3-one by copper-catalysed oxidation of indole-2-carboxamides. Adapted from Kong *et al.*[62] 18

Scheme 1.14 - Synthesis of C2-spiroindolin-3-one by nucleophile-induced spirocyclization cascade process. Adapted from Zhang *et al.*[63] 19

Scheme 1.15 - Synthesis of fluorescent dyes C2-spiroindolin-3-one. Adapted from Chen *et al.*[64] 19

Scheme 1.16 – Synthesis of C2-spiroindolin-3-one by regioselective gold(III)-catalyzed cycloisomerization. Adapted from Marien *et al.*[65] 20

Scheme 1.17 - Synthesis of C2-spiroindolin-3-one by oxidation with phenyliodine(III) bis(trifluoroacetate). Adapted from Zhang *et al.*[66] 20

Scheme 1.18 - Synthesis of C2-spiroindolin-3-one by rhodium (III) catalyzed hydroacylation. Adapted from Mu *et al*.[67] 20

Scheme 1.19 - Synthesis of spiroindolin-3-onethiobarbiturate from 2,1-benzisoxazole. Adapted from J. Serrano.[68] 21

Scheme 3.1 – Synthesis of 1,3-disubstituted(thio)ureas **3a-o.** 26

Scheme 3.2 - Synthesis of 1,3-diphenylurea **3p**. 26

Scheme 3.3 – Synthesis of 1,3-disubstituted(thio)barbituric acids **5a-e**. 28

Scheme 3.4 - Synthesis of 1,3-dimethylthiobarbituric acid **5f**. 30

Scheme 3.5 - Synthesis of 5-(2-nitrobenzylidene)pyrimidines **6a-i**. 32

Scheme 3.6 - Synthesis of 5-(benzisoxazol-3-ylidene)pyrimidines **7a-i.** 35

Scheme 3.7 - Synthesis of the spiroindolin-3-onethiobarbiturate **8a.** 38

Scheme 3.8 - Synthesis of the spiroindolin-3-one(thio)barbiturates **8a-i.** 40

Scheme 3.9 - Proposed mechanism for the synthesis of the spiroindolin-3-one(thio)barbiturates **8.** 43

Scheme 3.10 – Attempts to intermolecular trapping of the nitrene intermediate with respective alkenes. 44

List of Tables

Table 3.1 - FTIR spectra, melting points and yield for the synthetized 1,3-diphenylthioureas **3a-p.** 27

Table 3.2 - ^{1}H-NMR of the synthetized 1,3-diphenylthioureas **3a-p.**..... 29

Table 3.3 - FTIR spectra, melting points and yield for the synthetized 1,3-disubstituted(thio)barbituric acids **5a-f**. 30

Table 3.4 - ^{1}H-NMR of the synthetized 1,3-disubstituted(thio)barbituric acids **5a-f**..... 31

Table 3.5 - FTIR spectra, melting points and yield for the synthetized 5-(2-nitrobenzylidene)pyrimidines **6a-i**. 32

Table 3.6 - ^{1}H-NMR of the synthetized 5-(2-nitrobenzylidene)pyrimidines **6a-i**. 34

Table 3.7 - ^{13}C-NMR of the synthetized 5-(2-nitrobenzylidene)pyrimidines **6a-i**. 34

Table 3.8 - FTIR spectra, melting points and yield for the synthetized 5-(benzisoxazol-3-ylidene)pyrimidines **7a-i.**..... 36

Table 3.9 - ^{1}H-NMR of the synthetized 5-(benzisoxazol-3-ylidene)pyrimidines **7a-i.** 37

Table 3.10 - ^{13}C-NMR of the synthetized 5-(benzisoxazol-3-ylidene)pyrimidines **7a-i.** 37

Table 3.11 - Optimization of the synthesis of spiroindolin-3-onethiobarbiturate **8a**. 38

Table 3.12 - FTIR spectra, melting points and yield for the synthetized spiroindolin-3-one(thio)barbiturates **8a-i.** 40

Table 3.13 - ^{1}H-NMR of the synthetized spiroindolin-3-one(thio)barbiturates **8a-i.** 42

Table 3.14 - ^{13}C-NMR of the synthetized spiroindolin-3-one(thio)barbiturates **7a-i.** 42

Table 3.15 - Estimated IC_{50} values of 5-FU and **8a** in NHDF cells..... 45

Table 3.16 - Estimated IC_{50} values of ALO and **8c** for the inhibition of XO activity..... 48

Table 3.17 – Molecular docking results for Y-700, ALO and spiroindolin-3-one(thio)barbiturates **8a-f**. Presented interactions by hydrogen bond with XO. In bold is highlighted the main hydrogen bonding interactions for the inhibitory activity. 50

Table 3.18 - Prevision of the pharmacokinetics properties for the compounds **8a-f.** Grey highlights positive results. 53

List of Acronyms, Abbreviations and Symbols

^{1}H-NMR	Proton nuclear magnetic resonance
^{13}C-NMR	Carbon-13 nuclear magnetic resonance
5-FU	5-Fluorouracil
ADMET	Absorption, distribution, metabolism, excretion and toxicity
ALO	Alopurinol
ArC	Aromatic carbon
ArCH	Aromatic proton
ARG	Arginine
ATR	Attenuated total reflectance
ATCC	American type culture collection
BBB	Blood-brain barrier
BOC	*Tert*-butyloxycarbonyl
CNS	Central nervous system
DCM	Dichloromethane
DMF	Dimethylformamide
DMSO	Dimethyl sulfoxide
DMSO-d_6	Hexadeuterated dimethyl sulfoxide
d	Doublet
dd	Doublet of doublets
ddd	Doublet of doublet of doublets
DEPT	Distortionless Enhancement by Polarization Transfer
DMEM	Dulbecco's modified Eagle's medium
dt	Doublet of triplets
ELISA	Enzyme-linked immunosorbent assay
EMA	European medicines agency
EtOAc	Ethyl acetate
EWG	Electron withdrawing groups
FBS	Fetal bovine serum
FDA	Food and Drug Administration
FTIR	Fourier-transform infrared spectroscopy
GLU	Glutamine
hept	Heptet
hERG	Human *Ether-à-go-go*-Related Gene
HEPES	4-(2-hydroxyethyl)-1-piperazineethanesulfonic acid
HMBC	Heteronuclear multiple bond correlation
HSQC	Heteronuclear single bond correlation
IC_{50}	Half of the maximal inhibitory concentration

J	Coupling constant
Lit.	Literature
log P	Partition coefficient
mp	Melting points
MTT	3-(4,5-Dimethylthiazolyl-2)-2,5-diphenyltetrazolium bromide
m	Multiplet
MCF-7	Michigan cancer foundation-7
mw	Microwave
nH	Number of protons
NHC	N-heterocyclic carbene
NHDF	Normal human dermal fibroblasts
NMR	Nuclear magnetic resonance
OCT2	Organic cation transporter 2
PBS	Phosphate-buffered saline
PIFA	Phenyliodine(III) bis(trifluoroacetate)
ppm	Parts per million
QSAR	Quantitative structure−activity relationship
s	Singlet
SEM	Standard error of the means
ROS	Reactive oxygen species
RMSD	Root mean square deviation
SAR	Structure-activity relationships
SMILES	Simplified molecular-input line-entry system
t	Triplet
TBHP	*Tert*-butyl hydroperoxide
td	Triplet of duplets
THF	tetrahydrofuran
THR	Threonine
TLC	Thin layer chromatography
XO	Xanthine oxidase
Y-700	1-[3-Cyano-4-(2,2-dimethylpropoxy)phenyl]-1H-pyrazole-4-carboxylic acid
δ	Chemical shifts
Δ	Heating
υ_{max}	Maximum frequency of the absorption band (cm^{-1})

Chapter 1 - Introduction

In the present chapter will be introduced the theme of this project, starting with the notion of Medicinal Chemistry and the evolution of drug discovery and development. In a first instance it will be presented the different stages of drug discovery, highlighting chemical synthesis, *in silico*, *in vitro* and *in vivo* studies.

In the second part, it will be presented three different classes of compounds. In section 1.2 will be presented a historical contextualization of barbiturates, with special attention in the functionalization in C5 and its biological activities. In section 1.3 will be presented the importance of the benzisoxazole system, mainly 2,1-benzisoxazole, in the development of biologically activated compounds. And finally, in section 1.4 will be reviewed spiro compounds, mainly focusing on C2-spiroindolin-3-ones.

1.1. Medicinal Chemistry - Drug discovery and development

Medicinal Chemistry is a scientific area centered in the discovery and development of new chemical compounds with pharmacological interest. It also aims to identify their biological activity, side effects, metabolism and interpretation of their structure-activity relationships (SARs). The principal objective of a medicinal chemist is the obtention of a new lead compound.[1-2]

In the present days, creating new drugs is a complex process. The conventional methods involving the use of therapeutic plants for the treatment of diseases has evolved. In the nineteenth century, the extraction and identification of an active principle in their crude state from plants, animals or minerals, was a very common practice.[2] Morphine (figure 1.1) is a classic opioid drug which crystals were firstly isolated from *Papaver somniferum* L. (opium poppy), by the German chemist Friedrich Sertürner, in 1803.[3-4] With the evolution of organic chemistry, codeine and heroin (figure 1.1) were easily prepared from morphine when *O*-methylated at position 3 or *O*-acetylated at positions 3 and 6, respectively.[4-5]

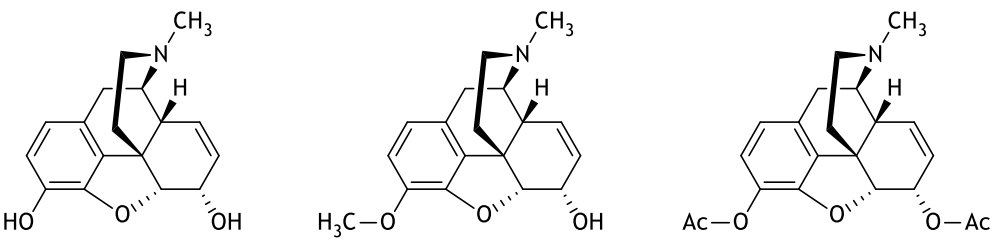

Figure 1.1 - Chemical structures of Morphine and its analogues codeine and heroine.[4]

At the end of the nineteenth century, not only was trivial to obtain drugs from natural sources but also to make changes in their chemical structures and to test their biological activities. With that, the pharmaceutic industry was born and led to various and new medicinal classes of drugs such as penicillin, an antibiotic, or different hormones like insulin, epinephrine and progesterone. Additionally, anesthetic, analgesics, hypnotics, anticonvulsants and anticancer agents are some of the examples of new drugs classes that were discovered/developed during the twentieth century and present days.[2, 4]

The history of Medicinal Chemistry and the development of drug research, over a period of a century, was an astonishing journey of accomplishments and, even though it changed over the past several years, the goal of finding new, more potent and safer medicines remained the same.[6]

Drug discovery can be divided in two different stages, the first one of preclinical studies and the second one of clinical studies (figure 1.2).[1]

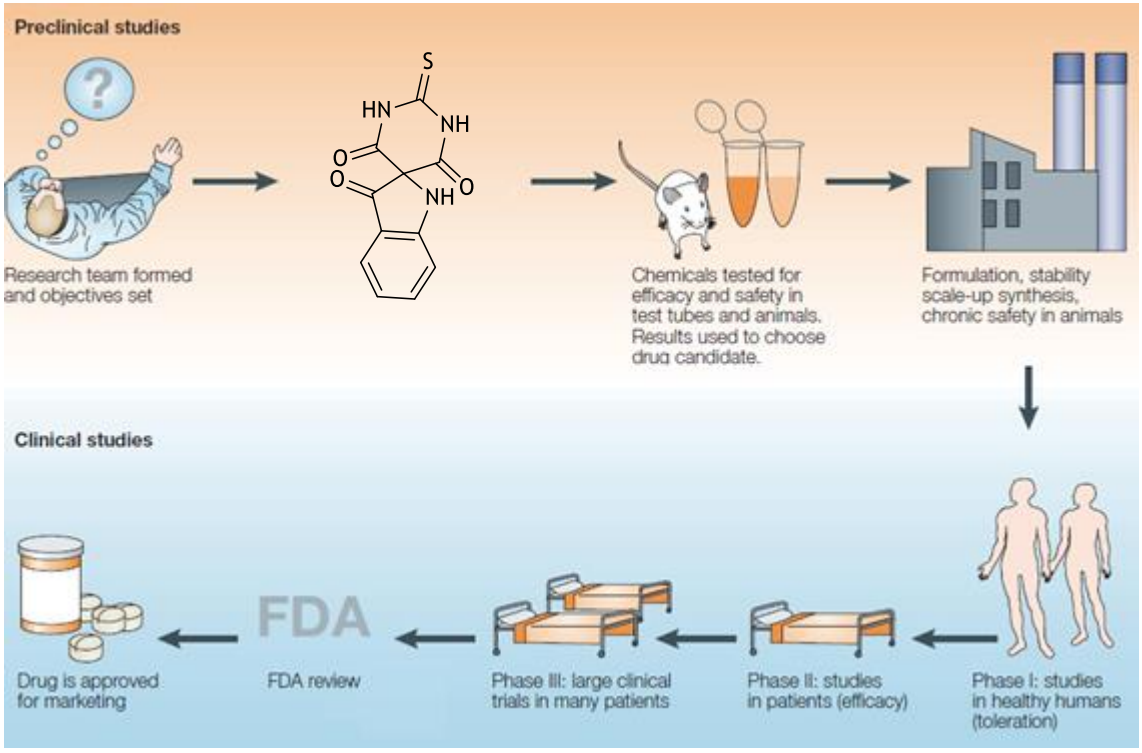

Figure 1.2 - Stages in the drug discovery process. Adapted from Lombardino *et al.*[1]

Initially, in a preclinical phase, usually the drug discovery process begins with the study of a pathology and its different therapies, if existing. From this analysis, hypotheses are raised on how to possibly improve the therapy and, after specifying the objectives, different compounds are designed.[1]

If the biological targets are well known and correctly characterized, computational studies of molecular docking can be performed. This *in silico* methodology is an application of computer-

based models which predicts the ideal orientation of a designed ligand or drug in the active site of the target when bound to each other to form a stable complex.[7] In addition, it is also possible to predict different pharmacokinetic properties, such as absorption, distribution, metabolism, excretion and toxicity (ADMET).[8] With the help of these techniques, a high number of molecules can be screened for a biological activity at an early stage of drug development, which contributes in the selection of a hit compound. However, this step can generate both false positives and false negatives. Molecules with possible therapeutic potential can be eliminated from the selection, although the human and financial resources spared by this approach compensate for this disadvantage.[7]

The next step can be the synthesis and biological evaluation of the selected compounds. A key subsequent step in this process include detecting the desired biological activity in *in vitro* studies and acquisition of SARs data, and then reflect it *in vivo* in an appropriate animal model. In addition, an optimization of the activity through preparation of structures analogous of the lead compound, and reevaluation of their activities, is usually required. Once all this process is optimized, a single lead compound can be selected as a drug development candidate. This drug candidate then undergoes several experiments to ensure its safety for human consumption, and if it has the required ADMET properties, to ensure minimal risks for the human test subjects in the next stage of the drug discovery – the clinical studies.[1, 6]

If the drug candidate passes to the clinical studies, the acquired research data is submitted to the specialized agencies, like the European Medicines Agency (EMA) in Europe Union or the Food and Drug Administration (FDA) in the United States, before clinical trials are initiated. In these trials, the drug candidate is sequentially evaluated in four phases.[1] In Phase I, is evaluated tolerance of the drug in healthy human volunteers. In Phase II, is determined the efficacy and dose range in different patients. In Phase III, is generalized a broad database on the drug efficacy and safety. In Phase IV, are performed studies of post drug commercialization.[1, 9]

For the few percentages of compounds that can be considered as drug candidates, only a small number of them can survive this series of development trials and become a drug. It's clearly a high-stake, long-term and risky procedure, but the potential benefits to the millions of patients with serious diseases provide a constant motivating force to go through with it, and every medicinal chemists can have a role in any of these stages — from drug design and chemical synthesis, to *in vitro* and *in vivo* screenings and clinical trials.[1, 6]

1.1.1. *In silico* studies

As depicted above, computational studies are advantageous technics in the early stages of drug discovery. With the power of predicting the different interactions of a ligand with his target,

or the pharmacokinetic properties of a compound, can taper the number of structures designed in the development of a new drug.[7, 10]

The goal of molecular docking is to understand and predict molecular recognition, both structurally, finding different binding modes, and energetically, predicting binding affinity. Molecular docking is strictly a computer-based analysis, with a well-defined protocol (scheme 1.1), usually performed between a small molecule (new chemical entities or drugs) and a target macromolecule (usually a protein). Mostly downloaded from Protein Data Bank, the macromolecule is prepared by minimization of its energy and by adding hydrogen ions and removing water molecules. The structure of ligands in study must has to be drawn in a drawing software and, like the protein, further energy minimization is required. Once both macromolecule and ligand are prepared, it is important to carry out a validation of the method. In the validation, a molecular docking of the protein with the original ligand that it was crystallized with is performed. When the method is validated, the docking for the ligands in study can start. It can be realized mainly by two types: rigid docking, where protein and ligand are fixed so that bond angles or lengths are not changeable, and flexible docking, which allows conformational shifts. The flexible docking is widely used, although it requires more time and computational throughput, where the rigid one is extremely faster but neglects the conformational degrees of freedom of ligands. After the molecular docking is realized, the results are usually sorted by affinity and, generally, the higher binding affinity molecule is considered to be the most potent and, in this way, the number of entries in the study can be narrowed down by choosing the best ones.[7, 10]

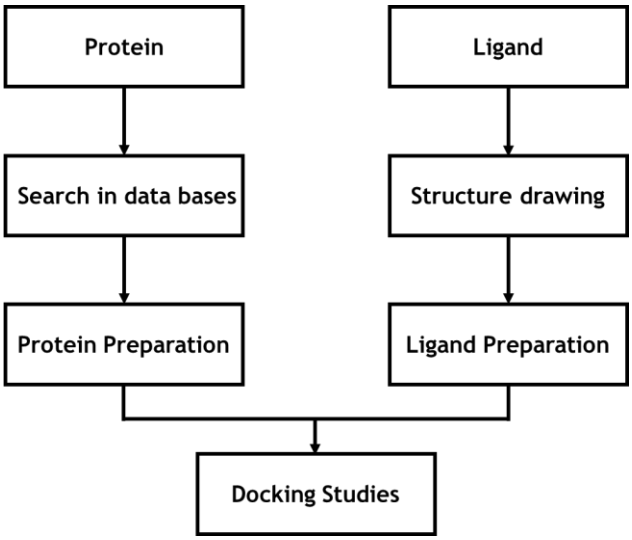

Scheme 1.1 - Overall steps involved in molecular dockings. Adapted from Gupta *et al.*[7]

In addition to the molecular docking and other studies, it is possible to also realize ADMET prediction studies. Since a large number of drug candidates tend to fail in the clinical trials due

to their poor ADMET properties, is important to have a notion of their pharmacokinetics to ensure that they can reach their target in sufficient concentrations to safely produce the desired pharmacological effect.[8]

The equilibrium between pharmacokinetics, toxicity, and potency is crucial for effectiveness of drugs. Many *in silico* approaches for predicting pharmacokinetic and toxicity properties of compounds from their chemical structure have been developed, being the most common ones based on quantitative structure–activity relationship (QSAR).[11] Usually they are not freely available, which limits their utility. pkCSM is a software that provides the analysis and optimization of pharmacokinetic and toxicity properties implemented in a user-friendly, freely available web interface (http://structure.bioc.cam.ac.uk/pkcsm/prediction). With a simplified molecular-input line-entry system (SMILES) notation it is possible to predict a large number of pharmacokinetic characteristics. For Absorption, water solubility, intestinal absorption and if the drug candidate is a p-glycoprotein substrate or inhibitor, are some of the parameters studied. For distribution, is important to know the blood-brain barrier (BBB) or central nervous system (CNS) permeabilities. Since the cytochrome P450 isoforms are responsible for the metabolism of many drugs, it is likely significant to assess whether a given drug candidate is its substrate or inhibitor. Regarding excretion, it is important to know if the compound is a renal organic cation transporter 2 (OCT2) substrate. Lastly, parameters like Ames toxicity, maximum tolerated dose in humans, inhibition of potassium channels (hERG, from human *Ether-à-go-go*-Related Gene) and hepatotoxicity, are of the same importance to partially predict the toxicity of the compounds in study.[8]

Additionally, the pkCSM software also calculates the Lipinski's "Rule of 5", which helps in the prediction the oral bioavailability of potential drug candidates. The Lipinski's "Rule of 5" are: the candidate can't have a molecular weight greater than 500 g/mol or a partition coefficient (log P) greater than 5 and it must have less than five hydrogen-bond donors and ten hydrogen-bond acceptors. If the drug candidate has no more than one violation it is considered to have a good oral bioavailability[12-13] Another parameter often considered are the parameters of Veber, where the drug candidate must have 10 or less rotatable bonds and polar surface area lower than 140 $Å^2$.[14]

1.1.2. Chemical synthesis

The traditional way of mixing different reagents in a round bottom flask to obtain new chemicals entities haven't changed. Nowadays the objective is to quickly synthesize and screen structures in order to find new lead compounds, identifying their SARs and finding analogues with good activities and minimal side effects.[15] Combinatorial and parallel synthesis are established tools in drug discovery, allowing the use of a defined reaction route to produce a large number of compounds in a short period of time.[2, 16]

In combinatorial chemistry is produced a mixture of different compounds within a sole vessel. The obtained structures are not separated or purified but tested for biological activity as a whole. If the mixture has shown a promising activity, further isolation of the active compound is required. This can become a disadvantage because purification methods are rather difficult, and the obtained activity can be due to co-action of two or more structures and the isolated compound could not show the same activity. In parallel synthesis, the syntheses are carried out in a series of vessels, with production of a single product in each one. The reactions are usually carried out on a small-scale so that the process can be almost automated and carried out under identical conditions but with small changes in the structures.[16-17]

The demand for diverse compound libraries for screening in drug discovery is the driving force behind the development of new technologies for a rapid combinatorial and parallel synthesis. One of those high-speed techniques is microwave-assisted organic synthesis, which has attracted a substantial amount of attention in the past few years.[18]

Located in the middle of infrared and radio frequency region, microwave (mw) is a part of electromagnetic spectrum between the frequencies 0.3 GHz to 300 GHz. Mw irradiation is widely applied in organic reactions.[19] It offers many advantages in heating based synthesis, including drastic shortening of the reaction time, suppression of side reactions, higher chemical yields, and a more eco-friendly chemistry.[20] In a mw-assisted reaction, the rate of a chemical reaction increases because of the heat generated from the interactions between the molecules and irradiated waves. It occurs due to a dipolar polarization, resulted from dipole-dipole interactions of polar molecules and the electric component of the mw. Under mw exposure, polar molecules tend to align themselves after absorbing certain amount of energy. When the direction of the applied field is changed, the molecules will also start to rotate along with it. With this destabilization, the molecules start to collide with each other, there is an increase in the kinetic energy, hence the increase of temperature, and the chemical reaction takes place.[19]

1.1.3. Biological activity evaluation

Regardless of the *in silico* studies realized to predict the biological activity of different compounds, it is highly important to also perform *in vitro* studies to determine if these results will be mirrored in biological means.[6]

Cell assays are often used for screening compounds namely to determine if they have effects on cell proliferation or show direct cytotoxic effects that eventually lead to cell death. These tests also are widely used for measuring target binding, signal transduction events, trafficking of cellular components, or monitoring organelle function. Depending on the study, different cell lines can be used. Cell lines are highly desirable, as they provide systems for a ready and direct access and evaluation of tissues. With origin in basically any biological tissue, they are a

valuable tool to study problems of clinical relevance related to diseases, screening, and studies of cell toxicity. Their easy access provides the possibility to perform cellular mechanisms studies that may suggest new potential drug targets and, in the case of pathological-derived tissues, allows the evaluation of therapeutic agents that potentially may treat a disease.[21]

Regardless of the type of screening used, it is important to know how many viable cells are remaining at the end of each experiment. There are a variety of quantification methods that can be used to estimate the number of viable cells. The most used one is the well-established 3-(4,5-dimethylthiazolyl-2)-2,5-diphenyltetrazolium bromide (MTT) cell proliferation assay. In this test, the cells are incubated with MTT, where it will be converted into purple and insoluble formazan crystals by active mitochondrial reductases of living/viable cells (scheme 1.2).[22]

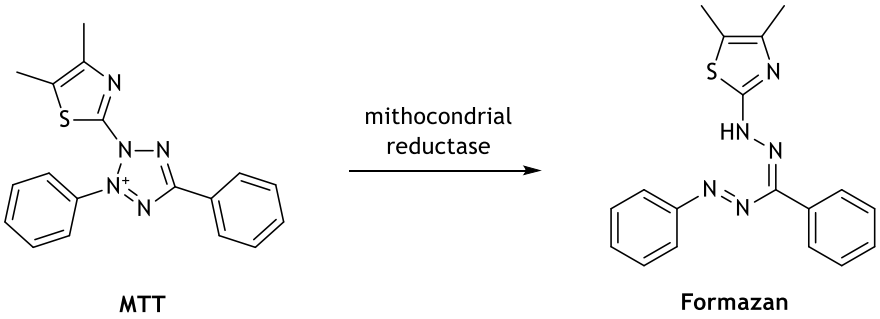

Scheme 1.2 – Reduction of MTT to formazan. Adapted from Mosmann *et al.*[22]

Other types of biological evaluation tests that can be performed in drug discovery and development are enzymatic assays, where is usually measured the inhibitory activity of compounds directly in the enzyme that is associated with a pathology. The xanthine oxidase (XO) inhibitory assay is a relevant example related to the present dissertation work. XO is a complex flavoprotein widely distributed in the human body. It is responsible for the metabolism of purines, oxidizing hypoxanthine through xanthine to uric acid, and also the formation of reactive oxygen species (ROS) (scheme 1.3). An increase in this enzyme's activity, as well as in its metabolites levels (uric acid and ROS), are associated with many pathological conditions, including gout and oxidative stress in tissues.[23]

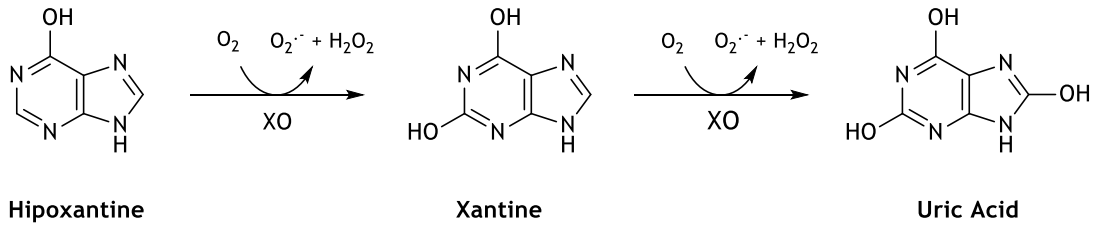

Scheme 1.3 - Oxidative hydroxylation of hypoxanthine through xanthine to uric acid, and formation of ROS. Adapted from Šmelcerović *et al.*[23]

The known XO inhibitors can be divided into two classes: purine inhibitors and nonpurine inhibitors.[24] Alopurinol (ALO) (figure 1.3) is a purine analogue and was the first XO inhibitor approved by FDA for the treatment of gout, and it is still being used in primary and secondary hyperuricemia. In low concentrations ALO behaves as a competitive enzyme inhibitor and, in higher concentrations the substrate behaves as a noncompetitive enzyme inhibitor. The use of ALO is associated with several side effects namely due to the fact that its purine analogue nature also allows interaction with to other purine receptors.[25] Febuxostat (figure 1.3), a thiazole derivative, is an example of a nonpurine XO inhibitor. It is more selective and potent than ALO, being mostly metabolized in the liver. It has a mixed inhibitory activity and, unlike ALO, Febuxostat can also inhibit ROS formation.[26] With these characteristics, which attracted a lot of researchers, the discovery of new nonpurine XO inhibitors is an important goal in Medicinal Chemistry.[27-28]

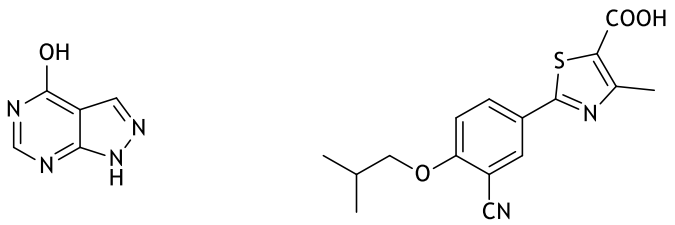

Alopurinol **Febuxostat**

Figure 1.3 - Purine and nonpurine inhibitors of xanthine oxidase.[24]

1.2. Barbiturates

Barbiturates constitutes a relevant class of compounds due to their wide range of biological activities and structural versatility. Initially synthetized in 1864 by German chemist Adolf von Baeyer, barbituric acid was obtained with the condensation of urea and malonic acid in acetyl chloride (Scheme 1.4).[29] Since its original synthesis, many other methods have been described in the literature, being the most common and widely used in the industry the condensation of urea with diethyl malonate in the presence of sodium ethoxide in anhydrous ethanol.[30]

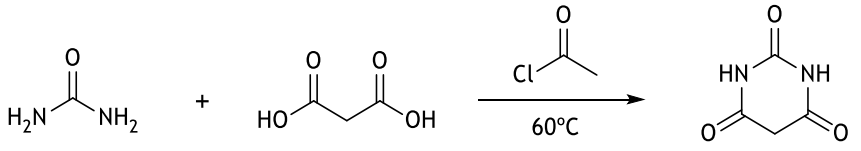

Urea **Malonic acid** **Barbituric acid**

Scheme 1.4 - Synthesis of barbituric acid.[29]

Barbituric acid itself lacks pharmacological effects. However, additions and/or substitutions in its backbone yields pharmacologically active compounds, such as CNS depressants, acting as anxiolytic, hypnotic, sedatives, anesthetic, and anticonvulsant agents[31], as well as antibacterial, anticancer, antiangiogenic, immunomodulatory, antifungal and antioxidant compounds.[32] The transformations in the barbituric acid backbone can be either in positions N1, C2, N3 and C5, especially the latter when is mono- or di-substituted, or is forming a spiro structure condensed with other types of heterocycles.[27, 32]

There are some examples of bioactive barbiturate derivatives (figure 1.4). Barbital was the first barbiturate to be developed. It has sedative and hypnotic activities and was used as a sleeping aid and as anxiolytic, but due to its toxicity and abusive nature was replaced for other compounds, mainly benzodiazepines, which are usually safer drugs.[33] Phenobarbital is one of the most used antiepileptic drugs in the world because of its easy accessibility and affordable cost. Although it was claimed to cause sedation and other cognitive and behavioral side effects, it is still recommended for partial and generalized tonic–clonic seizures.[34] Merbarone is a topoisomerase II inhibitor, which inhibits DNA synthesis and consequently tumor cells growth. Its antineoplastic characteristics showed positive results against leukemia and other types of tumors but, at Phase II of the clinical trials, failed as a drug because of its small effectiveness compared to other compounds.[32, 35]

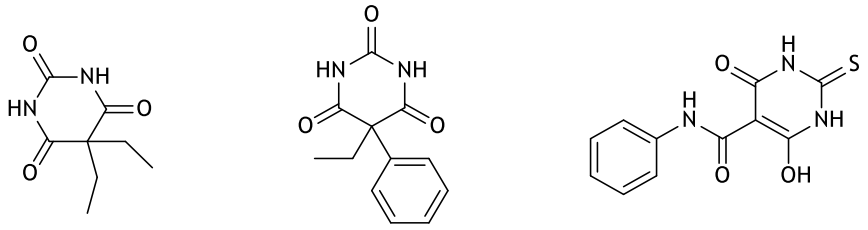

Figure 1.4 – Examples of bioactive barbiturate derivatives.[32]

The presence of an active methylene group at the C5 of barbituric acid allows this molecule to be easily involved in condensation reactions with other compounds. More recently, and among C5 functionalized barbiturates, there are 5-benzylidenes or 5-methylenes derivatives that show a variety of biological activities (scheme 1.5).[27, 36-37]

5-(Aminomethylene)barbiturate derivatives are easily obtained by reaction with triethyl orthoformate and primary amines in refluxing butan-1-ol. The introduction of the amines make these barbiturates good intermediates for the synthesis of new bioactive compounds because, since the addiction of the new functional groups, allows intramolecular reactions with the formation of spiro or fused heterocycles.[38-40] Jursic and co-workers, developed a series of 5-

(hydrazinylethyllidene)barbiturate derivatives with direct condensation of 5-acylbarbiturates with different hydrazines in an ethanol reflux. These derivatives showed to be potential antifungal compounds with the ability to inhibit fungal growth in the micromolecular range.[36] Additionally to these results, Figueiredo *et al.* also developed a series of new 5-(hydrazinylethyllidene)barbiturate derivatives with potential antimicrobial activity against *Acinetobacter baumannii*.[27] The 5-(benzylidene)barbiturate derivatives have been biologically evaluated and several compounds of this class were found to possess XO inhibitory effect and antimicrobial activity against a number of Gram-positive and Gram-negative bacteria, as well as against fungal strains.[27, 41-42] These benzylidenes can be obtained by Knoevenagel condensation between barbituric acid and an aromatic aldehyde. Initially these reactions were performed in organic solvents with or without a catalyst but, a reflux aqueous medium method, showed to be more advantageous, because of the resulted yields and low reactional time.[43] Finally, it was reported by Serrano *et al.* that when 5-(2-nitrobenzylidene)barbiturate derivatives were exposed to tin(II) chloride dihydrate (scheme 1.5) a partial reduction of the nitro group, into a nitroso as a key intermediate, was observed, and a consequential intramolecular cyclization occurred, forming a 2,1-benzisoxazole heterocycle with potential XO inhibitory activity.[37]

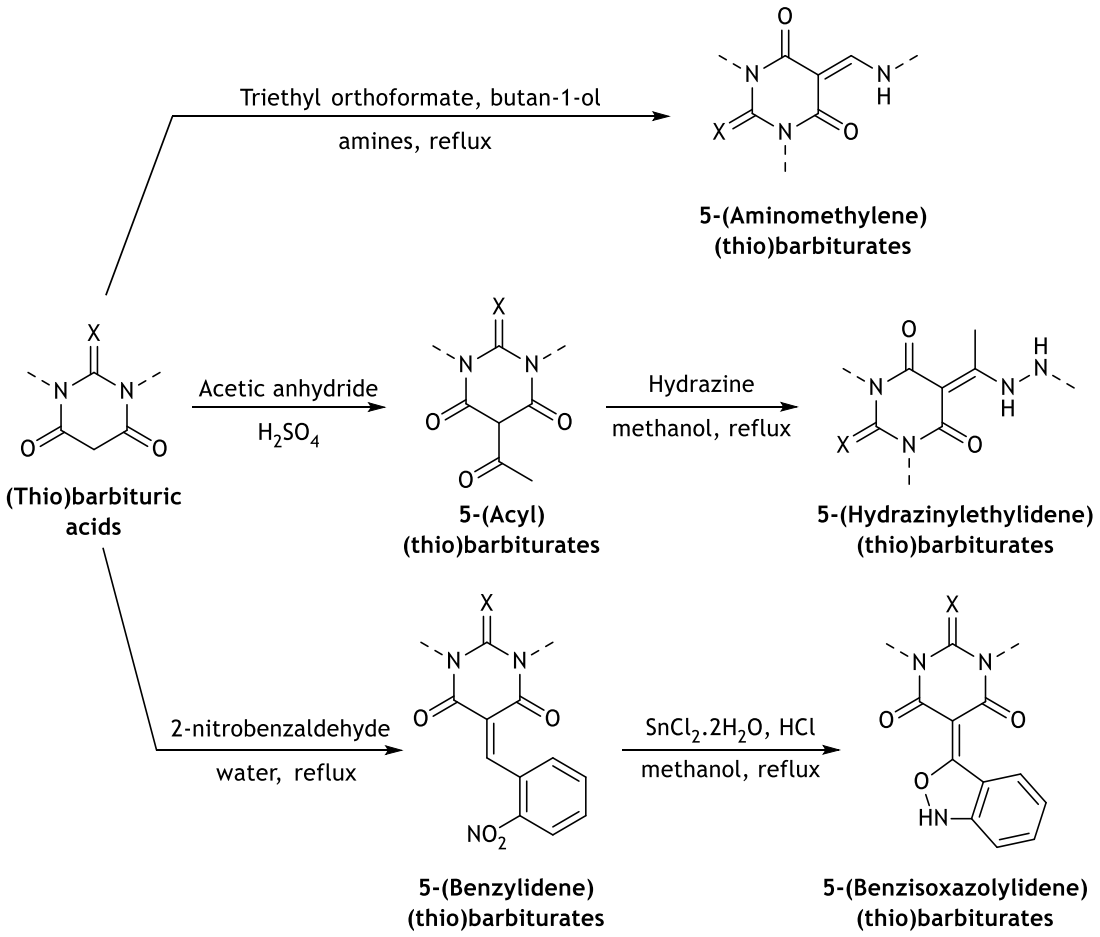

Scheme 1.5 - Chemical synthesis of barbiturates functionalized in C5. Adapted from Figueiredo *et al.*[27] and Serrano *et al.*[37]

1.3. Benzisoxazoles

Benzisoxazoles are aromatic ring heterocycles containing one oxygen atom adjacent to one nitrogen atom in a five-membered ring fused with a benzene ring. Benzisoxazoles can exist in two types, namely 1,2-benzisoxazoles (indoxazenes) and 2,1-benzisoxazoles (anthranils), where the difference are the position of the heteroatoms (figure 1.5).[37]

1,2-benzisoxazole **2,1-benzisoxazole**

Figure 1.5 – Molecular structures of 1,2-benzisoxazole (indoxazene) and 2,1-benzisoxazoles (anthranil).[37]

The 1,2-benzisoxazole is a privileged structure because it forms the centerpiece of small molecule chemical entities (figure 1.6) with a wide range of pharmacological properties, namely anticonvulsant and antipsychotic.[44]

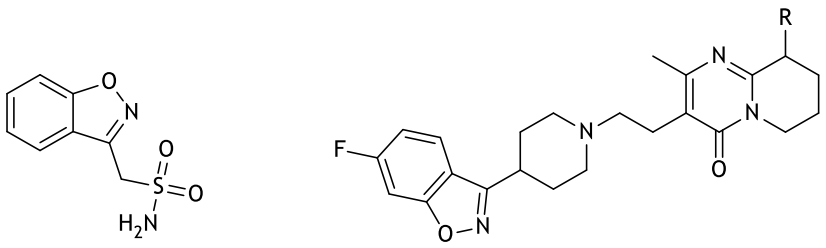

Zonisamide **Risperidone (R = H)**
Paliperidone (R = OH)

Figure 1.6 - Examples of drugs with a 1,2-benzisoxazole in their molecular structures.[44]

Zonisamide (figure 1.6), a sulphonamide derivative, is a new-generation anticonvulsant with multiple potential mechanisms that contribute to its antiepileptic efficacy mainly in partial-onset seizures and to its interest also in non-seizure disorders such as headaches, neuropathic pain, and weight loss. It has favorable pharmacokinetic characteristics and is well tolerated in a long-term dose usage.[45] Paliperidone and risperidone (figure 1.6), are atypical antipsychotics with high affinity for serotonin, dopamine D2, and alpha1- and alpha2-adrenergic receptors, being mainly indicated for the treatment of schizophrenia, bipolar mania and irritability associated with acoustic disorder.[46]

Although 1,2-benzisoxazole is more widely used due to its high therapeutic interest, 2,1-benzisoxazole is more notorious in the synthesis and preparation of other biologically active compounds.[37]

1.3.1. Synthesis of 2,1-benzisoxazoles

The 2,1-benzisoxazole is equally an interesting structure. Since the first described synthesis of 2,1-benzisoxazoles by reductive cyclization of *ortho*-nitrobenzaldehydes in 1882, by Friedlander[47], several methods have been described, and can be divided depending on the bond that is being formed in the isoxazole ring: the C-O bond, the N-O bond or both C-O and C-N bonds simultaneously.[37, 48]

C-O bond can be formed by the reaction between a carbonyl, from an aldehyde or ketone, and a nitro group after a partial reduction to a nucleophilic specie as a hydroxylamine (method A, scheme 1.6); by the reaction of a nitro derivative as nucleophilic species and a methylene bound to electron withdrawing groups (EWG) such as nitriles, esters, sulfones and phosphonates, followed by catalyzed dehydration (method B, scheme 1.6); and by the reaction of a methylene and a nitro group after partial reduction to a nucleophilic nitroso (method C, scheme 1.6).[37, 49]

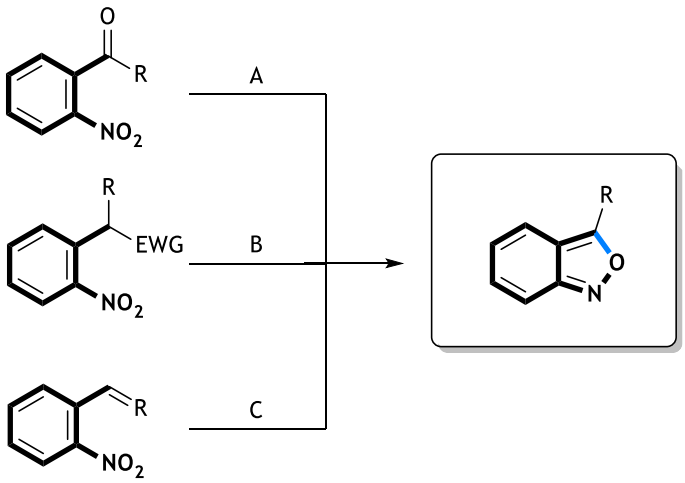

Scheme 1.6 – Methods of C-O bond formation to prepare 2,1-benzisoxazole. Blue bond – New C-O bond formed. Adapted from Serrano *et al.*[37]

N-O bond formation includes, for example, the thermolysis between a carbonyl, from a ketone or aldehyde, and an azido group (method A, scheme 1.7); or the oxidative cyclisation of *ortho*-aminobenzoarenes (method B, scheme 1.7).[37, 48]

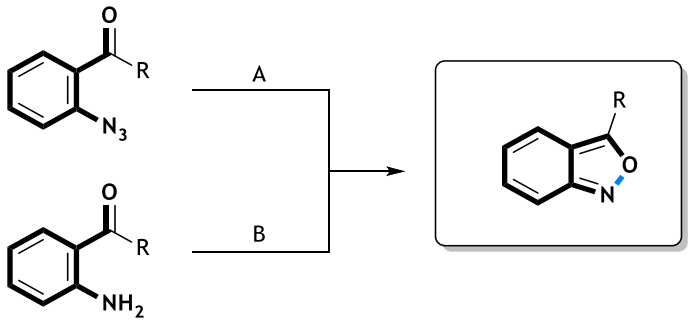

Scheme 1.7 - Methods of N-O bond formation to prepare 2,1-benzisoxazole. Blue bond – New N-O bond formed. Adapted from Serrano *et al.*[37]

Finally, the 2,1-benzisoxazole nucleus can also be obtained by the reaction of benzohydroxamic acid, as a methyl ester, and hydroxylamine, with *tert*-butyloxycarbonyl (BOC) protecting group, via co-catalysis of rhodium and copper involving the nitroso intermediate derived from the hydroxylamine (scheme 1.8).[37, 49]

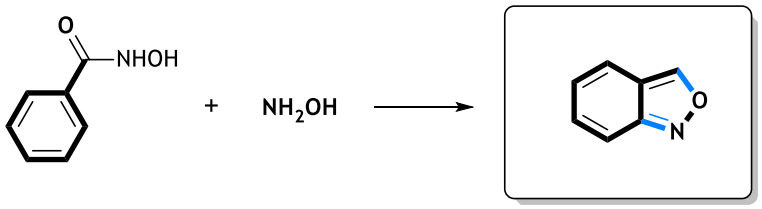

Scheme 1.8 – Simultaneous C-O and C-N bond formation to prepare 2,1-benzisoxazole. Red bonds – New C-O and C-N bonds formed. Adapted from Serrano *et al.*[37]

1.3.2. 2,1-Benzisoxazoles transformations

As depicted above, 2,1-benzisoxazole is more useful in the synthesis of other biologically active compounds. From these preparations highlights acridines, quinolines, quinazolines and benzodiazepines, from direct transformation of 2,1-benzisoxazoles or via aminoarylketones, which are easily obtained by treatment with iron in acetic acid (scheme 1.9).[48]

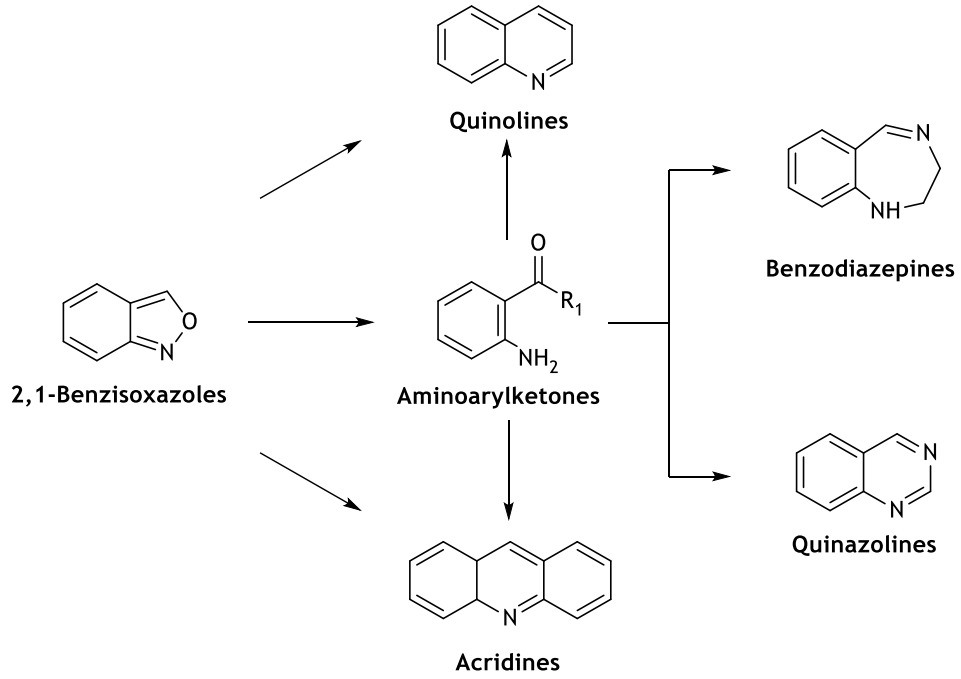

Scheme 1.9 - Obtention of biological active compounds via 2,1-benzisoxazoles. Adapted from Więcław *et al*.[48]

All these transformations are due to the cleavage of the N-O bond of 2,1-benzisoxazole ring. This cleavage was initially described in 1966 by Coe *et al*. with the formation a nitrene triplet intermediate, when a pentaflouroanthranil derivative was thermally exposed to form I,2,3,4-tetrafluoroacridone (scheme 1.10).[50]

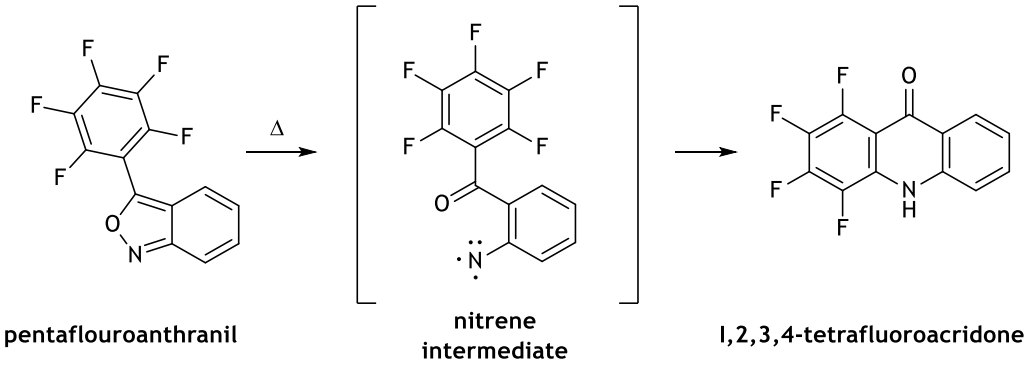

Scheme 1.10 – Cleavage of the N-O bond of the 2,1-benzisoxazole in the formation of I,2,3,4-tetrafluoroacridone. Adapted from Coe *et al*.[50]

Later, Hawkins *et al*. and Maki *et al*. postulated a spiro formation, namely spiroindolinone, from the nitrene intermediate, as a second intermediate of said cleavage in the development of acridones (scheme 1.11).[51-52]

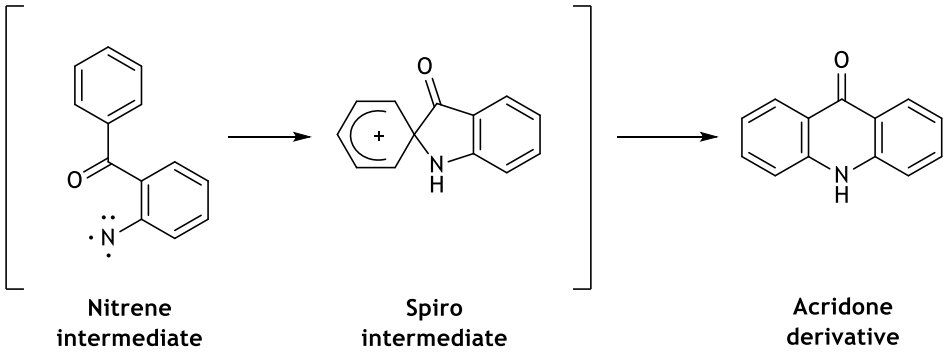

Scheme 1.11 – Spiro formation from a nitrene intermediate in the synthesis of acridones. Adapted from Hawkins *et al*.[51]

1.4. Spiro compounds - spiroindolinones

Spiro compounds, which are constituted by cyclic structures fused at a central carbon are vastly interesting. The tetrahedral nature of the spirolinked carbon gives a nearly perpendicular angle between the two ring planes.[53-54] This unique, rigid and three-dimensional conformation feature different implications on their biological activities.[54-55] Examples of these compounds include: Spirapril (figure 1.7), an angiotensin converting enzyme inhibitor mainly used in the treatment of hypertension, with a 1,3-thiolane spirolinked with a pyrrolidine in positions 2 and 3, respectively[56]; Griseofulvine (figure 1.7) an antifungal antibiotic, with a spiro formation between a benzofuran-3-one and a ciclohex-2-enone in positions 2 and 4, respectively[57]; and Fenspiride (figure 1.7) a drug used in the treatment of certain respiratory diseases, with a oxazolidinone spirolinked in position 5 with a piperidine in position 4.[58]

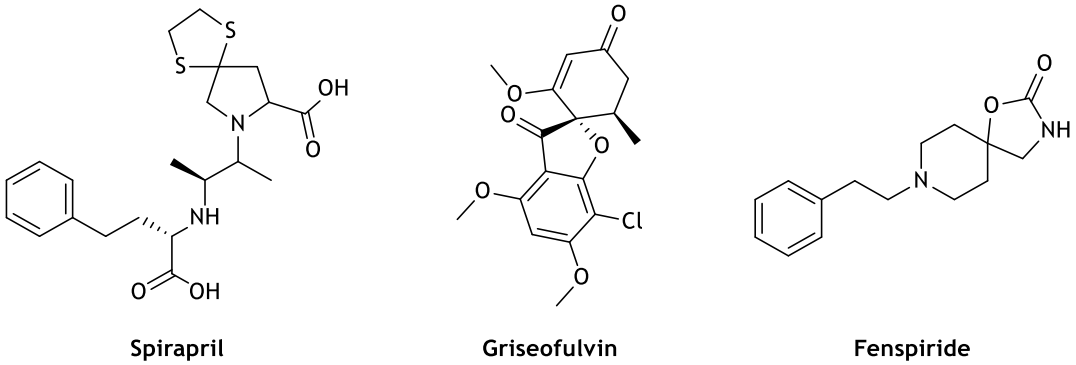

Figure 1.7 – Example of drugs with a spiro scaffold.[54]

Other important class of spiro compounds are the spiroindolinones. Indolinones are aromatic ring heterocycles containing nitrogen atom in a five-membered ring with a carbonyl fused with a benzene ring. There are two classes of spiroindolinones based on the position of the spirocarbon: C3-spiroindolin-2-one and C2-spiroindolin-3-ones (figure 1.8).[55]

C3-spiroindolin-2-one **C2-spiroindolin-3-one**

Figure 1.8 - Molecular structures of C3-spiroinlolin-2-one and C2-spiroindolin-3-one.[55]

Spiro heterocycles, particularly containing these spiroindolinones, have been identified as highly relevant structures in medicinal chemistry, being anti-tumor, antimicrobial, anti-HIV, antipyretics and antimalarial agents.[55] The C3-spiroindolin-2-one is intensively studied, and some molecules presented interesting biological activities, for example, cipargamin (also known as NITD609) (figure 1.9) an antimalarial agent in phase II of clinical studies.[59-60] On the other hand, C2-spiroindolin-3-ones are widespread in nature as alkaloids, such as mitragynine pseudoindoxyl and rauniticine pseudoindoxyl (figure 1.9).[55]

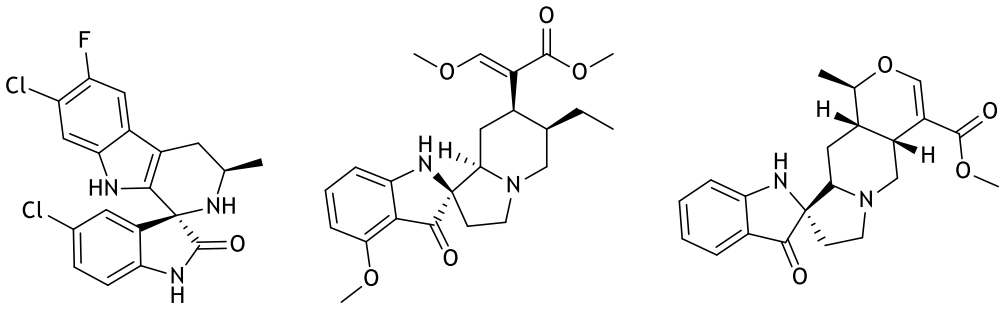

Cipargamin **Mitragynine pseudoindoxy** **Rauniticine pseudoindoxyl**

Figure 1.9 - Examples of drugs containing C3- and C2-spiroindolinone core structure.[55, 59]

1.4.1. Synthesis of spiroindolin-3-ones

Despite their important biological properties, C2-indolin-3-ones are scarcely explored as compared to C3-spiroindolin-2-one. The synthesis of C2-spiroindolin-3-ones are usually difficult. The general procedure can involve the spiro formation with or without an indole scaffold already in the starting material.[55] In this section, is presented some examples in the latest development of C2-spiroindolin-3-ones synthesis.

1.4.1.1. Spiro formation with an indole scaffold in the starting material

Guo *et al*. developed C2-spiroindolin-3-one derivatives with a highly enantioselective *N*-heterocyclic carbene (NHC) catalyzed formal [3+2] annulation of α,ß-unsaturated aldehydes with indolin-3-ones (scheme 1.12).[61]

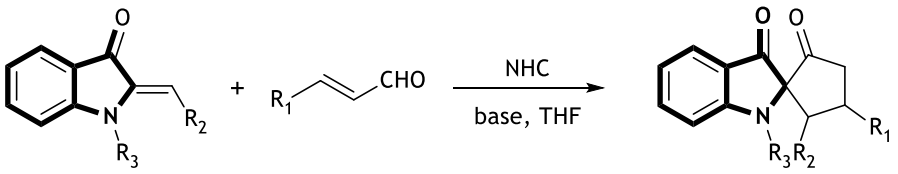

$R_{1,}$ R_2 and R_3 = Aryl or Alkyl group

Scheme 1.12 - Synthesis of C2-spiroindolin-3-one by [3+2] annulation of α,ß-unsaturated aldehydes with indolin-3-ones. Adapted from Guo *et al*.[61]

Kong *et al*. have reported a novel copper-catalyzed oxidative spirocyclization of indole-2-carboxamides using *tert*-butyl hydroperoxide (TBHP) as oxidant, giving access to C2-spiroindolin-3-one (scheme 1.13).[62]

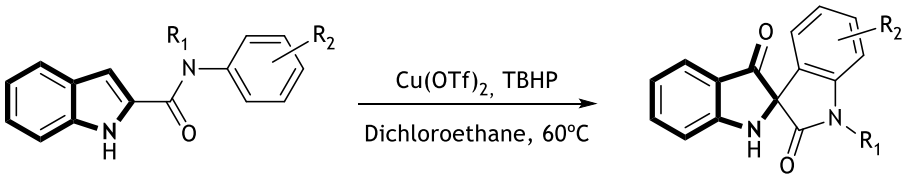

R_1 and R_2 = Aryl or Alkyl group

Scheme 1.13 - Synthesis of C2-spiroindolin-3-one by copper-catalysed oxidation of indole-2-carboxamides. Adapted from Kong *et al*.[62]

Zhang et al. described an efficient ring-contraction reaction of isochromeno[4,3-b]indol-5(11*H*)-ones via a nucleophile-induced spirocyclization cascade process in the absence of a transition-metal catalyst or oxidant (scheme 1.14).[63]

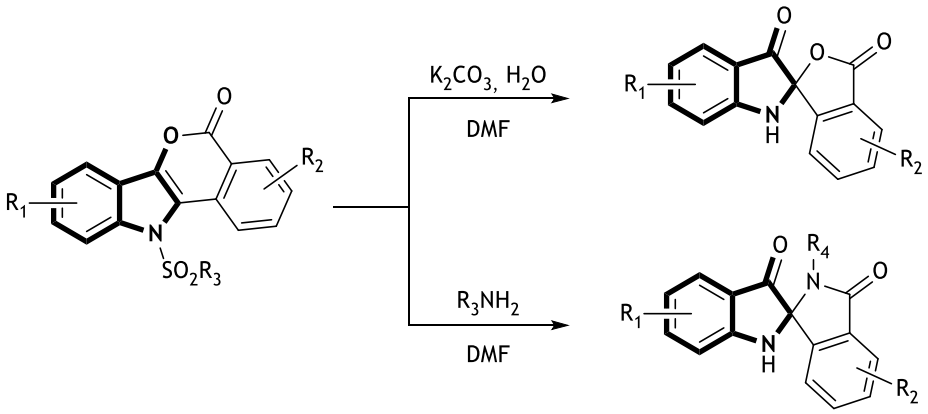

R_1, R_2, R_3, and R_4 = Aryl or Alkyl group

Scheme 1.14 - Synthesis of C2-spiroindolin-3-one by nucleophile-induced spirocyclization cascade process. Adapted from Zhang *et al.*[63]

Chen *et al.* developed new fluorescent dyes by treatment of 2,3,4,9-tetrahydro-1H-carbazole with iodomethane in the presence of potassium carbonated at 80°C which did not give the desired methylated compound, but instead of a novel C2-spiroindolin-3-one (scheme 1.15).[64]

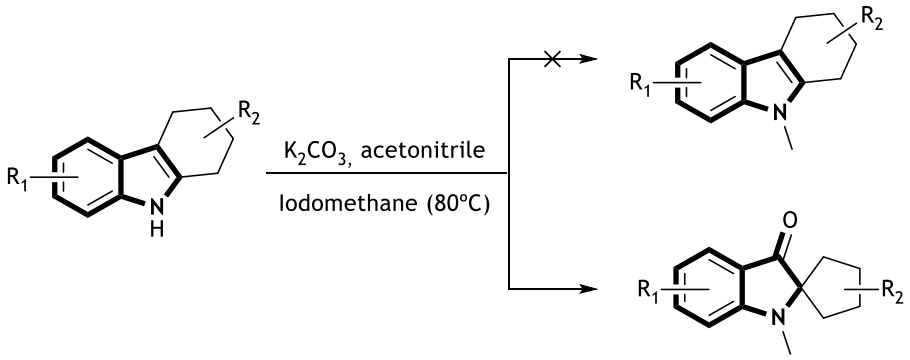

R_1 and R_2 = Aryl or Alkyl group

Scheme 1.15 - Synthesis of fluorescent dyes C2-spiroindolin-3-one. Adapted from Chen *et al.*[64]

1.4.1.2. Spiro formation without an indole scaffold in the starting material

Marien *et al.* produced novel C2-spiroindolin-3-one derivatives with a fully regioselective gold(III)-catalyzed cycloisomerization of o-nitrophenylpropiolamides, followed by an intramolecular dipolar cycloaddition (scheme 1.16).[65]

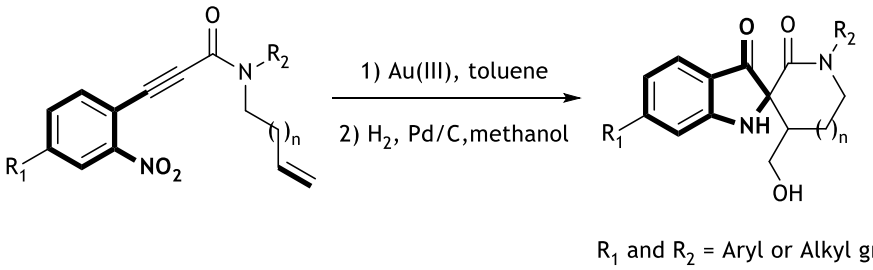

Scheme 1.16 – Synthesis of C2-spiroindolin-3-one by regioselective gold(III)-catalyzed cycloisomerization. Adapted from Marien *et al.*[65]

Later, Du and co-workers described a similar but metal-free reaction of phenylpropiolamides in C2-spiroindolin-3-one derivatives with phenyliodine(III) bis(trifluoroacetate) (PIFA) as the sole oxidant (scheme 1.17).[66]

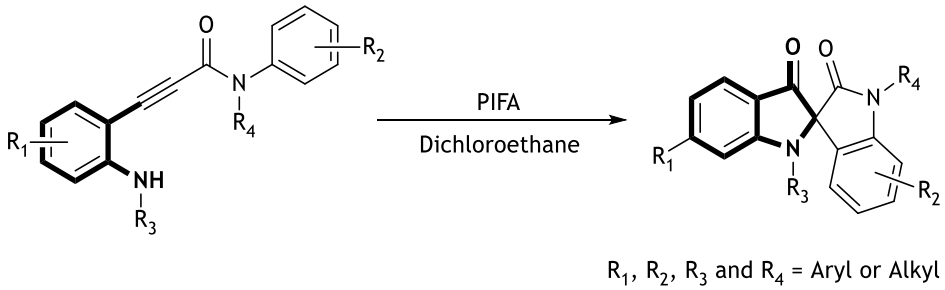

Scheme 1.17 - Synthesis of C2-spiroindolin-3-one by oxidation with phenyliodine(III) bis(trifluoroacetate). Adapted from Zhang *et al.*[66]

Other approach to obtain C2-spiroindolin-3-one was described by Mu et al. with a rhodium (III) catalyzed hydroacylation between 2-tolylsulfonyl-aminobenzaldehyde and *N*-methyl maleimide with silver carbonate in dichloroethane and an inert atmosphere of argon (scheme 1.18).[67]

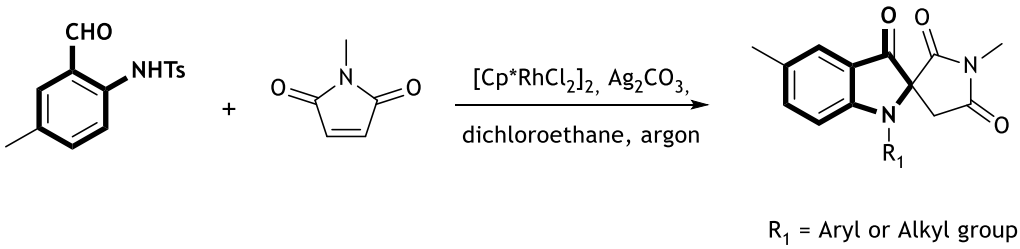

Scheme 1.18 - Synthesis of C2-spiroindolin-3-one by rhodium (III) catalyzed hydroacylation. Adapted from Mu *et al.*[67]

Finally, J. Serrano described the transformation of 2,1-benzisoxazole into spiroindolin-3-onethiobarbiturate in a reflux of dimethylformamide (DMF) (scheme 1.19).[68]

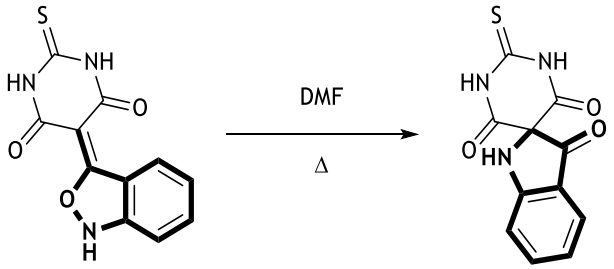

Scheme 1.19 - Synthesis of spiroindolin-3-onethiobarbiturate from 2,1-benzisoxazole. Adapted from J. Serrano.[68]

Nevertheless, and notwithstanding what was previously alleged, this transformation was not fully explained or extended for other examples of spiroindolin-3-one(thio)barbiturates. Therefore, it is of high interest their development and perception of possible biological activities.

Chapter 2 - Objectives

The objectives of this dissertation were:

- Optimization of reactional conditions in the synthesis of the spiroindolin-3-onethiobarbiturate transformation from 2,1-benzisoxazole.

- Preparation of new spiroindolin-3-one(thio)barbiturates using the optimized method, and spectroscopic characterization.

- Biological evaluation of the new spiroindolin-3-one(thio)barbiturates, namely determination of their potential for XO enzyme inhibition and cytotoxicity in Normal Human Dermal Fibroblasts (NHDF) and in a human breast adenocarcinoma (MCF-7, Michigan Cancer Foundation-7) cell line.

- Whenever necessary or suitable, to complement the biological activities, realize *in silico* studies.

Chapter 3 - Results and Discussion

3.1. Synthesis

In this topic the experimental results obtained in the preparation of new C2-spiroindolin-3-one, including their precursors, are here presented and discussed.

In a first instance will be shown the synthesis of 1,3-disubstituted(thio)urea and the obtention/attempts of obtention of their respective 1,3-disubstituted(thio)barbituric acids, the synthesis of the 5-(2-nitrobenzylidene)pyrimidines and their reduction into 5-(benzisoxazol-3-ylidene)pyrimidines.

In the second part will be presented the optimization methods for obtention of the C2-spiroindolin-3-one from the 5-(benzisoxazol-3-ylidene)pyrimidines. In this part, it will be also proposed a reactional mechanism for this transformation and the attempts of its validation.

Throughout the discussion will be presented comparative tables for the different results, comparing yields, melting points (mp), Fourier-Transform Infrared Spectroscopy (FTIR) spectra and ^{1}H and ^{13}C Nuclear Magnetic Resonance (NMR).

In ^{1}H-NMR tables will be presented the chemical shifts (δ, in part(s) per million (ppm)), the multiplicity of the signals (singlet (s), doublet (d), doublet of doublets (dd), doublet of doublet of doublets (ddd), doublet of triplets (dt), triplet (t), triplet of duplets (td), heptet (hept) or multiplet (m)), coupling constant (*J*, in Hz), relative intensity (nH as a number of protons) and assignment of the proton in the molecule, if possible. In ^{13}C-NMR tables will be presented chemical shifts (δ, in ppm), and the assignment of the carbon in the molecule. Characteristic and/or unidentified shifts are shown as "other signals" for each compound and, for a better distinction between protons or carbon atoms, the aromatic ones are represented as “ArCH” or “ArC”, respectively. This assignment was in some cases unequivocally established with the support of the Distortionless Enhancement by Polarization Transfer (DEPT), Heteronuclear Single Bond Correlation (HSQC) and Heteronuclear Multiple Bond Correlation (HMBC) spectra.

Additionally, and for a quick understanding of the molecular structure of some compounds mentioned during the discussion, is available a “book marker” with the most important structures.

3.1.1. Synthesis of 1,3-disubstituted(thio)ureas

1,3-Disubstitutedthioureas **3a-o** were obtained from the reaction between phenylisothiocyanate **1** and the amines **2a-o** in dichloromethane (DCM), as described by Lu *et al.*[69] (scheme 3.1). This method showed to be a fast procedure, with an easy isolation, since the product precipitates throughout the reaction, with a high purity and yields (table 3.1).

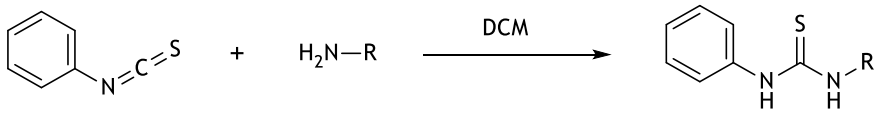

1 **2a**, R = Ph **3a**, R = Ph
b, R = H **b**, R = H
c, R = CH_3 **c**, R = CH_3
d, R = C_6H_{13} **d**, R = C_6H_{13}
e, R = Tz **e**, R = Tz
f, R = 3-Pyr **f**, R = 3-Pyr
g, R = 2-ClC_6H_4 **g**, R = 2-ClC_6H_4
h, R = 3-ClC_6H_4 **h**, R = 3-ClC_6H_4
i, R = 4-ClC_6H_4 **i**, R = 4-ClC_6H_4
j, R = 4-FC_6H_4 **j**, R = 4-FC_6H_4
k, R = 4-IC_6H_4 **k**, R = 4-IC_6H_4
l, R = 2-$(SCH_3)C_6H_4$ **l**, R = 2-$(SCH_3)C_6H_4$
m, R = 2-$(SC_6H_5)C_6H_4$ **m**, R = 2-$(SC_6H_5)C_6H_4$
n, R = 2-(*i*-Pr)C_6H_4 **n**, R = 2-(*i*-Pr)C_6H_4
o, R = 2-(*t*-Bu)C_6H_4 **o**, R = 2-(*t*-Bu)C_6H_4

Scheme 3.1 – Synthesis of 1,3-disubstitutedthioureas **3a-o.**

The 1,3-diphenylurea **3p** was obtained by the method described by Padiya *et al.*[70], where one equivalent of carbonyldiimidazole **4** reacted with two equivalents of aniline **2a** in water (scheme 3.2). In this case, the method was equally advantageous as the one described by Lu *et al.*, where **3p** was obtained pure and in a high yield (85%, table 3.1).

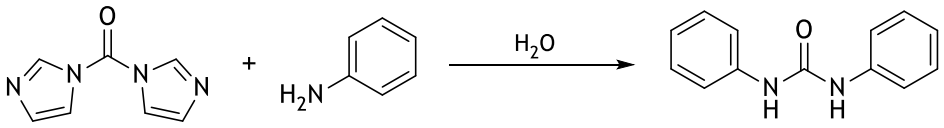

4 **2a** **3p**

Scheme 3.2 - Synthesis of 1,3-diphenylurea **3p**.

With the synthesis of the 1,3-disubstituted(thio)ureas **3a-p**, the 1,3-disubstitutedthioureas **3l** and **3m** have never been described.

In general, the melting points for the synthetized 1,3-disubstituted(thio)ureas **3a-p** were close to the literature, with the exception of **3p** which showed a difference of almost 10ºC, but its narrow melting range indicate a high degree of purity. In the cases of the 1,3-disubstitutedthioureas **3l** and **3m**, their melting points aren't described in the literature but, just like **3p**, their small melting range suggest a high degree of purity.

The FTIR spectra for the 1,3-disubstituted(thio)ureas **3a-p** showed the expected bands (Table 3.1) and it is worth noting the presence of the characteristic band for the vibrations of the N-H bond at 3500-3070 cm^{-1}, and the C=C bond at 1600-1500 cm^{-1}, characteristic of the aromatic

rings. In the case of the 1,3-diphenylurea **3p,** at 1645 cm^{-1}, it is present the band characteristic of the carbonyl of this compound.

Table 3.1 - FTIR spectra, melting points and yield for the synthetized 1,3-diphenylthiourea **3a-p.**

Compound	FTIR (characteristic bands)	Melting point (°C)		Yield (%)
		Obtained	Described	
3a	3202 (N-H)	142-144	140-142[71]	95
3b	3419 (N-H)	150-151	150-154[72]	84
3c	3257 (N-H)	117-118	115-117[73]	95
3d	3241 (N-H)	79-80	75-77[74]	87
3e	3152 (N-H)	142-144	140-142[75]	83
3f	3138 (N-H)	195-196	198[76]	89
3g	3303 (N-H)	178-179	181[77]	82
3h	3178 (N-H)	100-101	104[78]	97
3i	3201 (N-H)	156-157	150[78]	97
3j	3207 (N-H)	171-172	173-174[78]	90
3k	3200 (N-H)	169-170	170[79]	90
3l	3276 (N-H)	166-167	a)	98
3m	3276 (N-H)	150-151	a)	91
3n	3367 (N-H)	146-147	141-142[80]	71
3o	3338 (N-H)	175-176	172-173[80]	84
3p	3324 (N-H) and 1645 (C=O)	239-240	250-255[81]	85

a) not described in the literature.

The ^{1}H-NMR spectra (table 3.2) show the formation of the 1,3-disubstituted(thio)ureas **3a-p.** In the cases of the 1,3-diphenyl(thio)ureas **3a** and **3p** the chemical shifts confirm the symmetry observed in these compounds. A single singlet characterizes both protons of the amines, where the following duplet and two triplets, between 7.50 and 7.10 ppm, characterize the aromatic protons. In the 1,3-disubstitutedthioureas **3b-o** the ^{1}H-NMR spectra evidence their asymmetry in relation of the central thiocarbonyl, independently of the aromatic or aliphatic nature of substituent, since the protons of the amines are different. It is worth noticing that the further

is the location of a bulky group at the aromatic ring **(3h-k)** smaller is the difference between the two amine protons since only one singlet characterize both in each case. In the case of the 1,3-substitutedlthioureas **3c, 3d, 3l**, **3n** and **3o**, it is evident the presence of the aliphatic substituents: 1,3-substitutedlthiourea **3c** and **3l,** at 3.07 and 2.43 ppm, respectively, a single singlet characterizes the three protons of the methyl groups; 1,3-substitutedlthiourea **3d**, four different shifts characterizes the thirteen protons of the alkyl chain; 1,3-substitutedlthiourea **3n** the heptet at 3.15 ppm, integrated for one proton, and the duplet at 1.19 ppm, integrated for six protons, characterizes the *iso*-propyl group; and 1,3-substitutedlthiourea **3o,** the singlet at 1.37 ppm, integrated for nine protons, characterizes the *tert*-butyl group.

3.1.2. Synthesis of 1,3-disubstituted(thio)barbituric acids

The synthesis of 1,3-disubstituted(thio)barbituric acids was attempt by the reaction between the 1,3-disubstituted(thio)ureas **3a-p** and malonic acid. Initially, the reactions were carried out by the method described by Schulte *et al.*[82] (scheme 3.3) where the (thio)ureas were heated at 60ºC with malonic acid in acetyl chloride for 30 minutes.

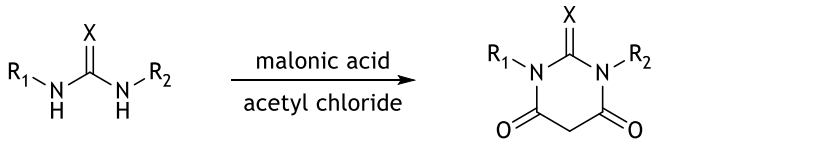

3a, X = S; $R_1 = R_2$ = Ph;
b, X = S; R_1 = Ph; R_2 = H;
c, X = S; R_1 = Ph; $R_2 = CH_3$;
d, X = S; R_1 = Ph; $R_2 = C_6H_{13}$;
e, X = S; R_1 = Ph; R_2 = Tz;
f, X = S; R_1 = Ph; R_2 = 3-Pyr;
g, X = S; R_1 = Ph; $R_2 = 2\text{-}ClC_6H_4$;
h, X = S; R_1 = Ph; $R_2 = 3\text{-}ClC_6H_4$;
i, X = S; R_1 = Ph; $R_2 = 4\text{-}ClC_6H_4$;
j, X = S; R_1 = Ph; $R_2 = 4\text{-}FC_6H_4$;
k, X = S; R_1 = Ph; $R_2 = 4\text{-}IC_6H_4$;
l, X = S; R_1 = Ph; $R_2 = 2\text{-}(SCH_3)C_6H_4$;
m, X = S; R_1 = Ph; $R_2 = 2\text{-}(SC_6H_5)C_6H_4$;
n, X = S; R_1 = Ph; $R_2 = 2\text{-}(i\text{-}Pr)C_6H_4$;
o, X = S; R_1 = Ph; $R_2 = 2\text{-}(t\text{-}Bu)C_6H_4$;
p, X = O; $R_1 = R_2$ = Ph.

5a, X = S; $R_1 = R_2$ = Ph;
b, X = O; $R_1 = R_2$ = Ph;
c, X = S; R_1 = Ph; $R_2 = 4\text{-}ClC_6H_4$;
d, X = S; R_1 = Ph; $R_2 = 4\text{-}FC_6H_4$;
e, X = S; R_1 = Ph; $R_2 = 4\text{-}IC_6H_4$.

Scheme 3.3 – Synthesis of 1,3-disubstituted(thio)barbituric acids **5a-e**.

It was noticed that when R_2 was a nonaromatic chain **(3b-d)**, a thiazole **(3e)** or a pyridine **(3f)** ring, or when the benzene ring was substituted in position 2 or 3 **(3g, h, l-o)**, the reaction didn't occur. This may be due to a stereochemical impediment of bulky groups, or a possible difference in the reactivity of the secondary amines, since R_1 and R_2 are different. During the reaction, it was observed by thin layer chromatography (TLC), that the formation of more than one product not being possible their isolation or characterization.

Table 3.2 - ^{1}H-NMR of the synthetized 1,3-disubstituted(thio)ureas **3a-p.**

Compound	Chemical Shifts (ppm)		
	1- and 2-NH	**Aromatics protons (*J* in Hz)**	**Aliphatic protons (*J* in Hz)**
3a	9.79 (s, 2H, 2 x NH)	7.48 (d, *J* = 7.4 Hz, 4H, 2' and 6'-ArCH), 7.33 (t, *J* = 8.2 and 7.6 Hz, 4H, 3' and 5'-ArCH) and 7.12 (t, *J* = 7.4 Hz, 2H, 4'-ArCH)	a)
3b	9.38 (s, 1H, NH) and 7.46 (s, 2H, 2 x NH)	7.37 – 7.20 (m, 4H, 2'- 3'- 5'- and 6'-ArCH) and 7.10 (t, *J* = 7.3 Hz, 1H, 4'-ArCH)	a)
3c	7.90 (s, 1H, NH) and 6.02 (s, 1H, NH)	7.37 (t, *J* = 7.7 Hz, 2H, 3' and 5'-ArCH), 7.25 (t, *J* = 7.5 Hz, 1H, 4'-ArCH) and 7.15 (d, *J* = 6.7 Hz, 2H, 2'- 6'-ArCH)	3.07 (s, 3H, 1-NCH_3)
3d	7.85 (s, 1H, NH) and 6.07 (s, 1H, NH)	7.44 (t, *J* = 7.8 Hz, 2H, 3''- and 5''-ArCH), 7.31 (t, *J* = 7.5 Hz, 1H, 4''-ArCH) and 7.20 (d, *J* = 7.5 Hz, 2H, 2''-ArCH)	3.61 (t, *J* = 7.3 Hz, 2H, 1'-CH_2), 1.56 (m, 2H, 2'-CH_2), 1.36 – 1.17 (m, 6H, 3'-, 4'- and 5'-CH_2) and 0.87 (d, *J* = 6.8 Hz, 3H, CH_3)
3e	12.44 (s, 1H, NH) and 10.44 (s, 1H, NH)	7.70 (d, *J* = 7.9 Hz, 2H, 2'- and 6'-ArCH), 7.45 (d, *J* = 4.2 Hz, 1H, CH), 7.31 (t, *J* = 7.9 Hz, 2H, 3'- and 5'-ArCH), 7.08 (t, *J* = 7.4 Hz, 1H, 4'-ArCH) and 7.00 (d, *J* = 4.2 Hz, 1H, ArCH)	a)
3f	10.02 (s, 1H, NH) and 9.87 (s, 1H, NH)	8.60 (d, *J* = 2.5 Hz, 1H), 8.32 (dd, *J* = 4.7 and 1.5 Hz, 1H), 7.94 (ddd, *J* = 8.2, 2.6 and 1.5 Hz, 1H), 7.48 (dd, *J* = 7.4 and 1.3 Hz, 2H), 7.39 – 7.32 (m, 4H) and 7.15 (t, *J* = 7.3 Hz, 1H)	a)
3g	10.01 (s, 1H, NH) and 9.44 (s, 1H, NH)	7.62 (dd, *J* = 6.4 and 1.6 Hz, 1H, ArCH), 7.56 – 7.49 (m, 3H, ArCH), 7.39 – 7.32 (m, 3H, ArCH), 7.26 (td, *J* = 7.7 and 1.7 Hz, 1H, ArCH) and 7.16 (t, *J* = 7.4 Hz, 1H, ArCH)	a)
3h	9.94 (s, 2H, 2 x NH)	7.71 (t, *J* = 2.0 Hz, 1H, ArCH), 7.47 (dd, *J* = 7.4 and 1.1 Hz, 2H, ArCH), 7.43 - 7.31 (m, 4H, ArCH) and 7.21 – 7.12 (m, 2H, ArCH)	a)
3i	9.88 (s, 2H, 2 x NH)	7.52 (dt, *J* = 4.6 and 3.1 Hz, 2H, ArCH), 7.47 (dd, *J* = 7.3 and 1.2 Hz, 2H, ArCH), 7.39 (dt, *J* = 4.6, 2.9 and 2.1 Hz, 2H, ArCH), 7.34 (t, *J* = 8.4 and 7.5 Hz, 2H, ArCH) and 7.14 (t, *J* = 7.4 Hz, 1H, 4''-ArCH)	a)
3j	9.78 (s, 2H, 2 x NH)	7.50 – 7.44 (m, 4H, ArCH), 7.34 (t, *J* = 8.3 Hz, 2H, ArCH) and 7.22 – 7.10 (m, 3H, ArCH)	a)
3k	9.87 (s, 2H, 2 x NH)	7.67 (d, *J* = 8.8 Hz, 2H, ArCH), 7.47 (dd, *J* = 7.3 and 1.2 Hz, 2H, ArCH) and 7.38 – 7.31 (m, 4H, ArCH), 7.15 (t, *J* = 7.3 Hz, 1H, 4''-ArCH)	a)
3l	9.85 (s, 1H, NH) and 9.20 (s, 1H, NH)	7.53 (dd, *J* = 7.6 and 1.1 Hz, 2H, ArCH), 7.39 (dd, *J* = 7.8 and 1.5 Hz, 1H, ArCH), 7.33 (t, *J* = 8.2 Hz, 3H, ArCH), 7.26 (td, *J* = 7.6 and 1.5 Hz, 1H, ArCH), 7.18 (dd, *J* = 7.6 and 1.5 Hz, 1H, ArCH) and 7.13 (t, *J* = 7.4 Hz, 1H, ArCH)	2.43 (s, 3H, SCH_3)
3m	10.02 (s, 1H, NH) and 9.40 (s, 1H, NH)	7.66 (dd, *J* = 8.0 and 1.4 Hz, 1H, ArCH), 7.47 (dd, *J* = 7.5 and 1.2 Hz, 2H, ArCH), 7.38 – 7.18 (m, 10H, ArCH) and 7.14 (t, *J* = 7.4 Hz, 1H, ArCH)	a)
3n	9.60 (s, 1H, NH) and 9.34 (s, 1H, NH)	7.50 (d, *J* = 7.7 Hz, 2H, ArCH), 7.37 – 7.24 (m, 4H, ArCH) and 7.23 – 7.17 (m, 2H, ArCH), 7.13 (t, *J* = 7.3 Hz, 1H, ArCH)	3.15 (hept, *J* = 6.9 Hz, 1H, 2'-CCH(CH_3)$_2$) and 1.19 (d, *J* = 6.9 Hz, 6H, 2'-CCH(CH_3)$_2$)
3o	9.54 (s, 1H, NH) and 9.10 (s, 1H, NH)	7.54 (d, *J* = 7.6 Hz, 2H, ArCH), 7.43 (dd, *J* = 4.9 and 2.7 Hz, 2H, ArCH), 7.33 (t, *J* = 8.2 Hz, 2H, ArCH), 7.29 – 7.21 (m, 2H, ArCH), 7.19 (dd, *J* = 3.1 and 1.8 Hz, 1H, ArCH), 7.13 (t, *J* = 7.5 Hz, 1H, ArCH)	1.37 (s, 9H, 2'-C(CH_3)$_3$)
3p	8.14 (s, 2H, 2 x NH)	7.36 (d, *J* = 8.3 Hz, 4H, 2' and 6'-ArCH), 7.18 (t, *J* = 7.9 Hz, 4H, 3' and 5'-ArCH), 6.90 (t, *J* = 7.8 Hz, 2H, 4'-ArCH)	a)

a) not applied.

Since it wasn't possible to obtain the respective 1,3-disubstituted(thio)barbituric acids from the 1,3-disubstitutedthioureas **3b-h** and **3l-o** by the method of Schulte *et al.*, the condensation was attempted by the method of Whiteley *et al.*[83] (scheme 3.4), where the reactions were realized in the presence of phosphoryl chloride, in chloroform. In this case it was only possible to obtain the 1,3-dimethylthiobarbituric acid **5f** from 1,3-dimethylthiourea **3q** after recrystallization with ethanol.

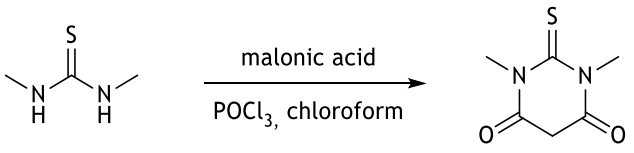

3q **5f**

Scheme 3.4 - Synthesis of 1,3-dimethylthiobarbituric acid **5f**.

The 1,3-disubstituted(thio)barbituric acids **5a-f,** where **5c-f** have never been described, were obtained pure and in good yields after recrystallization with ethanol (table 3.3).

Table 3.3 - FTIR spectra, melting points and yield for the synthetized 1,3-disubstituted(thio)barbituric acids **5a-f**.

Compound	FTIR (characteristic bands in ppm)	Melting point (ºC)		Yield (%)
		Obtained	Described	
5a	1727 and 1707 (C=O)	252-253	258-259[84]	95
5b	1683 (C=O)	241-242	222-223[85]	65
5c	1722 and 1701 (C=O)	259-260	a)	78
5d	1723 and 1700 (C=O)	238-239	a)	71
5e	1726 and 1697 (C=O)	230-231	a)	71
5f	1704 and 1672 (C=O)	193-194	a)	70

a) not described in the literature.

The melting point for the synthetized 1,3-disubstitutedthiobarbituric acid **5a** was close to what was described in the literature, where the melting point of **5b** showed a difference of almost 20ºC, but its narrow melting range indicate a high degree of purity. In the cases of the 1,3-disubstitutedthiobarbituric acids **5c-f**, their melting points aren't described in the literature but, just like **5b**, their small melting range suggest a high degree of purity.

The FTIR spectra for these 1,3-disubstituted(thio)barbituric acids **5a-f** showed the expected bands (Table 3.3). It is worth noting the disappearance of band representing the vibrations of the N-H bond at 3500-3100 cm^{-1} of the (thio)urea precursors, and, in the cases of **5a**, **c-f**, the appearance of band representing the vibrations of the C=O bond at approximately 1700 cm^{-1}.

The ^{1}H-NMR spectra (table 3.4) show the formation of the 1,3-disubstituted(thio)barbituric acids **5a-f.** The chemical shifts confirm the symmetry of **5a, 5b** and **5f,** and the asymmetry of compounds **5c-e.** It is worth noticing that the protons 5-C$\underline{H}_2$ of compounds **5a-e** demonstrate a similar singlet, all with chemical shifts between 4.13-4.04 ppm, and, even though compounds **5c-e** presents asymmetry, both protons of these compounds are characterized by the same signal. In the case of 1,3-dimethylthiobarbituric acid **5f**, the chemical shift of 5-C$\underline{H}_2$ is not in the same region as the others barbituric acids, but deviated to 3.77 ppm, this may be due to the inexistence of aromatic rings bonded to the positions N1 and N3.

Table 3.4 - ^{1}H-NMR of the synthetized 1,3-disubstituted(thio)barbituric acids **5a-f**.

Compound	Chemical Shifts (ppm)	
	5-C$\underline{H}_2$ (*J* in Hz)	Other Signals (*J* in Hz)
5a	4.10 (s, 2H, 5-C$\underline{H}_2$)	7.55 (m, 6H, ArC$\underline{H}$) and 7.21 (d, *J* = 7.3 Hz, 4H, 2' and 6' ArC$\underline{H}$)
5b	4.04 (s, 2H, 5-C$\underline{H}_2$)	7.48 (m, 6H, ArC$\underline{H}$) and 7.26 (d, *J* = 7.0 Hz, 4H, 2'- and 6'-ArC$\underline{H}$)
5c	4.11 (s, 2H, 5-C$\underline{H}_2$)	7.58 – 7.43 (m, 6H, ArC$\underline{H}$), 7.21 (d, *J* = 7.0 Hz, 2H, ArC$\underline{H}$), 7.15 (d, *J* = 8.6 Hz, 2H, ArC$\underline{H}$)
5d	4.13 (s, 2H, 5-C$\underline{H}_2$)	7.52 (d, *J* = 7.4 Hz, 2H, ArC$\underline{H}$), 7.33 – 7.13 (m, 7H, ArC$\underline{H}$)
5e	4.04 (s, 2H, 5-C$\underline{H}_2$)	7.81 – 7.71 (m, 2H, ArC$\underline{H}$), 7.53 – 7.33 (m, 3H, ArC$\underline{H}$), 7.23-7.09 (m, 2H, ArC$\underline{H}$) and 6.97 - 6.87 (m, 2H, ArC$\underline{H}$)
5f	3.77 (s, 2H, 5-C$\underline{H}_2$)	3.67 (s, 6H, 1- and 3-NC$\underline{H}_3$)

3.1.3. Synthesis of 5-(2-nitrobenzylidene)pyrimidines

The 5-(2-nitrobenzylidene)pyrimidines **6a-i** were obtained by Knoevenagel condensation, between 2-nitrobenzaldehyde and the respective 1,3-disubstituted(thio)barbituric acids **5a-i**, where the **5a-f** were the ones previously synthetized and **5g-i** were commercially obtained (scheme 3.5), just as described by Serrano *et al.*[37] Since the products were precipitating along the reaction, their isolation was simple and easy, affording the 2-nitrobenzylidene **6a-i** in high yields (table 3.5).

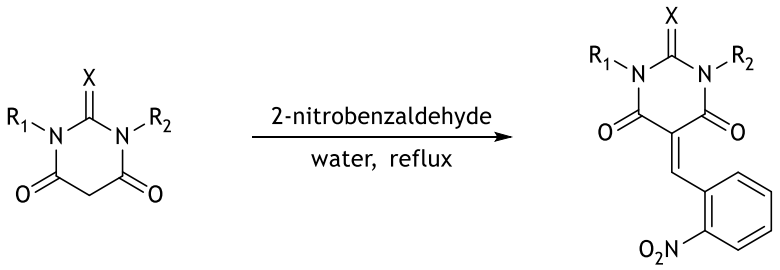

5a, X = S; $R_1 = R_2$ = Ph;
b, X = O; $R_1 = R_2$ = Ph;
c, X = S; R_1 = Ph; R_2 = 4-ClC_6H_4;
d, X = S; R_1 = Ph; R_2 = 4-FC_6H_4;
e, X = S; R_1 = Ph; R_2 = 4-IC_6H_4;
f, X = S; $R_1 = R_2 = CH_3$;
g, X = S; $R_1 = R_2$ = H;
h, X = O; $R_1 = R_2$ = H;
i, X = O; $R_1 = R_2 = CH_3$;

6a, X = S; $R_1 = R_2$ = H;
b, X = O; $R_1 = R_2$ = H;
c, X = S; $R_1 = R_2$ = Ph;
d, X = O; $R_1 = R_2 = CH_3$;
e, X = O; $R_1 = R_2$ = Ph;
f, X = S; $R_1 = R_2 = CH_3$;
g, X = S; R_1 = Ph; R_2 = 4-ClC_6H_4;
h, X = S; R_1 = Ph; R_2 = 4-FC_6H_4;
i, X = S; R_1 = Ph; R_2 = 4-IC_6H_4.

Scheme 3.5 - Synthesis of 5-(2-nitrobenzylidene)pyrimidines **6a-i**.

Table 3.5 - FTIR spectra, melting points and yield for the synthetized 5-(2-nitrobenzylidene)pyrimidines **6a-i**.

Compound	FTIR (characteristic bands in ppm)	Melting point (°C)		Yield (%)
		Obtained	Described	
6a	3255 (N-H), 1718 and 1692 (C=O), 1513 and 1351 (N-O).	239-241	246-250[86]	90
6b	3230 (N-H), 1739 and 1676 (C=O), 1516 and 1368 (N-O).	274-275	274-276[87]	97
6c	1717 and 1691 (C=O), 1520 and 1353 (N-O).	235-236	232-233[88]	90
6d	1663 (C=O), 1518 and 1377 (N-O).	158-159	159-161[88]	97
6e	1746 and 1681 (C=O), 1519 and 1355 (N-O).	239-240	a)	82
6f	1705 and 1678 (C=O), 1518 and 1342 (N-O).	161-162	a)	83
6g	1717 and 1690 (C=O), 1519 and 1393 (N-O).	238-239	a)	91
6h	1716 and 1690 (C=O), 1520 and 1394 (N-O).	249-250	a)	91
6i	1715 and 1688 (C=O), 1518 and 1392 (N-O).	193-194	a)	93

a) not described in the literature.

With the synthesis of the 5-(2-nitrobenzylidene)pyrimidines **6a-i**, the 5-(2-nitrobenzylidene) pyrimidines **6e-i** have never been described.

The melting points for the synthetized 5-(2-nitrobenzylidene)pyrimidines **6a-d** were close to what was described in the literature. In the cases of the 5-(2-nitrobenzylidene)pyrimidines **6e-i**, their melting points aren't described but their narrow melting range suggest a high degree of purity.

The FTIR spectra for these 5-(2-nitrobenzylidene)pyrimidines **6a-i** showed the expected bands (Table 3.5). All compounds presented a band at approximately at 1700 cm^{-1}, corresponding of a carbonyl group, and bands at 1600-1500 cm^{-1} for the C=C bonds, characteristic of the aromatic rings. It is also worth noting the appearance of a band representing the vibrations of the N-O bond at approximately 1500 and 1300 cm^{-1}.

The ^{1}H- and ^{13}C-NMR spectra (table 3.6 and 3.7) show all the expected signals of the synthetized 5-(2-nitrobenzylidene)pyrimidines **6a-i**. Overall, all 5-(2-nitroenzylidene)pyrimidines **6a-f** present a singlet between the shifts of 8.60 and 8.85 ppm characteristic of the proton of the methylene (5-CC<u>H</u>). The substituents in N1 and N3 were characterized by different signals, and the same goes to the carbonyls in positions 4 and 6, both have different chemical shifts in the ^{13}C-NMR. The chemical shifts of the benzylidenes overlap each other in the same region. In the cases of **6a** and **6b**, two singlets at 12.60-11.24 ppm, represent both protons of positions N1 and N3, of the barbiturate ring, where, at the aliphatic region of 3.70-3.00 ppm, two singlets represent the protons of the methyl groups of **6d** and **6f**. In **6c**, **6e**, **6g**, **6h** and **6i** the signals for the protons at positions C5', C4' and C6' were undefined, because of the overlapping signals of the phenyls groups. It should also be noted that the substituents of the pyrimidine ring have no influence on the spectroscopic signals. In the ^{13}C-NMR, the carbonyls at positions C4 and C6, the carbons of the methylene and position C5, and all the aromatic carbons in position C1', C2', C3', C4', C5' and C6', have similar chemical shifts between each 5-(2-nitrobenzylidene)pyrimidine. Additionally, some chemical shifts obtained for the 5-(2-nitrobenzylidene)pyrimidines **6g-i**, suggest that these compounds are found in a nearly equimolar a mixture of their *E* and *Z* diastereoisomers.

Table 3.6 - ^{1}H-NMR of the synthetized 5-(2-nitrobenzylidene)pyrimidines **6a-i**.

Compound	Chemical Shifts (ppm)					
	5-CC<u>H</u>	3'-ArC<u>H</u> (*J* in Hz)	5'-ArC<u>H</u> (*J* in Hz)	4'-ArC<u>H</u> (*J* in Hz)	6'-ArC<u>H</u> (*J* in Hz)	Other Signals (*J* in Hz)
6a	8.63 (s, 1H)	8.24 (dd, *J* = 8.3 and 1.0 Hz, 1H)	7.80 (td, *J* = 7.6 and 1.1 Hz, 1H)	7.72-7.66 (m, 1H)	7.62 (dt, *J* = 7.7 and 1.2 Hz, 1H)	12.56 (s, 1H, N<u>H</u>) and 12.33 (s, 1H, N<u>H</u>)
6b	8.60 (s, 1H)	8.23 (d, *J* = 7.9 Hz, 1H)	7.79 (t, *J* = 7.4 Hz, 1H)	7.68 (t, *J* = 7.7 Hz, 1H)	7.57 (d, *J* = 7.7 Hz, 1H)	11.49 (s, 1H, N<u>H</u>) and 11.24 (s, 1H, N<u>H</u>)
6c	8.80 (s, 1H)	8.19 (d, *J* = 8.2 Hz, 1H)	7.71 (t, *J* = 7.5 Hz, 1H)	a)	a)	7.59 (t, *J* = 7.9 Hz, 2H, ArC<u>H</u>), 7.45 (t, *J* = 7.6 Hz, 2H, ArC<u>H</u>), 7.40-7.28 (m, 6H, ArC<u>H</u>) and 7.20 (d, *J* = 7.7 Hz, 2H, ArC<u>H</u>)
6d	8.71 (s, 1H)	8.26 (dd, *J* = 8.3 and 1.2 Hz, 1H)	7.80 (td, *J* = 7.6 and 1.3 Hz, 1H)	7.69 (t, J = 7.7 Hz, 1H)	7.53 (d, *J* = 7.8 Hz, 1H)	3.25 (s, 3H, NC<u>H</u>$_3$) and 3.06 (s, 3H, NC<u>H</u>$_3$)
6e	8.82 (s, 1H)	8.25 (dd, *J* = 8.2 and 1.2 Hz, 1H)	7.82 (td, *J* = 7.6 and 1.2 Hz, 1H)	a)	a)	7.71-7.61 (m, 2H, ArC<u>H</u>), 7.57-7.50 (m, 2H, ArC<u>H</u>), 7.49-7.36 (m, 6H, ArC<u>H</u>) and 7.34-7.27 (m, 2H, ArC<u>H</u>)
6f	8.78 (s, 1H)	8.28 (d, *J* = 8.3 Hz, 1H)	7.83 (t, *J* = 7.5 Hz, 1H)	7.72 (t, *J* = 7.9 Hz, 1H)	7.60 (d, *J* = 7.7 Hz, 1H)	3,67 (s, 3H, NC<u>H</u>$_3$) and 3,48 (s, 3H, NC<u>H</u>$_3$)
6g	8.82 (s, 1H)	8.25 (d, *J* = 8.2 Hz, 1H)	a)	a)	a)	7.98 – 7.16 (m, 12H, ArC<u>H</u>)
6h	8.83 (s, 1H)	8.26 (d, *J* = 8.3 Hz, 1H)	a)	a)	a)	7.76 (t, J = 7.6 Hz, 4H) and 7.56 – 7.19 (m, 8H, ArCH)
6i	8.81 (s, 1H)	8.25 (d, J = 8.0 Hz, 1H)	a)	a)	a)	7.96 – 6.99 (m, 12H)

a) Undefined.

Table 3.7 - ^{13}C-NMR of the synthetized 5-(2-nitrobenzylidene)pyrimidines **6a-i**.

Compound	Chemical Shifts (ppm)									
	<u>C</u>O	5-C<u>C</u>H	2'-Ar<u>C</u>	5'-Ar<u>C</u>H	1'-Ar<u>C</u>	4'-Ar<u>C</u>H	6'-Ar<u>C</u>H	3'-Ar<u>C</u>H	5-<u>C</u>	Other Signals
6a	160.63 and 159.18	153.31	146.28	133.77	131.58	130.49	130.39	124.08	120.61	179.05 (2-<u>C</u>S)
6b	162.38 and 161.20	152.45	146.28	133.76	131.72	130.41	130.16	124.06	120.54	150.26 (2-<u>C</u>O)
6c	160.28 and 158.81	155.03	146.20	134.04	131.76	130.40	130.16	124.12	121.30	181.43 (2-<u>C</u>S), 140.02 (Ar<u>C</u>), 139.72 (Ar<u>C</u>), 129.05 (Ar<u>C</u>H), 128.88 (Ar<u>C</u>H),128.85 (Ar<u>C</u>H),128.83 (Ar<u>C</u>H),128.28 (Ar<u>C</u>H) and 128.10 (Ar<u>C</u>H)
6d	161.20 and 159.96	153.65	146.15	133.90	132.01	130.09	130.02	124.06	120.14	151.10 (2-<u>C</u>O), 28.44 (N-<u>C</u>H$_3$) and 27.82 (N-<u>C</u>H$_3$)
6e	161.86 and 160.63	154.56	146.67	134.49	132.36	130.69	130.54	124.58	121.45	151.05 (2-<u>C</u>O), 135.98 (Ar<u>C</u>), 135.62 (Ar<u>C</u>), 129.42 (Ar<u>C</u>H), 129.32 (Ar<u>C</u>H), 129.25 (Ar<u>C</u>H), 129.02 (Ar<u>C</u>H) and 128.86 (Ar<u>C</u>H)
6f	160.10 and 158.60	155.78	146.14	134.00	131.97	130.36	130.04	124.12	120.47	180.92 (2-<u>C</u>S), 35.54 (N-<u>C</u>H$_3$), 34.96 (N-<u>C</u>H$_3$)
6g	160.29 and 160.26 158.81 and 158.79	155.26	146.22	134.08	131.71 and 131.70	130.20	130.11	124.16	121.20 and 121.18	181.34 (2-<u>C</u>S), 139.92 and 139.62, 138.90 and 138.62, 132.90 and 132.76, 130.84 and 130.81, 130.50 and 130.48, 129.22, 129.12, 129.05, 128.95, 128.79, 128.36, and 128.19
6h	160.37 and 160.31 158.90 and 158.83	155.21	146.22	134.09	131.74	130.20	130.12	124.16	121.25 and 121.22	181.55 (2-<u>C</u>S), 140.02 and 139.71, 136.24 and 135.94, 134.28 and 134.21, 131.02 and 130.93, 130.48 and 130.46, 129.86, 129.11, 128.94, 128.81, 128.80, 128.34, and 128.17
6i	160.29 and 158.82	155.26	146.23	134.09	131.73 and 131.71	130.20	130.14	124.35	121.21	181.24 (2-<u>C</u>S), 139.93 and 139.89, 139.62 and 139.59, 138.08, 137.93, 134.30 and 134.23, 131.27 and 131.25, 130.52 and 130.50, 129.89, 129.14, 128.97, 128.82, 128.67, 128.39 and 128.22

3.1.4. Synthesis of 5-(benzisoxazol-3-ylidene)pyrimidines

Nine 5-(benzisoxazol-3-ylidene)pyrimidines **7a-1** were obtained by a partial reduction of the 5-(2-nitrobenzylidenes)barbiturates **6a-i** with tin(II) chloride dihydrate and concentrate hydrochloric acid (scheme 1.5). This method was adapted from Serrano *et al.*[37], where instead of using methanol as described, tetrahydrofuran (THF) was used as a solvent, giving the 5-(benzisoxazol-3-ylidene)pyrimidines **7a-i**, five of them **(7e-i)** were new, pure and in good yields (table 3.8).

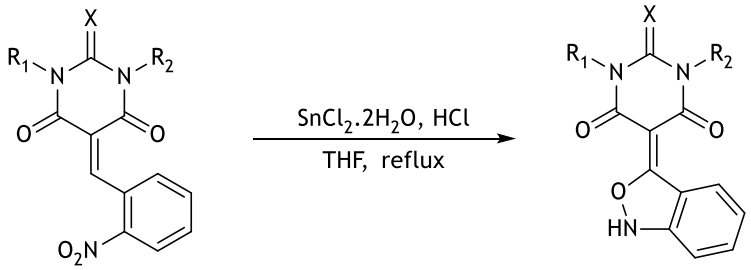

6a, X = S; $R_1 = R_2$ = H;
b, X = O; $R_1 = R_2$ = H;
c, X = S; $R_1 = R_2$ = Ph;
d, X = O; $R_1 = R_2 = CH_3$;
e, X = O; $R_1 = R_2$ = Ph;
f, X = S; $R_1 = R_2 = CH_3$;
g, X = S; R_1 = Ph; R_2 = 4-ClC_6H_4;
h, X = S; R_1 = Ph; R_2 = 4-FC_6H_4;
i, X = S; R_1 = Ph; R_2 = 4-IC_6H_4.

7a, X = S; $R_1 = R_2$ = H;
b, X = O; $R_1 = R_2$ = H;
c, X = S; $R_1 = R_2$ = Ph;
d, X = O; $R_1 = R_2 = CH_3$;
e, X = O; $R_1 = R_2$ = Ph;
f, X = S; $R_1 = R_2 = CH_3$;
g, X = S; R_1 = Ph; R_2 = 4-ClC_6H_4;
h, X = S; R_1 = Ph; R_2 = 4-FC_6H_4;
i, X = S; R_1 = Ph; R_2 = 4-IC_6H_4.

Scheme 3.6 - Synthesis of 5-(benzisoxazol-3-ylidene)pyrimidines **7a-i.**

The melting points for the synthetized 5-(benzisoxazol-3-ylidene)pyrimidines **7a-d** were according to what was described in the literature. In the cases of the 5-(benzisoxazol-3-ylidene)pyrimidines **7e-i**, their melting points aren't described but their small melting range suggest a high degree of purity.

The FTIR spectra for these 5-(benzisoxazol-3-ylidene)pyrimidines **7a-i** showed the expected bands (Table 3.8). All compounds presented a band nearly at 1700 cm^{-1}, corresponding of a carbonyl group, and bands at 1600-1500 cm^{-1} for the C=C bonds, characteristic of the aromatic rings. It is also worth noting the appearance of a band representing the vibrations of the N-H bond at approximately 3500-3100 cm^{-1}, for 5-(benzisoxazol-3-ylidene)pyrimidines **7c-i**.

Table 3.8 - FTIR spectra, melting points and yield for the synthetized 5-(benzisoxazol-3-ylidene) pyrimidines **7a-i.**

Compound	FTIR (characteristic bands in ppm)	Melting point (ºC)		Yield (%)
		Obtained	Described	
7a	3381 (N-H) and 1664 (C=O)	207-208	207-208[37]	87
7b	3174 (N-H), 1722 and 1666 (C=O)	267-268	266-268[37]	87
7c	3187 (N-H) and 1684 (C=O)	254-255	255-256[37]	73
7d	3195 (N-H), 1707 and 1644 (C=O)	212-213	211-213[37]	84
7e	3133 (N-H), 1719 and 1656 (C=O)	264-265	a)	70
7f	3142 (N-H), 1667 and 1606 (C=O)	218-219	a)	84
7g	3143 (N-H) and 1682 (C=O)	248-249	a)	67
7h	3145 (N-H) and 1682 (C=O)	249-250	a)	65
7i	3141 (N-H) and 1683 (C=O)	258-259	a)	60

a) not described in the literature.

The ^{1}H- and ^{13}C-NMR spectra (table 3.9 and 3.10) show all the expected signals of **7a-i**. Four signals, observed for **7a-b**, **7d** and **7f** in the range of 7.90-6.60 ppm indicated an ortho substituted benzene ring. Unlikely the 5-(2-nitrobenzylidene)pyrimidines **6a-f**, there are some chemical shifts of the 5-(benzisoxazol-3-ylidene)pyrimidines **7a-f** that appear as equivalents. In **7a** and **7b**, one singlet at 11.50-10.50 ppm, represent both protons of positions N1 and N3, of the barbiturate scaffold, where, at the aliphatic region of 3.70-3.00 ppm, one singlet represents the protons of the methyl groups of **7d** and **7f**. In **7c**, **7e**, **7g**, **7h** and **7i** the signals for the protons at positions C7', C6' and C4 were undefined, because of overlapping signals of the phenyl groups. In the ^{13}C-NMR, the signals at 178.80-174.50 and 152.30-150.80 ppm were attributed to carbons directly attached to a sulfur atom and an oxygen atom, respectively. Additionally, the signal at 128.44, 162.20 and 92.69 ppm, in **7g-i**, where attributed to the 4''-ArC, attached to an atom of chlorine, fluorine and iodine, respectively. It should also be noted that the substituents of the pyrimidine ring have no influence on the spectroscopic signals. The aromatic carbons in position C3', C3a', C4', C5', C6', C7', C7a', and the carbon at position C5, have similar chemical shifts between each 5-(benzisoxazol-3-ylidene)pyrimidines.

Table 3.9 - ^{1}H-NMR of the synthetized 5-(benzisoxazol-3-ylidene)pyrimidines **7a-i.**

Compound	Chemical Shifts (ppm)				
	4'-ArCH (*J* in Hz)	7'-ArCH (*J* in Hz)	6'-ArCH (*J* in Hz)	5'-ArCH (*J* in Hz)	Other signals (*J* in Hz)
7a	7.88 (d, *J* = 8.8 Hz, 1H)	7.34 (d, *J* = 9.0 Hz, 1H)	7.22 (dd, *J* = 9.0 and 6.3 Hz, 1H)	6.73 (dd, *J* = 8.8 and 6.3 Hz, 1H)	11.05 (s, 2H, 1- and 3-NH)
7b	7.77 (dt, *J* = 8.8 and 1.7 Hz, 1H)	7.46 (dt, *J* = 9.1 and 1.7 Hz, 1H)	7.32 (ddd, *J* = 9.1, 6.4, and 0.8 Hz, 1H)	6.89 (ddd, *J* = 8.8, 6.4, and 0.8 Hz, 1H)	10.69 (s, 2H, 1- and 3-NH)
7c	7.80 (d, *J* = 8.8 Hz, 1H)	7.35 (d, *J* = 8.9 Hz, 1H)	a)	6.71 (dd, *J* = 8.9 and 6.2 Hz, 1H)	7.40 (t, *J* = 7.7 Hz, 4H, 3''- and 5''-ArCH), 7.24-7.19 (m, 5H, 2''-, 6''- and 6'-ArCH), 7.29 (t, *J* = 7.4 Hz, 2H, 4''-ArCH)
7d	7.90 (dt, *J* = 8.8 and 1.1 Hz, 1H)	7.37 (dt, *J* = 8.9 and 1.0 Hz, 1H)	7.29 (ddd, *J* = 8.9, 6.2, and 1.1 Hz, 1H)	6.80 (ddd, *J* = 8.8, 6.3, and 0.9 Hz, 1H)	3.17 (s, 6H, 1- and 3-NCH_3)
7e	7.83 (d, *J* = 8.8 Hz, 1H)	a)	7.21 (dd, *J* = 8.9 and 6.3 Hz, 1H)	6.70 (dd, *J* = 8.8 and 6.2 Hz, 1H)	7.42 (dd, *J* = 8.3 and 6.9 Hz, 4H, 3''- and 5''-ArCH), 7.36-7.26 (m, 7H, 7'-, 2''-, 4''- and 6''-ArCH)
7f	7.77 (dt, *J* = 8.8 and 1.1 Hz, 1H)	7.38 (dt, *J* = 9.0 and 1.0 Hz, 1H)	7.24 (ddd, *J* = 9.0, 6.3 and 1.1 Hz, 1H)	6.77 (ddd, *J* = 8.8, 6.3 and 0.9 Hz, 1H)	3.62 (s, 6H, 1- and 3-NCH_3)
7g	7.78 (dt, *J* = 8.8 and 1.1 Hz, 1H)	a)	a)	6.71 (dd, *J* = 8.9 and 6.2 Hz, 1H)	7.48 – 7.36 (m, 4H), 7.34 (d, *J* = 9.0 Hz, 1H, 7'-ArCH), 7.32 – 7.24 (m, 3H) and 7.24 – 7.17 (m, 3H)
7h	7.78 (d, *J* = 8.8 Hz, 1H)	a)	a)	6.71 (dd, *J* = 8.9 and 6.3 Hz, 1H)	7.39 (t, *J* = 7.6 Hz, 2H) and 7.37 – 7.15 (m, 9H)
7i	a)	a)	a)	6.71 (t, *J* = 7.5 Hz, 1H)	7.75 (t, *J* = 9.4 Hz, 3H), 7.39 (t, *J* = 7.5 Hz, 2H), 7.32 (dd, *J* = 15.8, 8.1 Hz, 2H), 7.21 (d, *J* = 7.5 Hz, 3H) and 7.05 (d, *J* = 8.0 Hz, 2H)

a) Undefined.

Table 3.10 - ^{13}C-NMR of the synthetized 5-(benzisoxazol-3-ylidene)pyrimidines **7a-i.**

Compound	Chemical Shifts (ppm)								
	3'-C	4 and 6-CO	7a'-ArC	6'-ArCH	4'-ArCH	5'-ArCH	3a'-C	7'-ArCH	5-C	Other Signals
7a	166.10	161.02	156.35	130.32	125.43	119.34	114.25	113.16	85.07	174.5 (2-CS)
7b	163.68	162.71	156.40	131.82	124.15	122.01	116.21	113.76	82.71	150.8 (2-CO)
7c	166.33	159.62	156.11	130.28	125.32	119.39	114.39	113.13	85.45	178.6 (2-CS), 141.8 (1''-ArC), 129.6 (2''- and 6''-ArCH), 128.4 (3''- and 5''-ArCH) and 126.9 (4''-ArCH)
7d	167.45	160.91	155.93	131.15	125.51	120.01	114.92	112.92	82.54	152.3 (2-CO) and 27.7 (1 and 3-NCH_3)
7e	167.79	161.23	156.52	130.81	126.01	119.43	114.49	113.30	85.33	152.17 (2-CO), 137.84 (1''-ArC), 130.13 (2''- and 6''-ArCH), 128.79 (3''- and 5''-ArCH), 127.60 (4''-ArCH)
7f	166.53	159.21	156.19	130.42	125.06	119.77	114.78	113.32	84.69	177.12 (2-CS) and 34.86 (1- and 3-NCH_3)
7g	166.09	159.55 and 159.43	156.14	130.27	125.29	119.36	114.30	113.14	85.33	178.45 (2-CS), 141.73 (ArC), 140.78 (ArC), 131.56 (ArCH), 131.50 (ArCH), 129.53 (ArCH), 128.49 (ArCH), 128.44 (4''-ArC) and 127.00 (ArCH)
7h	166.26	159.79 and 159.63	156.10	130.43	125.38	119.48	114.39	113.11	85.49	178.76 (2-CS), 162.20 (4''-ArC), 141.84 (ArC), 138.07 (ArC), 131.58 (ArCH), 131.50 (ArCH), 129.56 (ArCH), 128.49 (ArCH), 127.03 (ArCH), 115.36 (ArCH) and 115.14 (ArCH)
7i	166.05	159.52 and 159.35	156.14	130.22	125.27	119.31	114.27	113.14	85.28	178.30 (2-CS), 141.76 (ArC), 141.71 (ArC), 137.35 (ArCH), 132.11 (ArCH), 129.52 (ArCH), 128.42 (ArCH), 126.98 (ArCH) and 92.89 (4''-ArC)

3.1.5. Synthesis of spiroindolin-3-one(thio)barbiturates

As previously depicted, the principal objective of this work was the optimization of the transformation of the 5-(benzisoxazol-3-ylidene)pyrimidines into the spiroindolin-3-one(thio)barbiturates (scheme 3.7). Since the cleavage of the 2,1-benzisoxazoles is described as a merely thermal process[50], methods of heating in an oil bath or a muffle, photolysis and mw, varying the solvents and temperatures, were studied (table 3.11).

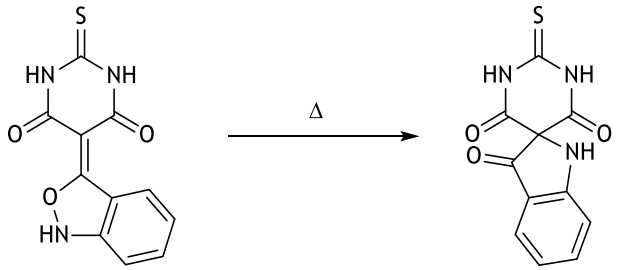

7a **8a**

Scheme 3.7 - Synthesis of the spiroindolin-3-one(thio)barbiturate **8a.**

Table 3.11 - Optimization of the synthesis of spiroindolin-3-onethiobarbiturate **8a**.

Entry	Method	Solvent	T(°C)	Time	Yield (%)
1	Heating	DMF	140	5 min	30
2		DMF	120	20 min	55
3		DMF	100	1 hour	70
4		DMSO	140	5 min	a)
5		NaOH (50%)	100	8 hours	b)
6	Melting	-	210	5 min	10
7		-	210	10 min	c)
8	Photolysis	DMF	50	1 day	40
9	Microwave	DMF	140	2 min	20
10		DMF	120	5 min	65
11		DMF	100	10 min	80
12		EtOAc	100	10 min	b)
13		NaOH (50%)	100	10 min	b)

a) Product formed by TLC but not isolated; b) No reaction was observed; c) Product/starting material decomposes.

Initially, a full product formation was verified by TLC within 5 minutes of reflux in DMF (table 3.11, entry 1). In this context, the isolation of the product proved to be a very difficult process, since the total removal of the DMF revealed to be a hard task. Thus, and given the low solubility of these 2,1-benzisoxazole(thio)barbiturate derivatives, other solvents capable of dissolving them were used (table 3.11, entries 4 and 5). In dimethyl sulfoxide (DMSO), **8a** was easily obtained, but the isolation was just as difficult as in DMF. In a solution of sodium hydroxide (NaOH) 50%, no reaction was observed. To resolve this situation, an early evaporation at reduced pressure of the DMF proved to be a key step in the isolation process, followed by an extraction with ethyl acetate (EtOAc). Therefore, the spiroindolin-3-onethiobarbiturate **8a** was obtained pure, in a yield of 30% (table 3.11, entry 1). This yield may due to the product and/or the starting material decompose with the high temperature, which was observed when the reaction time was prolonged at this temperature. Therefore, other temperatures were tried. At 120 and 100ºC, **8a** was obtained in higher yields however the reaction revealed to be slower, which was expected. The full consumption of the starting materials and formation of product was at 20 and 60 minutes of reaction, in yields of 55 and 70%, respectively (table 3.11, entries 2 and 3).

Additionally, other thermal processes like melting, photolysis and mw, were tried. In melting, **8a** was obtained in low yields of 10% or decomposes (table 3.11, entries 6 and 7), which was expected, since the product and/or the starting material would decay with high temperatures. The one of photolysis afforded **8a** with a no optimized yield of 40% (table 3.11, entry 8).

Finally, with mw irradiation other solvents where tried. Neither EtOAc or NaOH 50% gave good results of the expected product (table 3.11, entries 12 and 13). DMF still proved to be the best solvent, replicating what previously happened: at lower temperatures, the reaction revealed to be slower, but the product was obtained in higher yields. Therefore, the use of mw using DMF as solvent at 100°C optimized **8a** yield from 70 to 80%, reducing the reaction time from 60 to 10 minutes (table 3.11, entry 11).

Overall, mw irradiation was a better method to obtain the spiroindolin-3-onethiobarbiturate **8a**. This condition enabled an isolated system, providing a better control and homogenous distribution of the temperature, which eased the formation of the product with a shortened reaction time.

Using the same optimized procedure depicted above, spiroindolin-3-one(thio)barbiturates **8b-i** were synthetized from their respective 5-(benzisoxazol-3-ylidene)pyrimidines **7b-i** (scheme 3.8). **8b-i** were obtained by mw irradiation, pure and in high yields of 70 to 85% (table 3.12).

All the nine spiroindolin-3-one(thio)barbiturates **8a-i** prepared have not hitherto been described.

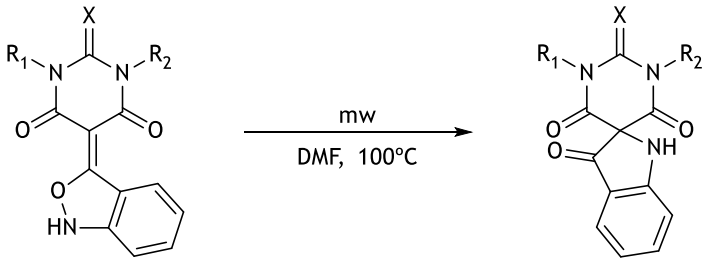

7a, X = S; $R_1 = R_2$ = H;
b, X = O; $R_1 = R_2$ = H;
c, X = S; $R_1 = R_2$ = Ph;
d, X = O; $R_1 = R_2 = CH_3$;
e, X = O; $R_1 = R_2$ = Ph;
f, X = S; $R_1 = R_2 = CH_3$;
g, X = S; R_1 = Ph; R_2 = 4-ClC_6H_4;
h, X = S; R_1 = Ph; R_2 = 4-FC_6H_4;
i, X = S; R_1 = Ph; R_2 = 4-IC_6H_4.

8a, X = S; $R_1 = R_2$ = H;
b, X = O; $R_1 = R_2$ = H;
c, X = S; $R_1 = R_2$ = Ph;
d, X = O; $R_1 = R_2 = CH_3$;
e, X = O; $R_1 = R_2$ = Ph;
f, X = S; $R_1 = R_2 = CH_3$;
g, X = S; R_1 = Ph; R_2 = 4-ClC_6H_4;
h, X = S; R_1 = Ph; R_2 = 4-FC_6H_4;
i, X = S; R_1 = Ph; R_2 = 4-IC_6H_4.

Scheme 3.8 - Synthesis of the spiroindolin-3-one(thio)barbiturate **8a-i.**

Table 3.12 - FTIR spectra, melting points and yield for the synthetized spiroindolin-3-one(thio)barbiturates **8a-i.**

Compound	FTIR (characteristic bands in ppm)	Melting point (°C)	Yield (%)
8a	3508 and 3355 (N-H) and 1700 (C=O)	219-220	85
8b	3391 (N-H), and 1762 and 1693 (C=O)	198-199	70
8c	3351 (N-H) and 1698 (C=O)	170-171	78
8d	3356 (N-H), and 1720 and 1669 (C=O)	222-223	75
8e	3398 (N-H), and 1688 and 1660 (C=O),	188-189	80
8f	3391 (N-H) and 1693 (C=O)	212-213	85
8g	3350 (N-H) and 1704 (C=O)	180-181	77
8h	3354 (N-H) and 1682 (C=O)	179-180	74
8i	3358 (N-H) and 1704 (C=O)	208-209	81

The melting points of the synthetized spiroindolin-3-one(thio)barbiturates **8b-i** presented a small melting range which suggest a high degree of purity for these compounds.

The FTIR spectra for these spiroindolin-3-one(thio)barbiturates **8b-i** showed the expected bands (Table 3.12). All compounds presented a band at nearly 1700 cm^{-1}, corresponding of a carbonyl group, and bands at 1600-1500 cm^{-1} for the C=C bonds, characteristic of the aromatic rings. Comparatively with the 5-(benzisoxazol-3-ylidene)pyrimidines **7a-i**, the band which correspond to the N-O bond at 1500 and 1300cm^{-1}, disappeared in some cases.

The ^{1}H- and ^{13}C-NMR spectra (table 3.13 and 3.14) show all the expected signals of the synthetized spiroindolin-3-one(thio)barbiturates **8a-i.** All spiroindolin-3-one(thio)barbiturates **8b-i**, presented a singlet at 8.10-7.40 ppm, characteristic of the new N-H formed. Just like the 5-(benzisoxazol-3-ylidene)pyrimidines **7a-i,** the four signals observed in the range of 7.70-6.75 ppm indicated an *ortho*-substituted benzene ring. In **8a-b**, **8d** and **8f**, some chemical shifts can be found, suggesting the symmetry of the pyrimidine: **8a** and **8b**, one singlet at 12.70-11.50 ppm, represent both protons of positions N1 and N3, of the barbiturate ring, where, at the aliphatic region of 3.60-3.15 ppm, one singlet represents the protons of the methyl groups of **8d** and **8f**. In the cases of **8c**, **8e**, **8g**, **8h** and **8i** the signals for the protons at positions C4 and C6 were undefined, because of overlapping signals of the phenyl groups. In the ^{13}C-NMR, the signals at 182.20-179.66 and 151.46-150.51 ppm were attributed to carbons directly attached to a sulfur atom and an oxygen atom, respectively. Within these, the signal at 164.02-161.84 ppm was associated to two carbonyls, also confirming the symmetry of **8a-f**. Additionally, the signal at 133.22, 160.43 and 95.04 ppm, in **8g-i**, where attributed to the 4''-Ar<u>C</u>, attached to an atom of chlorine, fluorine and iodine, respectively. It should also be noted that the substituents of the pyrimidine ring have no significant influence on the spectroscopic signals, where the chemical shifts of the benzylidenes overlap each other in the same region. The carbonyls of positions C3, C4' and C6', all the aromatic carbons in position C3', C3a', C4', C5', C6', C7', C7a', and the methylenic carbon at position C2,5, have similar chemical shifts between each spiroindolin-3-one(thio)barbiturates **8a-i**.

Taking in mind the possible formation of a nitrene intermediate, a possible mechanism for the formation of the spiroindolin-3-one(thio)barbiturates is herein proposed. As previously described by Coe *et al.*[50], when the 2,1-benzisoxazole ring is exposed to an increasing temperature, the O-N bound is cleaved to afford a highly electrophilic electron-rich nitrene intermediate. Following this ring disruption, the spirocyclization is ensued through an intermolecular nucleophilic attack by a barbiturate enolate in the nitrene triplet. The enough structural stability of the C2-spiroindolin-3-one so formed, allows the formation and isolation of the new spiroindolin-3-one(thio)barbiturates **8**.

Table 3.13 - ^{1}H-NMR of the synthetized spiroindolin-3-one(thio)barbiturates **8a-i.**

Compound	Chemical Shifts (ppm)				
	6-ArCH (*J* in Hz)	4-ArCH (*J* in Hz)	7-ArCH (*J* in Hz)	5-ArCH (*J* in Hz)	Other signals (*J* in Hz)
8a	7.57 (ddd, *J* = 8.4, 7.0 and 1.3 Hz, 1H)	7.42 (dt, *J* = 7.9 and 0.7 Hz, 1H)	7.17 (dt, *J* = 8.3 and 0.9 Hz, 1H)	6.81 (ddd, *J* =7.8, 7.0 and 0.9 Hz, 1H)	12.63 (s, 2H, 1'- and 3'-NH) and 7.47 (s, 1H, 1-NH)
8b	7.57 (ddd, *J* = 8.5, 7.2 and 1.4 Hz, 1H)	7.42 (d, *J* = 7.8 Hz, 1H)	7.16 (d, *J* = 8.3 Hz, 1H)	6.80 (t, *J* = 7.4 Hz, 1H)	11.62 (s, 2H, 1' and 3'-NH) and 7.50 (s, 1H, 1-NH)
8c	7.64 (ddd, *J* = 8.4, 7.0 and 1.4 Hz, 1H)	a)	7.22 (d, *J* = 8.3 Hz, 1H)	6.89 (t, *J* = 8.0 Hz, 1H)	8.04 (s, 1H, 1-NH), 7.58 – 7.38 (m, 7H, ArCH), 7.34 (dt, *J* = 8.0 and 1.6 Hz, 2H, ArCH), 7.06 (dt, *J* = 7.8 and 1.7 Hz, 2H, ArCH)
8d	7.60 (ddd, *J* = 8.4, 6.9 and 1.4 Hz, 1H)	7.41 (d, *J* = 7.8 Hz, 1H)	7.18 (d, *J* = 8.4 Hz, 1H)	6.82 (t, *J* = 7.4, 1H)	7.79 (s, 1H, 1-NH) and 3.19 (s, 6H, 1'- and 3'-NCH_3)
8e	7.64 (ddd, *J* = 8.3, 7.0 and 1.3 Hz, 1H)	a)	7.22 (d, *J* = 8.3 Hz, 1H)	6.89 (ddd, *J* = 7.8, 7.0 and 0.8 Hz, 1H)	8.06 (s, 1H, 1-NH), 7.59 – 7.42 (m, 7H, ArCH) and 7.26 (d, *J* = 7.5 Hz, 4H, ArCH)
8f	7.61 (t, *J* = 7.7 Hz, 1H)	7.41 (d, *J* = 7.9 Hz, 1H)	7.20 (d, *J* = 8.4 Hz, 1H)	6.83 (t, *J* = 7.4, 1H)	7.82 (s, 1H, 1-NH) and 3.59 (s, 6H, 1'- and 3'-NCH_3)
8g	a)	a)	7.21 (d, *J* = 8.3 Hz, 1H)	6.89 (t, *J* = 8.0 Hz, 1H)	8.09 (s, 1H, 1-NH), 7.77 – 7.28 (m, 8H) and 7.15 – 7.01 (m, 4H)
8h	7.63 (t, *J* = 7.8 Hz, 1H)	a)	7.21 (d, *J* = 8.3 Hz, 1H)	6.88 (t, *J* = 7.5 Hz, 1H)	8.07 (s, 1H, 1-NH), 7.58 – 7.25 (m, 8H) and 7.13 – 7.02 (m, 2H)
8i	7.63 (t, *J* = 7.8 Hz, 1H)	a)	7.21 (d, *J* = 8.3 Hz, 1H)	6.87 (t, *J* = 7.5 Hz, 1H)	8.09 (s, 1H, 1-NH), 7.86 (dd, *J* = 17.7, 8.4 Hz, 2H, 3''- and 5''-ArCH), 7.58 – 7.28 (m, 6H) and 7.10 – 6.98 (m, 2H)

a) Undefined.

Table 3.14 - ^{13}C-NMR of the synthetized spiroindolin-3-one(thio)barbiturates **7a-i.**

Compound	Chemical Shifts (ppm)									
	3-CO	7a-ArC	4'- and 3'-CO	6-ArCH	4-ArCH	5-ArCH	3a-ArC	7-ArCH	2,5'-C	Other Signals
8a	189.32	164.99	162.42	138.94	125.35	119.07	114.27	113.18	78.33	179.66 (2'-CS)
8b	189.63	165.10	164.02	138.91	125.34	119.00	114.45	113.14	78.05	150.51 (2'-CO)
8c	188.61	165.28	161.87	140.00	126.29	120.11	114.17	113.95	80.30	182.20 (2'-CS), 139.90 (1''-ArC), 129.89 (ArCH), 129.76 (ArCH), 129.48 (ArCH), 129.07 (ArCH) and 128.48 (ArCH)
8d	188.90	165.13	162.88	139.22	125.51	119.25	113.91	113.24	78.35	151.46 (2'-CO) and 29.11 (1'- and 3'-NCH3)
8e	188.57	165.10	162.58	139.58	125.87	119.65	113.87	113.52	79.48	150.92 (2'-CO), 135.05 (1''-ArC), 129.38 (ArCH), 128.98 (ArCH) and 128.49 (ArCH)
8f	188.24	164.92	161.84	139.37	125.62	119.38	113.67	113.30	79.12	181.48 (2'-CS) and 36.07 (1'- and 3'-NCH_3)
8g	188.00	164.84	161.35	139.58	125.85	119.70	113.66	113.52	79.86	181.60 (2'-CS), 139.33 (ArC), 138.24 (ArC), 133.22 (4''-ArC), 131.55 (ArCH), 130.96 (ArCH), 130.05 (ArCH), 129.52 (ArCH), 129.34 (ArCH), 128.98 (ArCH), 128.67 (ArCH), 128.46 (ArCH) and 127.95 (ArCH)
8h	188.05	164.84	161.38	139.57	125.85	119.67	113.68	113.52	79.86	181.82 (2'-CS), 160.43 (4''-ArC), 139.42, (ArC), 135.61 (ArC), 135, 58 (ArCH), 131.21 (ArCH), 131.12 (ArCH), 130.21 (ArCH), 129.46 (ArCH), 129.32 (ArCH), 128.99 (ArCH), 128.64 (ArCH) and 127.97 (ArCH)
8i	188.01	164.84	161.34	139.59	125.86	119.67	113.66	113.53	79.84	181.50 (2'-CS),), 139.27, (ArC), 138.38 (ArC), 132.12 (ArCH), 131.33 (ArCH), 130.38 (ArCH), 129.47 (ArCH), 129.34 (ArCH), 128.98 (ArCH), 128.67 (ArCH), 128.42 (ArCH), 127.96 (ArCH) and 95.04 (4''-ArC)

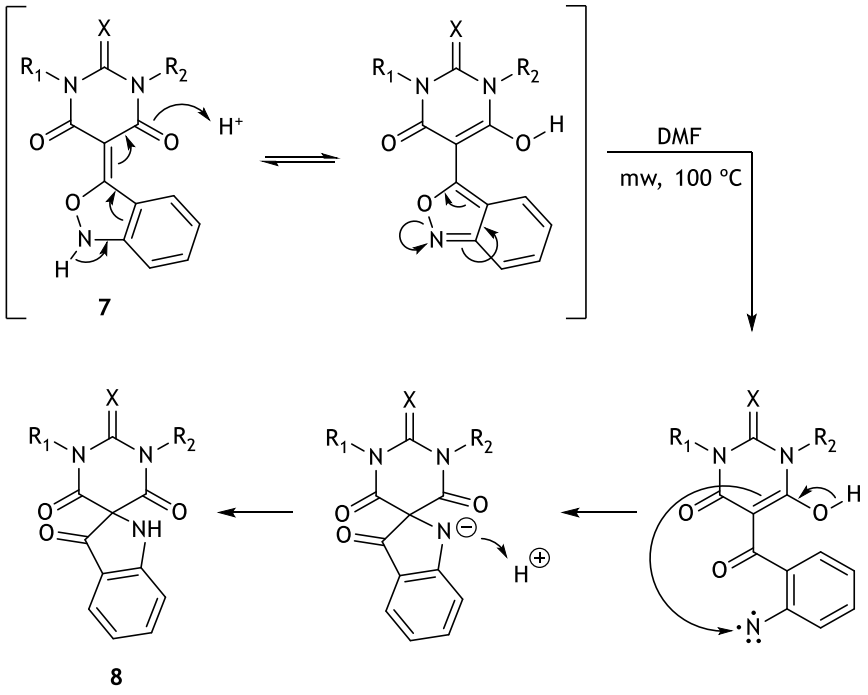

X = S, O
R_1 = H, Me, Ph
R_2 = H, Me, Ph, 4-ClC_6H_4,4-FC_6H_4, 4-IC_6H_4.

Scheme 3.9 - Proposed mechanism for the synthesis of the spiroindolin-3-one(thio)barbiturate **8.**

This proposed mechanism could be validated with the trapping of the referred nitrene triplet. Atkinson *et al.*[89], described this trapping with an inter- or intramolecular reaction of the nitrene with an alkene, forming the three-membered heterocycle aziridine.[90]

Therefore, attempts to trap the nitrene intermediate in the reaction of 5-(benzisoxazol-3-ylidene)pyrimidine **7a** and four different alkenes (2-methylbut-2-ene **9a**, 4-bromobut-1-ene **9b**, allyl alcohol **9c** and cyclohexene **9d**), to afford the respective aziridines **10a-d** (scheme 3.10) was performed. For one equivalent of **7a**, ten equivalents of alkene **9** were used, but no reaction was observed. This may be explained by a not so favored intermolecular trapping reaction in relation to the intramolecular spiro formation described. A possible solution to overcome this issue could be a future intramolecular reaction of the 5-(benzisoxazol-3-ylidene)pyrimidines **7a** substituted with a vinyl group, which will potentially be able to compete with the spiro formation of **8a.**

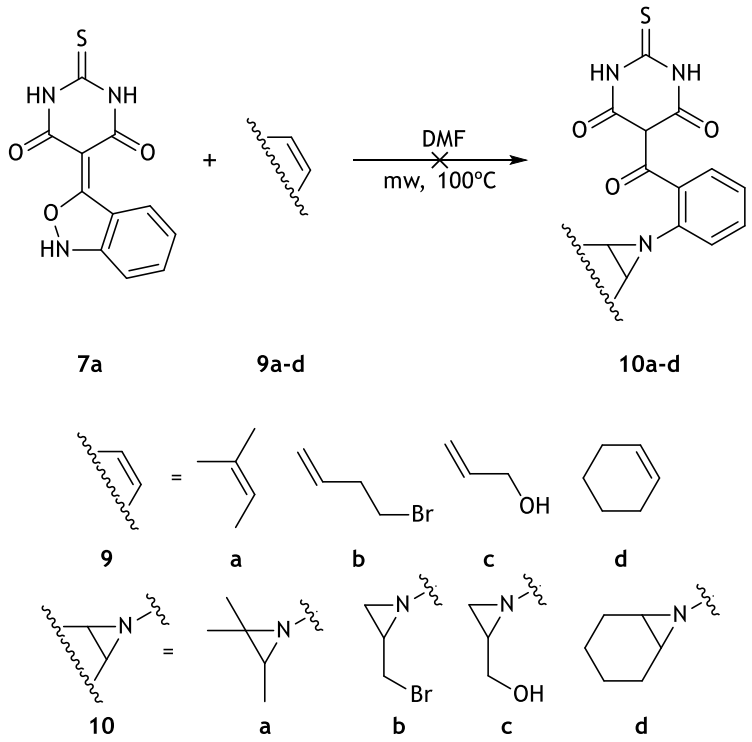

Scheme 3.10 – Attempts to intermolecular trapping of the nitrene intermediate with respective alkenes.

3.2. Evaluation of Biological Activity

In this section the experimental results obtained in the screenings for the biological evaluation of the new spiroindolin-3-one(thio)barbiturates **8a-f**, are presented and discussed. In the subtopic 3.2.1. will treated the results of the cell viability assays in NHDF and MCF-7 cells, where in the subtopic 3.2.2. will be treated the results of the XO inhibitory activity assay.

Finally, the general SAR of the synthesized spiroindolin-3-one(thio)barbiturates **8a-f** for the different biological activities tested in this work will be presented.

The results are presented as average values with their standard error of the means (SEM) and the difference between groups was considered statistically significant at $p < 0.05$ (Student's *t*-test).

3.2.1. Cell viability assays

To evaluate the effect of spiroindolin-3-one(thio)barbiturates **8a-f** on cell proliferation, the MTT assay was performed, after 72 hours of exposure of these compounds in the cells. The effects on the proliferation were compared to the 5-fluorouracil (5-FU) as positive control in both NHDF and MCF-7 cell lines.[27]

In order to determine the cytotoxic potential of compounds **8a-f** in NHDF cells, a screening at a concentration of 30 μM was performed. By analyzing the results (figure 3.1) it can be concluded that there is no relevant cytotoxicity of the compounds on NHDF cells, with the exception of **8a,** which showed a percentage of relative cell proliferation of 57%, comparatively close to the observed with 5-FU.

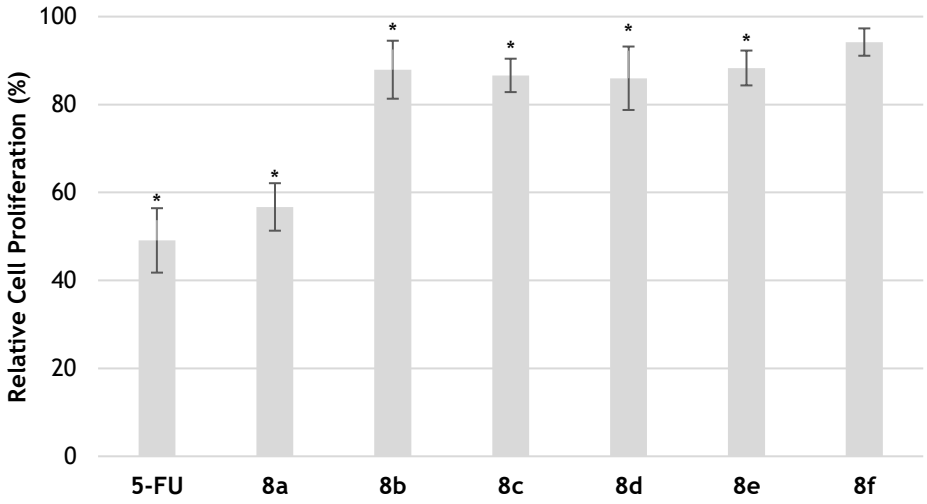

Figure 3.1 - Percentage of relative cell proliferation of NHDF cells after 72 hours exposure to 5-FU and compounds **8a, 8b, 8c, 8d, 8e** and **8f** at a concentration of 30 μM. The data are presented as average values with their SEM and are representatives of the two independent experiments performed. * $p < 0.05$ versus the control (Student's *t*-test).

After the initial screening, concentration-response studies were performed for the spiroindolin-3-onethiobarbiturate **8a** and 5-FU. In this study, the cells were exposed to concentrations of 0.1, 1, 10, 30, 50 and 100 μM of the selected compounds during 72 h.

By the analysis of the results (table 3.15), it was found that, despite the cytotoxicity observed in the initial screening, **8a** didn't show a potency similar to the one determined for 5-FU, with a half of the maximal inhibitory concentration (IC_{50}) value higher than 100 μM.

Table 3.15 - Estimated IC_{50} values of compounds 5-FU and **8a** in NHDF cells.

Compound	IC_{50} (μM)	r^2
5-FU	4.744	0,9750
8a	>100	-

After performing the cytotoxicity assay on NHDF cells, it was determined the anti-proliferative activity of these compounds in the MCF-7 cancer cell line. Thus, all the synthesized compounds were again screened at a concentration of 30μM. By the analysis of the results (figure 3.2) it can be stated that any of the studied compounds showed a relevant anti-proliferative effect in these cells. The results were similar to the ones obtained in NHDF, with the exception of spiroindolin-3-onethiobarbiturate **8c,** which showed a percentage of relative cell proliferation of almost 60%, 30% lower than in NHDF. After this initial screening, a concentration-response study is pertinent, particularly for compound **8c**.

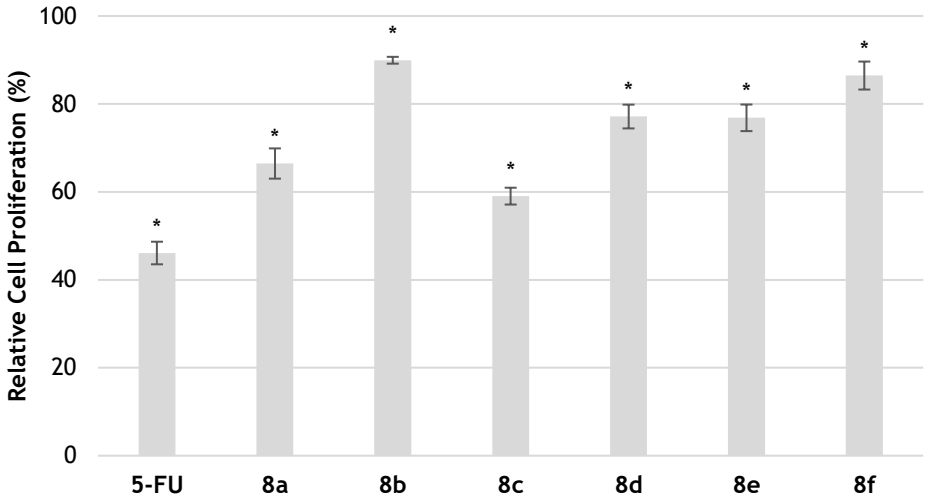

Figure 3.2 - Percentage of relative cell proliferation of MCF-7 cells after 72 hours exposure to 5-FU and compounds **8a, 8b, 8c, 8d, 8e** and **8f** at a concentration of 30 μM. The data are presented as average values with their SEM and are representatives of one independent experiment performed. * $p < 0.05$ versus the control (Student's *t*-test).

3.2.2. Xanthine Oxidase inhibitory activity assay

The XO inhibitory activity of the synthetized spiroindolin-3-one(thio)barbiturates **8a-f** was spectrophotometrically evaluated using ALO as a positive control and measuring the formation of uric acid at a wavelength of 295 nm. In order to guarantee the concentration range in which there is linearity of absorbance, a calibration curve was performed for various concentrations of uric acid at 295 nm, being observed linearity at least between 1.5 and 400 μM (figure 3.3).

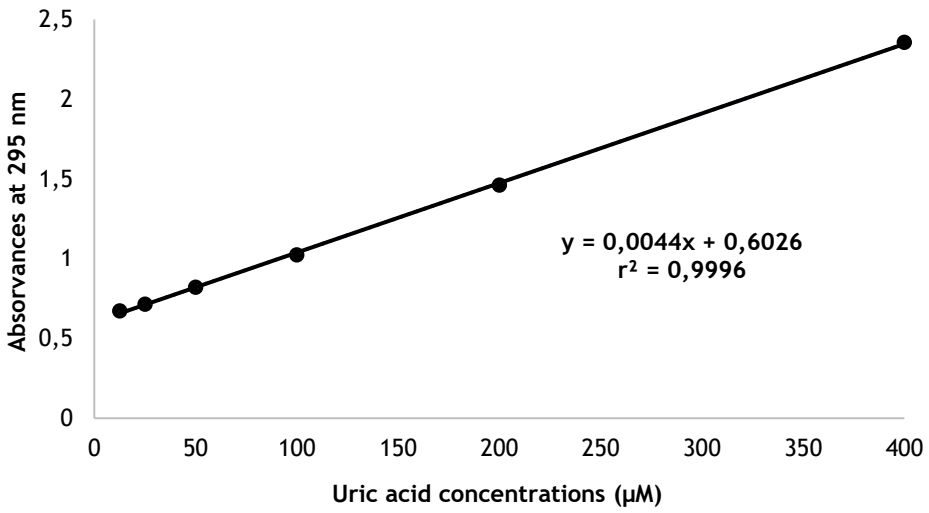

Figure 3.3 - Calibration curve for uric acid at 295 nm, with respective equation of line and r^2.

The inhibitory potential of the spiroindolin-3-one(thio)barbiturates **8a-f** in the enzyme activity was determined with a screening at 30 µM, just as described by Figueiredo *et al*.[27] In order to interpret the results, the minute five was chosen as representative, since it was at this time that the ALO inhibition reached its maximum (figure 3.4 and figure 3.5). By the analysis of results (figure 3.4) it can be referred that none of the spiroindolin-3-one(thio)barbiturates **8a-f** showed a relevant XO inhibitory activity. The best results were observed for compounds **8c** and **8e**, which can be due to their lipophilicity, therefore they can make hydrophobic interactions with the enzyme. After analyzing the data on the inhibition of enzyme activity over the 10 minutes of reaction (figure 3.5), even with a lower inhibitory activity than ALO, the spiroindolin-3-onethiobarbiturate **8c** showed an inhibitory profile similar the control.

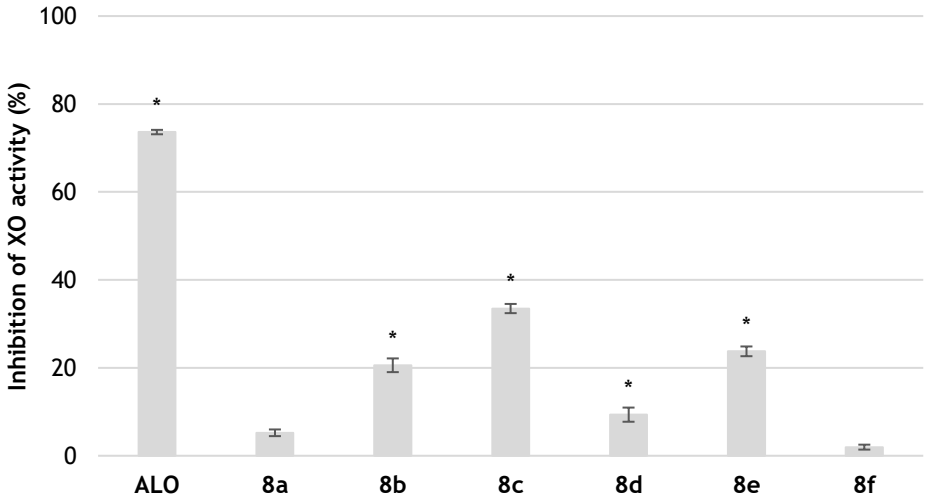

Figure 3.4 - Inhibition of XO activity, at 5 minutes of incubation, of ALO and the compounds **8a, 8b, 8c, 8d, 8e** and **8f** at a concentration of 30 µM. The data are presented as average values with their SEM and are representative of the two independent experiments performed. * $p < 0.05$ versus the control (Student's *t*-test).

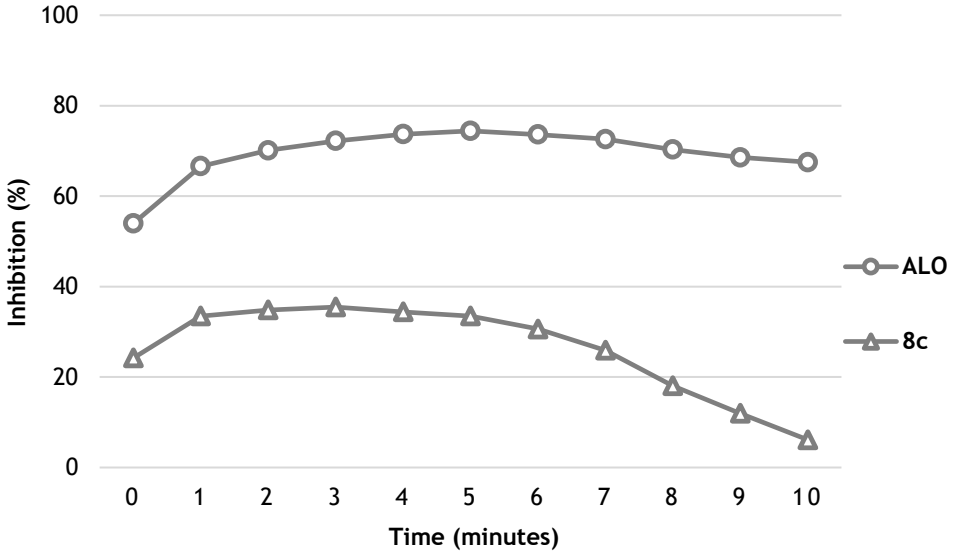

Figure 3.5 - Over time inhibition of XO activity for spiroindolin-3-one(thio)barbiturates **8c, 8e** and ALO at a concentration of 30μM.

After the initial screening, concentration-response studies were performed for the spiroindolin-3-onethiobarbiturate **8c** and ALO. In this study were used concentrations of 0.01, 0.1, 1, 7.5, 15 and 30 μM of the selected compounds.

After the concentration-response study, it was possible to estimate the IC_{50} values (table 3.16). For ALO the calculated IC_{50} was of 10,78 μM, close to the value of 11.23 μM reported by Shi *et al.*[91] When compared with ALO, the spiroindolin-3-onethiobarbiturate **8c** present a IC_{50} value higher than 30 μM.

Table 3.16 - Estimated IC_{50} values of compounds ALO and **8c** for the inhibition of XO activity.

Compound	IC_{50} (μM)	r^2
ALO	10.78	0,9151
8c	>30	-

3.2.3. Structure-Activity Relationship

A brief systematization of SAR information for the spiroindolin-3-one(thio)barbiturates **8a-f** (Figure 3.6) here presented for a simpler and faster interpretation of the obtained results. Overall, when the chalcogen was a sulfur atom, the spiroindolin-3-one(thio)barbiturates

showed higher cytotoxicity in both cell lines, where the R substituents seems to not influence this effect. For XO inhibitory activity, when the chalcogen was an oxygen atom and the barbiturate nuclei was substituted with a phenyl, the spiroindolin-3-one(thio)barbiturates had a more prominent activity.

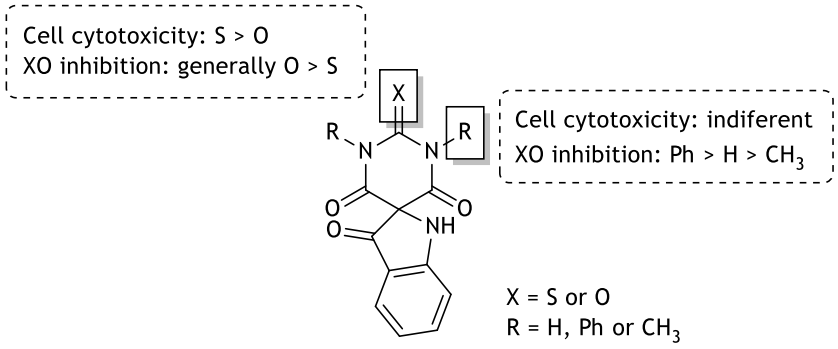

Figure 3.6 – SAR of spiroindolin-3-one(thio)barbiturates **8a-f** for cell cytotoxicity in NHDF and MCF-7 and XO inhibition.

3.3. *In silico* studies

3.3.1. Molecular docking

From the experimental results obtained for the inhibition of XO activity, a molecular docking study was performed for ALO and for the spiroindolin-3-one(thio)barbiturates **8a-f**. This computational study was performed to obtain more information on the preferred relative orientation of these compounds when bonded to the enzyme, for a better understanding of the *in vitro* results.

The crystallized XO structure with the code of 1VDV (1.98 Å resolution) was obtained through the Protein Data Bank.[92] In this case the protein was recrystallized with 1-[3-Cyano-4-(2,2-dimethylpropoxy)phenyl]-1H-pyrazole-4-carboxylic acid (Y-700), a potent XO inhibitor.

In order to validate the method, a re-docking of Y-700 with the XO was performed.[93] For this ligand, a root mean square deviation (RMSD) value of 0.78 Å was obtained, and, since it is below the standard of 2 Å, the method was considered validated. After the validation, the simulations were carried out between ALO and spiroindolin-3-one(thio)barbiturates **8a-f** with XO (table 3.17).

Table 3.17 – Molecular docking results for Y-700, ALO and spiroindolin-3-one(thio)barbiturates **8a-f**. Presented interactions by hydrogen bond with XO. In bold is highlighted the main hydrogen bond interactions for the inhibitory activity.

Ligand	Binding energy (Kcal/mol)	Interactions by hydrogen bond
Y-700	-8.17	ASN768, LYS771, **GLU802** and **ARG880**
ALO	-6.29	**GLU802**, **ARG880** and MOS3004
8a	-5.95	**THR1010** and VAL1011
8b	-5.76	**THR1010** and VAL1011
8c	-6.20	LYS771
8d	-6.11	SER876
8e	-6.33	LEU648 and SER876
8f	-6.50	SER876

By the analysis of these results, it can be considered that the molecular docking results don't reflect what was observed in the *in vitro* assays. In fact, the spiroindolin-3-one(thio)barbiturates **8e** and **8f** showed a lower energy than the determined for ALO, which goes against the in *vitro* results, since a low inhibitory activity was observed for these compounds.

According to the literature, the most important interactions between the enzyme and ligands are hydrogen bonds with residues of glutamine 802 (GLU802), arginine 880 (ARG880) and threonine 1010 (THR1010).[94] As expected Y-700 and ALO have some of these interactions (figure 3.6, A and B), where only **8a** and **8b** interact with THR1010 (figure 3.6, C and D), which may be due to the inexistence of substituents in positions N1 and N3, that, in the case of **8c-f,** may have prevented these bonds.

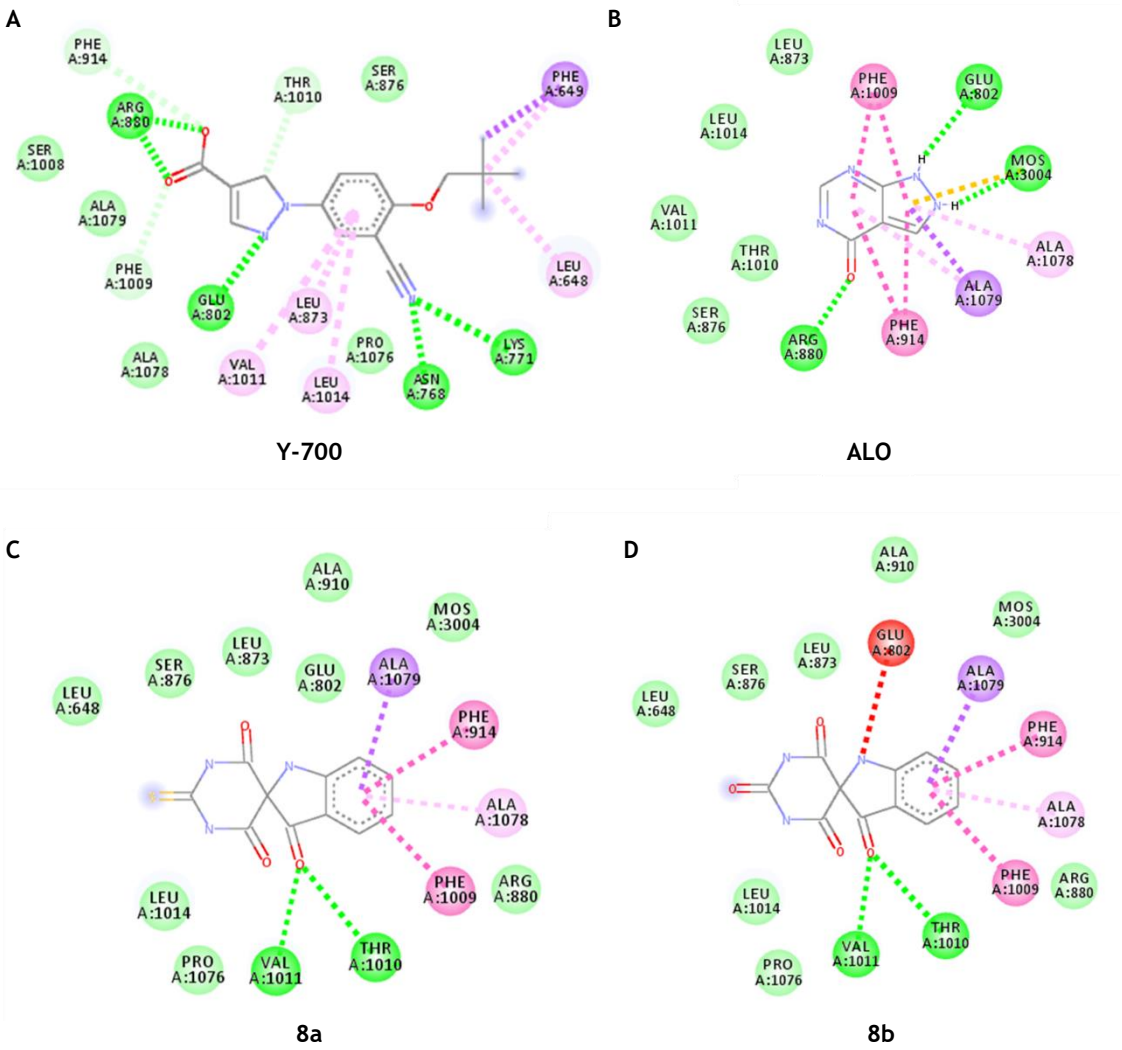

Figure 3.7 – Interactions of Y-700, ALO, **8a** and **8b** with XO. Green dashes – Hydrogen bonds; Light green dashes – van der Waals interactions; Purple dashes – Pi-Sigma interactions; Yellow – Pi-Sulfur interactions; Pink – Pi-Pi Stacked interactions; Light pink dashes – Pi-Alkyl interactions; Red dashes – Unfavorable Acceptor-Acceptor interactions.

3.3.2. Pharmacokinetics and toxicity properties prediction

In order to obtain a greater information about these compounds, predictions of relevant the pharmacokinetic and toxicity properties for the synthesized spiroindolin-3-one(thio) barbiturates **8a-f,** were performed in the online pkCSM software (table 3.18).

Concerning the absorption properties, none of the spiroindolin-3-one(thio)barbiturates demonstrated good water solubility. About the intestinal absorption (table 3.18), a percentage higher than 30% was determined for all compounds, which means that they can be well absorbed in the intestines. Compounds **8c** and **8e** were predicted as P-glycoprotein substrates, which may be due to the presence of phenyl groups which increase hydrophobic interactions with this protein.

Regarding the distribution (table 3.18), it can be noted that all spiroindolin-3-one(thio) barbiturates **8a-f** may cross the BBB, where and only **8b** and **8e** may have the capacity of penetrate the CNS.

Spiroindolin-3-one(thio)barbiturates **8c, 8e** and **8f** can be CYP3A4 substrates, and, the first two, can also be inhibitors (table 3.18). Additionally, these compounds can also be inhibitors of the CYP1A2, CYP2C19 and CYP2C9 isoforms. These metabolic characteristics suggest that cytochrome P450 can dramatically alter **8c** and **8e** pharmacokinetics, and interactions with other drugs can be expected.

Furthermore, any advertences were presented at the level of excretion (table 3.18), since they do not appear to be substrates of renal OCT2.

Concerning the toxicity properties (table 3.18), a low maximum recommended tolerated dose was predicted for spiroindolin-3-one(thio)barbiturates **8c, 8e** and **8f**, and compounds **8c** and **8e** where considered hERG II inhibitors and might led to hepatotoxicity, which may be due to their lipophilicity, compared with the other spiroindolin-3-one(thio)barbiturates.

Finally, spiroindolin-3-one(thio)barbiturates **8c** and **8e** violates only one parameter, where **8a**, **8b**, **8d** and **8f** doesn't violated any as of Lipinski rules and Verber parameters. This can indicate that all spiroindolin-3-one(thio)barbiturates **8a-f** may have a good oral bioavailability.

Table 3.18 - Prevision of the pharmacokinetics properties for the compounds **8a-f.** Grey highlights positive results.

Pharmacokinetic and model of study	Compounds					
	8a	**8b**	**8c**	**8d**	**8e**	**8f**
Absorption						
Water solubility (mol/L)	0.0016	0.0024	0.0002	0.0012	0.0002	-0.0005
Intestinal absorption (%)[a]	**85**	**66**	**96**	**85**	**96**	**92**
P-glycoprotein substrate	**No**	**No**	Yes	**No**	Yes	**No**
P-glycoprotein I inhibitor	**No**	**No**	Yes	**No**	Yes	**No**
P-glycoprotein II inhibitor	**No**	**No**	Yes	**No**	Yes	**No**
Distribution						
BBB permeability (log BB)[b]	-0,605	-0,721	-0,371	-0,723	-0.442	-0,941
CNS permeability (log PS)[c]	**-2,750**	**-2,846**	-1,854	**-2,667**	-1.95	**-2,672**
Metabolism						
CYP2D6 substrate	**No**	**No**	**No**	**No**	**No**	**No**
CYP3A4 substrate	**No**	**No**	Yes	**No**	Yes	Yes
CYP1A2 inhibitor	**No**	**No**	**No**	**No**	Yes	**No**
CYP2C19 inhibitor	**No**	**No**	Yes	**No**	Yes	**No**
CYP2C9 inhibitor	**No**	**No**	Yes	**No**	Yes	**No**
CYP2D6 inhibitor	**No**	**No**	**No**	**No**	**No**	**No**
CYP3A4 inhibitor	**No**	**No**	Yes	**No**	Yes	**No**
Excretion						
Renal OCT2 substrate	**No**	**No**	**No**	**No**	**No**	**No**
Toxicity						
AMES toxicity	**No**	**No**	**No**	**No**	**No**	**No**
Max dose (mg/kg/day)[d]	**0.644**	**0.745**	0.351	**0.520**	0.307	0.427
hERG I inhibitor	**No**	**No**	**No**	**No**	**No**	**No**
hERG II inhibitor	**No**	**No**	Yes	**No**	Yes	**No**
Hepatotoxicity	**No**	**No**	Yes	**No**	Yes	**No**
Lipinski's rules and Verber parameters						
Molecular Weight (g/mol)[e]	**261,26**	**245,19**	**413,46**	**273,25**	**289.32**	**397,39**
Log P[f]	**-0,4355**	**-0,6004**	**3,3985**	**0,0840**	**0.2489**	**3,2336**
Rotatable Bonds[g]	**0**	**0**	**2**	**0**	**0**	**2**
Hydrogen Acceptors[h]	**5**	**5**	**5**	**5**	**5**	**5**
Hydrogen Donors[i]	**3**	**3**	**1**	**1**	**1**	**1**
Surface Area (Å^2)[j]	**106,74**	**100,54**	177,27	**113,69**	**119.89**	171,07
Violations	**0**	**0**	1	**0**	**0**	1

[a] < 30% poorly absorbed; [b] > 0.3 cross the blood-brain barrier or < −1 poorly distributed to the brain; [c] > -2 penetrate the CNS or < -3 unable to penetrate the CNS; [d] ≤ 0.48 low or ≥ 0.48 high; [e] < 500 g/mol; [f] < 5; [g] < 10; [h] < 10; [i] < 5; [j] < 140.[8]

Chapter 4 - Conclusions

In this work, a total of twenty-six new (thio)barbiturates derivatives have been synthetized. All compounds were obtained in overall good yields and were equally characterized. With the synthesis of the spiroindolin-3-one(thio)barbiturates, it was possible to obtain nine new spiro compounds, by means of new, optimized and greener route of mw irradiation synthesis, in yields of 70-85%.

In addition, the activity of the spiroindolin-3-one(thio)barbiturates as anti-proliferative agents and xanthine oxidase inhibitors, was also evaluated. None spiroindolin-3-one(thio)barbiturate **8a-f** showed significant cytotoxicity on the cell lines studied, with **8a** being the most cytotoxic in NHDF (58% of cell proliferation), and **8c** the most cytotoxic in MCF-7 (59% of cell proliferation). Further cell viability assays will have to be performed in MDF-7 cells, in order to have consistency in the obtained results for this cell line, as well as concentration-response studies. Spiroindolin-3-onethiobarbiturate **8c** showed 33% of xanthine oxidase inhibition, which was very low when compared to ALO (inhibition of 79%).

In the molecular docking results, is important to note that some of the spiroindolin-3-one(thio)barbiturates, namely **8e** and **8f**, showed higher affinities to the enzyme then ALO, however these results did not reflect those obtained in the in vitro assays. Regarding the predictions of relevant pharmacokinetic properties and toxicity, all spiroindolin-3-one(thio)barbiturates **8a-f,** fulfil the Lipinski's rule of five and Verber parameters, as well as most of the pharmacokinetic and toxicity criteria determined for the different ADMET parameters.

As future work, more studies should be performed to improve not only the potency and selectivity of this family of compounds but also its pharmacokinetics properties. It will also be important to continue the synthesis of more spiroindolin-3-one(thio)barbiturates derivatives, variating the substituents in positions N1 and N3 or in the indolinone scaffold, to optimize the biological results, and for a better understanding of the structure-activity relationship. It is also of great importance to continue the synthesis of new asymmetric spiroindolin-3-one(thio)barbiturates, as well as the separation of their enantiomers, to determine the individual biological activity of each one.

Chapter 5 - Experimental Section

5.1. Synthesis and Structural characterization

All solvents and reagents used were commercially available, having the analytically pure degree of purity and, when necessary, the solvents were dried on 4Å molecular sieves.

Melting reactions were realized in a Selecta muffle oven. Photolysis reactions were performed with a halogen lamp of 500 W. Mw assisted reactions were carried out in a Milestone MultiSYNTH Single and Multi-Mode Microwave Synthesis System.

All reactions were followed by TLC using 0.2 mm aluminum plates coated with silica gel (Macherey-Nagel 60 G / UV254). The eluent is referred mentioning the volumetric ratio of the various components of the mixed eluents, if the case. After elution, the plates were visualized by UV light at the wavelength of 254 and/or 365 nm.

Melting points (mp) were determined for products in the form of crystal or solid with open capillary tubes in a Büchi B-540 melting point apparatus and were not corrected.

FTIR spectra were registered on a Thermo Fisher Scientific Nicolet iS10: smart iTR spectrophotometer, obtained by attenuated total reflectance (ATR) and Omnic 8.2 software, according to the main definitions of: background with 32 scans; sample with 32 scans; resolution of 4 cm^{-1}, between 4000 and 600 cm^{-1}. In the description of the compounds, the data obtained are indicated by the following order: maximum frequency of the absorption band (υ_{max} in cm^{-1}) and assignment to a group of atoms in the molecule in the case of the characteristic bands.

^{1}H-NMR and ^{13}C-NMR spectra were performed on a Brüker Avance III 400 MHz spectrometer (400.13 and 100.62 MHz, respectively), and processed in MestReNova 12.0.3 software. The hexadeuterated dimethylsulfoxide (DMSO-d_6), or deuterated chloroform ($CDCl_3$), were used as solvents and as internal standards (DMSO-d_6, δ = 2.50 ppm and 39.52 ppm, or $CDCl_3$, δ = 7.26 ppm and 77.16 ppm, in ^{1}H- and ^{13}C-NMR, respectively). Heteronuclear Single Bond Correlation (HSQC) and heteronuclear multiple bond correlation (HMBC) spectra were performed for some of the compounds. In the description of the compounds, the data obtained are indicated in the following order: for ^{1}H-NMR – solvent; chemical shift (δ, in ppm); signal multiplicity (s, d, dd, ddd, dt, t, td, or m); coupling constant (*J*, in Hz); relative intensity (nH, number of protons); and attribution of the proton in the molecule, if possible; for ^{13}C-NMR - solvent; chemical shift (δ, in ppm); attribution of carbon in the molecule, if possible.

For each synthesized compound is presented the two-dimensional structure (2D) and its SMILES notation, which were obtained with ChemBridgeSoft® Chembiodraw 14.0 drawing software.

5.1.1. Synthesis of precursors

5.1.1.1. 1,3-Disubstituted(thio)ureas

The 1,3-disubstituted(thio)ureas **3a-p** were obtained by the following conditions:

Condition A: To a stirred solution of phenylisothiocyanate **1** (1.00 mmol, 135 mg) in DCM (0.5 mL) at room temperature, was added dropwise a solution of the respective aniline **2** (1.00 mmol) in DCM (0.5 mL). The reaction was followed by TLC (DCM). Once completed, the resulting suspension was filtered and washed with diethyl ether (10 mL).[69]

Condition B: To suspension of aniline **2** (2.00 mmol) in water (5 mL) at room temperature, carbonyldiimidazole **4** (1.00 mmol, 162 mg) was added. The reaction was followed by TLC (DCM). Once completed, the resulting suspension was filtered and washed with diethyl ether (10 mL).Adapted from 70

1,3-Diphenylthiourea (3a)

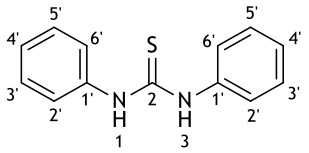

From phenylisothiocyanate **1** and aniline (**2a)** (1.00 mmol, 93 mg); Condition A; Completed in 3 hours; Yield 95%; white crystals; mp 142-144°C (lit.[71] 140-142 °C); FTIR υ_{max} (cm^{-1})[27] 3202 (N-H), 3053, 1598 (C=C), 1526, 1491, 1449, 1342, 1313, 1288, 1242, 1171, 1069, 1021, 1003, 933, 756, 694, 642, 629, 610; ^{1}H-NMR (400 MHz, DMSO-d_6) δ (ppm)[27] 9.79 (s, 2H, 2 x NH), 7.48 (d, *J* = 7.4 Hz, 4H, 2' and 6'-ArCH), 7.33 (t, *J* = 8.2 and 7.6 Hz, 4H, 3' and 5'-ArCH), 7.12 (t, *J* = 7.4 Hz, 2H, 4'-ArCH); ^{13}C-NMR (101 MHz, DMSO-d_6) δ (ppm)[27] 179.63 (2-CS), 139.46 (1'-ArC), 128.45 (ArCH), 124.44 (4'-ArCH), 123.66 (ArCH); SMILES S=C(NC1=CC=CC=C1)NC2=CC=CC=C2.

1-Phenylthiourea (3b)

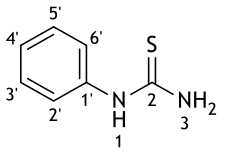

From phenylisothiocyanate **1** and ammonia (**2b)** (1.00 mmol, 17 mg); Condition A; Completed in 2 hours; Yield 84%; white solid; mp 150-151 °C (lit.[72] 150-154°C); FTIR υ_{max} (cm^{-1}) 3419 (N-H), 3266, 3167, 3000, 1607, 1588, 1517, 1485, 1460, 1443, 1315, 1295, 1259, 1229, 1169, 1058, 809, 747, 692, 636; ^{1}H-NMR (400 MHz, DMSO-d_6) δ (ppm) 9.38 (s, 1H, 1-NH), 7.46 (s, 2H, 2 x 3-NH), 7.37 – 7.20 (m, 4H, 2'- 3'- 5'- and 6'-ArCH), 7.10 (t, *J* = 7.3 Hz, 1H, 4'-ArCH); SMILES NC(NC1=CC=CC=C1)=S.

1-Methyl-3-phenylthiourea (3c)

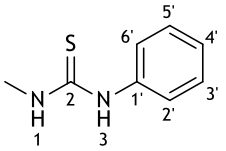

From phenylisothiocyanate **1** and methylamine (**2c)** (31 mg); Condition A; Completed in 2 hours; Yield 95%; White solid; mp 117-118 °C (lit.[73] 115-117 ºC); FTIR υ_{max} (cm^{-1}) 3257.22 (N-H), 3154, 2989, 1594, 151, 1490, 1449, 1365, 1307, 1287, 1246, 1211, 1154, 1069, 1027, 1001, 723, 689, 640; ^{1}H-NMR (400 MHz, $CDCl_3$) δ (ppm) 7.90 (s, 1H, 3-N<u>H</u>), 7.37 (t, *J* = 7.7 Hz, 2H, 3' and 5'-ArC<u>H</u>), 7.25 (t, *J* = 7.5 Hz, 1H, 4'-ArC<u>H</u>), 7.15 (d, *J* = 6.7 Hz, 2H, 2'- 6'-ArC<u>H</u>), 6.02 (s, 1H, 1-N<u>H</u>), 3.07 (s, 3H, 1-NC<u>H_3</u>); SMILES S=C(NC)NC1=CC=CC=C1.

1-Hexyl-3phenylthiourea (3d)

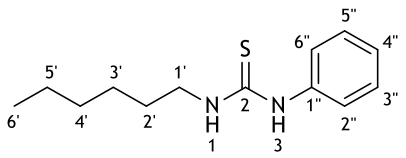

From phenylisothiocyanate **1** and hexylamine (**2d)** (1.00 mmol, 101 mg); Condition A; Completed in 2 hours; Yield 87%; White solid; mp 79-80 ºC (lit.[74] 75-77 ºC); FTIR υ_{max} (cm^{-1}) 3241.13 (N-H), 3189, 3137, 3078, 2946, 2924, 2852, 1598, 1547, 1496, 1465, 1432, 1382, 1353, 1340, 1316, 1295, 1266, 1254, 1227, 1192, 1144, 1075, 1032, 756, 721, 699, 684; ^{1}H-NMR (400 MHz, $CDCl_3$) δ (ppm) 7.85 (s, 1H, N<u>H</u>), 7.44 (t, *J* = 7.8 Hz, 2H, 3''- and 5''-ArC<u>H</u>), 7.31 (t, *J* = 7.5 Hz, 1H, 4''-ArC<u>H</u>), 7.20 (d, *J* = 7.5 Hz, 2H, 2''-ArC<u>H</u>), 6.07 (s, 1H, N<u>H</u>), 3.61 (t, *J* = 7.3 Hz, 2H, 1'-C<u>H_2</u>), 1.56 (m, 2H, 2'-C<u>H_2</u>), 1.36 – 1.17 (m, 6H, 3'-, 4'- and 5'-C<u>H_2</u>), 0.87 (d, *J* = 6.8 Hz, 3H, C<u>H_3</u>); SMILES S=C(NCCCCCC)NC1=CC=CC=C1.

1-Phenyl-3-(thiazol-2-yl)thiourea (3e)

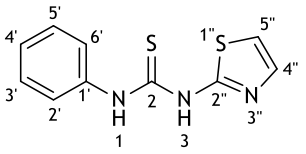

From phenylisothiocyanate **1** and 2-aminothiazole (**2e)** (1.00 mmol, 100 mg); Condition A; Completed in 3 hours; Yield 83%; Brown solid; mp 142-144 ºC (lit.[75] 140-142 ºC); FTIR υ_{max} (cm^{-1}) 3152 (N-H), 3105, 3081, 2972, 1559, 1542, 1506, 1469, 1448, 1362, 1304, 1253, 1204, 1183, 1152, 1131, 1068, 1027, 866, 819, 769, 753, 725, 684, 639; ^{1}H-NMR (400 MHz, DMSO-d_6) δ (ppm) 12.44 (s, 1H, N<u>H</u>), 10.44 (s, 1H, N<u>H</u>), 7.70 (d, *J* = 7.9 Hz, 2H, 2'- and 6'-ArC<u>H</u>), 7.45 (d, *J* = 4.2 Hz, 1H, C<u>H</u>), 7.31 (t, *J* = 7.9 Hz, 2H, 3'- and 5'-ArC<u>H</u>), 7.08 (t, *J* = 7.4 Hz, 1H, 4'-ArC<u>H</u>), 7.00 (d, *J* = 4.2 Hz, 1H, C<u>H</u>); SMILES S=C(NC1=NC=CS1)NC2=CC=CC=C2.

1-Phenyl-3-(pyridin-3-yl)thiourea (3f)

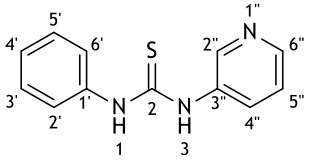

From phenylisothiocyanate **1** and 2-aminopyridine (**2f)** (1.00 mmol, 94 mg); Condition A; Completed in 2 hours; Yield 89%; White solid; mp 195-196 ºC (lit.[76] 198 ºC); FTIR υ_{max} (cm^{-1}) 3138.60 (N-H), 3036, 2976, 1586, 1578, 1529, 1507, 1487, 1449, 1420, 1376, 1309, 1290, 1267, 1229, 1119, 1186, 1099, 1041, 1026, 959, 936, 780, 734, 708, 689, 644; ^{1}H-NMR (400 MHz, DMSO-d_6) δ (ppm) 10.02 (s, 1H, NH), 9.87 (s, 1H, NH), 8.60 (d, *J* = 2.5 Hz, 1H), 8.32 (dd, *J* = 4.7 and 1.5 Hz, 1H), 7.94 (ddd, *J* = 8.2, 2.6 and 1.5 Hz, 1H), 7.48 (dd, *J* = 7.4 and 1.3 Hz, 2H), 7.39 – 7.32 (m, 4H), 7.15 (t, *J* = 7.3 Hz, 1H); SMILES S=C(NC1=CC=CN=C1)NC2=CC=CC=C2.

1-(2-Chlorophenyl)-3-phenylthiourea (3g)

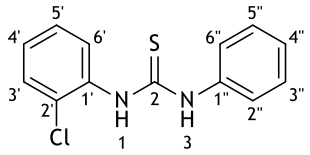

From phenylisothiocyanate **1** and 2-chloroaniline (**2g)** (1.00 mmol, 128 mg); Condition A; Completed in 3 hours; Yield 82%; White solid; mp 178-179 ºC (lit.[77] 181 ºC); FTIR υ_{max} (cm^{-1}) 3303 (N-H), 3165, 3000, 1590, 1577, 1538, 1502, 1481, 1448, 1439, 1362, 1314, 1292, 1266, 1247, 1226, 1202, 1156, 1127, 1060, 1031, 950, 933, 763, 746, 721, 692, 682, 648; ^{1}H-NMR (400 MHz, DMSO-d_6) δ (ppm) 10.01 (s, 1H, NH), 9.44 (s, 1H, NH), 7.62 (dd, *J* = 6.4 and 1.6 Hz, 1H, ArCH), 7.56 – 7.49 (m, 3H, ArCH), 7.39 – 7.32 (m, 3H, ArCH), 7.26 (td, *J* = 7.7 and 1.7 Hz, 1H, ArCH), 7.16 (t, *J* = 7.4 Hz, 1H, ArCH); SMILES S=C(NC1=CC=CC=C1)NC2=CC=CC=C2Cl.

1-(3-Chlorophenyl)-3-phenylthiourea (3h)

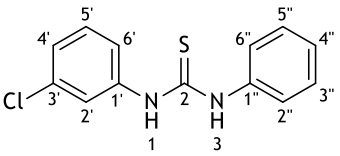

From phenylisothiocyanate **1** and 3-chloroaniline (**2h)** (1.00 mmol, 128 mg); Condition A; Completed in 3 hours; Yield 97%; White solid; mp 100-101 ºC (lit.[78] 104); FTIR υ_{max} (cm^{-1}) 3178 (N-H), 3026, 1589, 1534, 1494, 1473, 1449, 1428, 1326, 1310, 1243, 1160, 1087, 1073, 1028, 998, 950, 895, 856, 845, 784, 763, 718, 687, 667; ^{1}H-NMR (400 MHz, DMSO-d_6) δ (ppm) 9.94 (s, 1H, 2 x NH), 7.71 (t, *J* = 2.0 Hz, 1H, ArCH), 7.47 (dd, *J* = 7.4 and 1.1 Hz, 2H, ArCH), 7.43 - 7.31 (m, 4H, ArCH), 7.21 – 7.12 (m, 2H, ArCH); SMILES S=C(NC1=CC=CC=C1) NC2=CC=CC(Cl)=C2.

1-(4-Chlorophenyl)-3-phenylthiourea (3i)

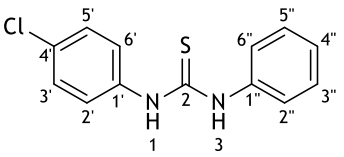

From phenylisothiocyanate **1** and 4-chloroaniline (**2i)** (1.00 mmol, 128 mg); Condition A; Completed in 3 hours; Yield 97%; White solid; mp 156-157 ºC (lit.[78] 150 ºC); FTIR υ_{max} (cm^{-1}) 3201 (N-H), 3029, 3005, 1599, 1583, 1523, 1487, 1450, 1404, 1339, 1282, 1244, 1170, 1087, 1015, 931, 916, 841, 811, 769, 724, 707, 697, 660; ^{1}H-NMR (400 MHz, DMSO-d_6) δ (ppm) 9.88 (s, 2H, 2 x NH), 7.52 (dt, *J* = 4.6 and 3.1 Hz, 2H, ArCH), 7.47 (dd, *J* = 7.3 and 1.2 Hz, 2H, ArCH), 7.39 (dt, *J* = 4.6, 2.9 and 2.1 Hz, 2H, ArCH), 7.34 (t, *J* = 8.4 and 7.5 Hz, 2H, ArCH), 7.14 (t, *J* = 7.4 Hz, 1H, 4''-ArCH); SMILES S=C(NC1=CC=CC=C1)NC2=CC=C(Cl)C =C2.

1-(4-Flourophenyl)-3-phenylthiourea (3j)

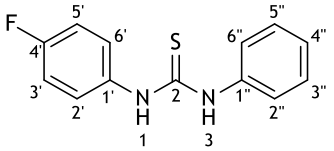

From phenylisothiocyanate **1** and 4-flouroaniline (**2j)** (1.00 mmol, 111 mg); Condition A; Completed in 3 hours; Yield 90%; White solid; mp 171-172 ºC (lit.[78] 173-174 ºC); FTIR υ_{max} (cm^{-1}) 3207 (N-H), 3011, 1597, 1528, 1501, 1449, 1412, 1360, 1336, 1290, 1247, 1226, 1207, 1151, 1089, 1026, 1014, 1003, 932, 915, 848, 831, 786, 758, 726, 700, 676, 645; ^{1}H-NMR (400 MHz, DMSO-d_6) δ (ppm) 9.78 (s, 2H, NH), 7.50 – 7.44 (m, 4H, ArCH), 7.34 (t, *J* = 8.3 Hz, 2H, ArCH), 7.22 – 7.10 (m, 3H, ArCH); SMILES S=C(NC1=CC=CC=C1)NC2=CC=C(F)C=C2.

1-(4-Iodophenyl)-3-phenylthiourea (3k)

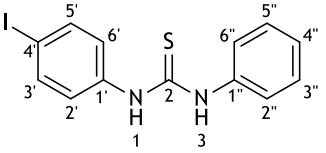

From phenylisothiocyanate **1** and 4-iodoaniline (**2k)** (1.00 mmol, 219 mg); Condition A; Completed in 3 hours; Yield 90%; White solid; mp 169-170 ºC (lit.[79] 170 ºC); FTIR υ_{max} (cm^{-1}) 3200 (N-H), 3025, 1599, 1587, 1523, 1479, 1450, 1479, 1450, 1396, 1327, 1282, 1243, 1218, 1097, 1072, 1054, 1009, 932, 917, 837, 806, 769, 699, 642; ^{1}H-NMR (400 MHz, DMSO-d_6) δ (ppm) 9.87 (s, 2H, NH), 7.67 (d, *J* = 8.8 Hz, 2H, ArCH), 7.47 (dd, *J* = 7.3 and 1.2 Hz, 2H, ArCH), 7.38 – 7.31 (m, 4H, ArCH), 7.15 (t, *J* = 7.3 Hz, 1H, 4''-ArCH); SMILES S=C(NC1=CC=CC=C1) NC2=CC=C(I)C=C2.

1-(2-(Methylthio)phenyl)-3-phenylthiourea (3l)

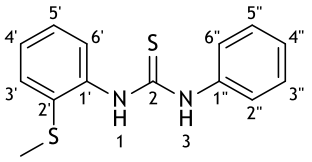

From phenylisothiocyanate **1** and 2-(methylthio)aniline (**2l)** (1.00 mmol, 139 mg); Condition A; Completed in 3 hours; Yield 98%; White solid; mp 166-167 ºC; FTIR υ_{max} (cm^{-1}) 3276 (N-H), 3155, 3059, 3023, 2992, 2915, 1592, 1534, 1490, 1471, 1447, 1436, 1356, 1311, 1291, 1269, 1244, 1225, 1203, 1162, 1069, 1038, 1024, 965, 928, 863, 845, 758, 741, 726, 718, 690, 647; ^{1}H-NMR (400 MHz, DMSO-d_6) δ (ppm) 9.85 (s, 1H, N<u>H</u>), 9.20 (s, 1H, N<u>H</u>), 7.53 (dd, *J* = 7.6 and 1.1 Hz, 2H, ArC<u>H</u>), 7.39 (dd, *J* = 7.8 and 1.5 Hz, 1H, ArC<u>H</u>), 7.33 (t, *J* = 8.2 Hz, 3H, ArC<u>H</u>), 7.26 (td, *J* = 7.6 and 1.5 Hz, 1H, ArC<u>H</u>), 7.18 (dd, *J* = 7.6 and 1.5 Hz, 1H, ArC<u>H</u>), 7.13 (t, *J* = 7.4 Hz, 1H, ArC<u>H</u>), 2.43 (s, 3H, SC<u>H</u>$_3$); SMILES S=C(NC1=CC=CC=C1)NC2=CC=CC=C2SC.

1-Phenyl-3-(2-(phenylthio)phenyl)thiourea (3m)

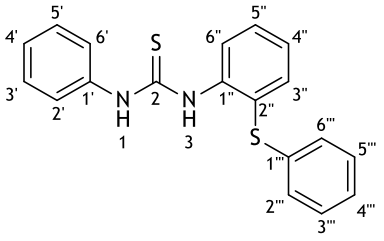

From phenylisothiocyanate **1** and 2-(phenylthio)aniline (**2m)** (1.00 mmol, 201 mg); Condition A; Completed in 3 hours; Yield 91%; White solid; mp 150-151 ºC; FTIR υ_{max} (cm^{-1}) 3276 (N-H), 3155, 3059, 3023, 2992, 2915, 1592, 1534, 1490, 1471, 1447, 1436, 1356, 1311, 1291, 1269, 1244, 1225, 1203, 1069, 1038, 1024, 965, 928, 863, 845, 758, 741, 726, 718, 690, 679, 647; ^{1}H-NMR (400 MHz, DMSO-d_6) δ (ppm) 10.02 (s, 1H, N<u>H</u>), 9.40 (s, 1H, N<u>H</u>), 7.66 (dd, *J* = 8.0 and 1.4 Hz, 1H, ArC<u>H</u>), 7.47 (dd, *J* = 7.5 and 1.2 Hz, 2H, ArC<u>H</u>), 7.38 – 7.18 (m, 10H, ArC<u>H</u>), 7.14 (t, *J* = 7.4 Hz, 1H, ArC<u>H</u>); SMILES S=C(NC1=CC=CC=C1)NC2=CC=CC=C2SC3=CC=CC=C3.

1-(2-Isopropylphenyl)-3-phenylthiourea (3n)

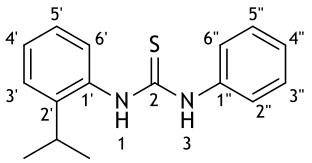

From phenylisothiocyanate **1** and 2-isopropylaniline (**2n)** (1.00 mmol, 135 mg); Condition A; Completed in 3 hours; Yield 71%; White solid; mp 146-147 ºC (lit.[80] 141-142); FTIR υ_{max} (cm^{-1}) 3367 (N-H), 3152, 2962, 2862, 2864, 1592, 1536, 1503, 1443, 1360, 1311, 1285, 1261, 1234, 1204, 1204, 1155, 1080, 1026, 927, 759, 729, 694, 651; ^{1}H-NMR (400 MHz, DMSO-d_6) δ (ppm) 9.60 (s, 1H, N<u>H</u>), 9.34 (s, 1H, N<u>H</u>), 7.50 (d, *J* = 7.7 Hz, 2H, ArC<u>H</u>), 7.37 – 7.24 (m, 4H, ArC<u>H</u>), 7.23 – 7.17 (m, 2H, ArC<u>H</u>), 7.13 (t, *J* = 7.3 Hz, 1H, ArC<u>H</u>), 3.15 (hept, *J* = 6.9 Hz, 1H, 2'-CC<u>H</u>(CH$_3$)$_2$), 1.19 (d, *J* = 6.9 Hz, 6H, 2'-CCH(C<u>H</u>$_3$)$_2$); SMILES S=C(NC1=C(C(C)C)C=CC=C1)NC2=CC =CC=C2.

1-(2-(*tert*-butyl)phenyl)-3-phenylthiourea (3o)

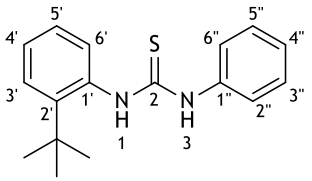

From phenylisothiocyanate **1** and 2-*tert*-butylaniline (**2o)** (1.00 mmol, 149 mg); Condition A; Completed in 3 hours; Yield 84%; White solid; mp 175-176 ºC (lit.[80] 172-173 ºC); FTIR υ_{max} (cm^{-1}) 3338 (N-H), 3140, 2959, 1596, 1529, 1496, 1478, 1450, 1439, 1395, 1361, 1338, 1263, 1226, 1199, 1088, 1070, 1049, 1023, 1003, 927, 907, 871, 761, 721, 692, 638; ^{1}H-NMR (400 MHz, DMSO-d_6) δ (ppm) 9.54 (s, 1H, NH), 9.10 (s, 1H, NH), 7.54 (d, *J* = 7.6 Hz, 2H, ArCH), 7.43 (dd, *J* = 4.9 and 2.7 Hz, 2H, ArCH), 7.33 (t, *J* = 8.2 Hz, 2H, ArCH), 7.29 – 7.21 (m, 2H, ArCH), 7.19 (dd, *J* = 3.1 and 1.8 Hz, 1H, ArCH), 7.13 (t, *J* = 7.5 Hz, 1H, ArCH), 1.37 (s, 9H, 2'-C(CH_3)$_3$); SMILES S=C(NC1=C(C(C)(C)C)C=CC=C1)NC2=CC=CC=C2.

1,3-Diphenylurea (3p)

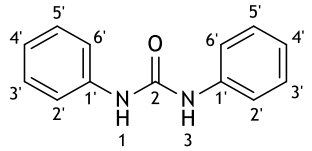

From carbonyldiimidazole **4** and aniline (**2a)** (1.00 mmol, 186 mg); Condition B; Completed in 4 hours; Yield 85%; white solid; mp 239-240 °C (lit.[81] 250-255°C); FTIR υ_{max} (cm^{-1}) 3324.18 (N-H), 3279.83 (N-H), 3035.06, 1645.45 (C=O), 1592.78, 1496.58, 1447.18, 1439.50, 1314.08, 1294.72, 1230.43, 1155.95, 1082.87, 1052.06, 1026.19, 985.49, 912.72, 894.33, 751.90, 695.10, 641.00; ^{1}H-NMR (400 MHz, DMSO-d_6) δ (ppm) 8.14 (s, 2H, 2 x NH), 7.36 (d, *J* = 8.3 Hz, 4H, 2' and 6'-ArCH), 7.18 (t, *J* = 7.9 Hz, 4H, 3' and 5'-ArCH), 6.90 (t, *J* = 7.8 Hz, 2H, 4'-ArCH); SMILES O=C(NC1=CC=CC=C1)NC2=CC=CC=C2.

5.1.1.2. 1,3-Disubstituted(thio)barbituric acids

The 1,3-disubstituted(thio)barbituric acids **5a-f** were obtained by the following conditions:

Condition A: A stirred solution of 1,3-disubstituted(thio)urea **3** (1.00 mmol), malonic acid (1.30 mmol, 137 mg) and acetyl chloride (3.00 mmol, 240 mg) was heated at 60°C for 30 min. The reaction was followed by TLC (DCM). Water was added to the obtained mixture and the solid was filtered, washed with water (10 mL) and recrystallized from ethanol.[82]

Condition B: To a solution of 1,3-disubstituted(thio)urea **3** (1.00 mmol) and malonic acid (1.00 mmol, 137 mg) in chloroform (5 ml), phosphoryl chloride (2.00 mmol, 310 mg) was added dropwise, and heated at 50°C. The reaction was followed by TLC (DCM). Once completed, the solvent was removed at reduced pressure, water was added (10 mL) and the obtained solid was filtered and recrystallized from ethanol.[83]

1,3-Diphenyl-2-thioxodihydropyrimidine-4,6(1*H*,5*H*)-dione (5a)

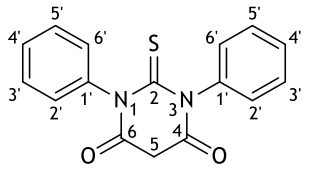

From 1,3-diphenylthiourea (**3a)** (1.00 mmol, 228 mg) and malonic acid; Condition A; Yield 95%; yellow solid; mp 252-253 °C (lit.[84] 258-259 °C); FTIR υ_{max} (cm^{-1})[27] 3053, 2895, 1727 (C=O), 1707 (C=O), 1594, 1490, 1454, 1381, 1338, 1260, 1212, 1165, 1169, 1037, 1003, 927, 747, 696, 687, 667; ^{1}H-NMR (400 MHz, $CDCl_3$) δ (ppm) [27] 7.55 (m, 6H, ArC<u>H</u>), 7.21 (d, *J* = 7.3 Hz, 4H, 2' and 6' ArC<u>H</u>), 4.10 (s, 2H, 5-C<u>H</u>$_2$); ^{13}C-NMR (101 MHz, $CDCl_3$) δ (ppm)[27] 181.64 (2-<u>C</u>S), 163.32 (4 and 5-<u>C</u>O), 138.75 (Ar<u>C</u>), 129.68 (Ar<u>C</u>H), 129.20 (Ar<u>C</u>H), 128.64 (Ar<u>C</u>H), 41.23 (5-<u>C</u>H$_2$); SMILES S=C(N(C(CC1=O)=O)C2=CC=CC=C2)N1C3=CC=CC=C3.

1,3-Diphenylpyrimidine-2,4,6(1*H*,3*H*,5*H*)-trione (5b)

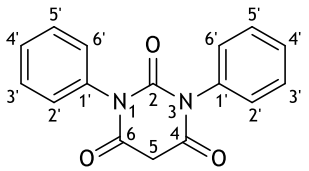

From 1,3-diphenylurea (**3p)** (1.00 mmol, 212 mg) and malonic acid; Condition A; Yield 65%; yellow solid; mp 241-242 °C (lit.[85] 222-223 °C); FTIR υ_{max} (cm^{-1}) 3064, 2898, 1683 (C=O), 1595, 1490, 1455, 1388, 1354, 1296, 1253, 1220, 1196, 1178, 1071, 1027, 1003, 931, 811, 752, 701, 690; ^{1}H-NMR (400 MHz, $CDCl_3$) δ (ppm) 7.48 (m, 6H, ArC<u>H</u>), 7.26 (d, *J* = 7.0 Hz, 4H, 2'- and 6'-ArC<u>H</u>), 4.04 (s, 2H, 5-C<u>H</u>$_2$); SMILES O=C(N(C(CC1=O)=O)C2=CC=CC=C2)N1C3=CC=CC=C3.

1-(4-Chlorophenyl)-3-phenyl-2-thioxodihydropyrimidine-4,6(1*H*,5*H*)-dione (5c)

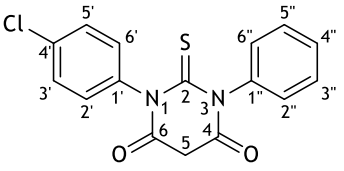

From 1-(4-chlorophenyl)-3-phenylthiourea (**3i)** (1.00 mmol, 262 mg) and malonic acid; Condition A; Yield 78%; light yellow solid; mp 259-260 ºC; FTIR υ_{max} (cm^{-1}) 3091, 2897, 1722 (C=O), 1701 (C=O), 1595, 1488, 1380, 1337, 1257, 1214, 1197, 1178, 1085, 1011, 955, 928, 829, 794, 750, 727, 709, 690, 666; ^{1}H-NMR (400 MHz, $CDCl_3$) δ (ppm) 7.58 – 7.43 (m, 6H, ArC<u>H</u>), 7.21 (d, *J* = 7.0 Hz, 2H, ArC<u>H</u>), 7.15 (d, *J* = 8.6 Hz, 2H, ArC<u>H</u>), 4.11 (s, 2H, 5-C<u>H</u>$_2$); SMILES S=C(N(C(CC1=O)=O)C2=CC=C(Cl)C=C2)N1C3=CC=CC=C3.

1-(4-Fluorophenyl)-3-phenyl-2-thioxodihydropyrimidine-4,6(1*H*,5*H*)-dione (5d)

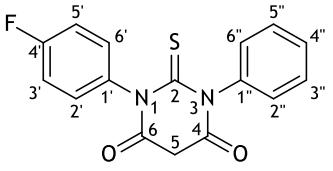

From 1-(4-fluorophenyl)-3-phenylthiourea (**3j)** (1.00 mmol, 246 mg) and malonic acid; Condition A; Yield 71%; light yellow solid; mp 238-239 ºC; FTIR υ_{max} (cm^{-1}) 3065, 2897, 1723 (C=O), 1700 (C=O), 1597, 1504, 1455, 1381, 1336, 1259, 1381, 1336, 1259, 1212, 1196, 1178, 1150, 1093, 928, 834, 822, 779, 744, 692, 654.95; ^{1}H-NMR (400 MHz, $CDCl_3$)

δ (ppm) 7.52 (d, *J* = 7.4 Hz, 2H, ArC<u>H</u>), 7.33 – 7.13 (m, 7H, ArC<u>H</u>), 4.13 (s, 2H, 5-C<u>H</u>$_2$); SMILES S=C(N(C(CC1=O)=O)C2=CC=C(F)C=C2)N1C3=CC=CC=C3.

1-(4-Iodophenyl)-3-phenyl-2-thioxodihydropyrimidine-4,6(1*H*,5*H*)-dione (5e)

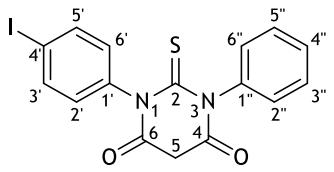

From 1-(4-iodophenyl)-3-phenylthiourea (**3k)** (1.00 mmol, 354 mg) and malonic acid; Condition A; Yield 71%; beige solid; mp 230-231 ºC; FTIR υ_{max} (cm^{-1}) 3075, 2897, 1726 (C=O), 1697 (C=O), 1639, 1595, 1557, 1481, 1456, 1379, 1363, 1325, 1255, 1212, 1197, 1171, 1093, 1055, 1034, 1012, 1002, 953, 927, 823, 802, 787, 762, 747, 732, 715, 703, 688, 664; ^{1}H-NMR (400 MHz, $CDCl_3$) δ (ppm) 7.81 – 7.71 (m, 2H, ArCH), 7.53 – 7.33 (m, 3H, ArCH), 7.23-7.09 (m, 2H, ArCH) and 6.97 - 6.87 (m, 2H, ArCH), 4.04 (d, J = 5.7 Hz, 1H, 5-C<u>H</u>$_2$); SMILES S=C(N(C(CC1=O)=O)C2=CC=C(I)C=C2)N1C3=CC=CC=C3.

1,3-Dimethyl-2-thioxodihydropyrimidine-4,6(1*H*,5*H*)-dione (5f)

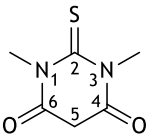

From 1,3-dimethylthiourea (**3q)** (1.00 mmol, 105 mg) and malonic acid; Condition B; Yield 70%; yellow solid; mp 193-194 °C; FTIR υ_{max} (cm^{-1}) 3101, 2949, 1704 (C=O), 1672 (C=O), 1633, 1540, 1473, 1434, 1387, 1321, 1257, 1235, 1201, 1175, 1095, 903, 788, 691, 644; ^{1}H-NMR (400 MHz, DMSO-d_6) δ (ppm) 3.77 (s, 2H, 5-C<u>H</u>$_2$), 3.62 (s, 6H, 1- and 3-NC<u>H</u>$_3$); SMILES S=C(N(C(CC1=O)=O)C)N1C.

5.1.1.3. 5-(2-Nitrobenzylidene)pyrimidines

To a solution of 1,3-disubstituted(thio)barbituric acids **5** (1.00 mmol) in water (5 mL), 2-nitrobenzaldehyde (1.00 mmol, 154 mg) was added and refluxed for 2 h. After cooling, the solid was filtered, washed with water (5 mL), ethanol (5 mL) and diethyl ether (5 mL) to give the following 5-(2-nitrobenzylidene)pyrimidines:[37]

5-(2-Nitrobenzylidene)-2-thioxodihydropyrimidine-4,6(1*H*,5*H*)-dione (6a)

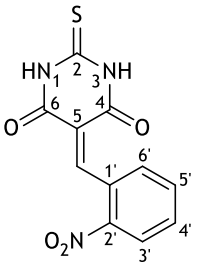

From thiobarbituric acid **(5g)** (1.00 mmol, 147 mg) and 2-nitrobenzaldehyde; Yield 90%; pale yellow solid; mp 239-241 °C (lit.[86] 246-250 ºC); FTIR υ_{max} (cm^{-1})[27] 3255 (N-H), 3156, 2876, 1718 (C=O), 1692 (C=O), 1626, 1540, 1513 (N-O), 1439, 1351 (N-O), 1288, 1203, 1141, 785, 759, 732; ^{1}H-NMR (400 MHz, DMSO-d_6) δ (ppm)[27] 12.56 (s, 1H, N<u>H</u>), 12.33 (s, 1H, N<u>H</u>), 8.63 (s, 1H, 5-CC<u>H</u>), 8.24 (dd, *J* = 8.3 and 1.0 Hz, 1H, 3'-ArC<u>H</u>), 7.80 (td, *J* = 7.6 and 1.1 Hz, 1H, 5'-

ArCH), 7.72-7.66 (m, 1H, 4'-ArCH), 7.62 (dt, *J* = 7.7 and 1.2 Hz, 1H, 6'-ArCH); ^{13}C-NMR (101 MHz, DMSO-d_6) δ (ppm)[27] 179.05 (2-CS), 160.63 (CO), 159.18 (CO), 153.31 (5-CCH), 146.28 (2'-ArC), 133.77 (5'-ArCH), 131.58 (1'-ArC), 130.49 (4'-ArCH), 130.39 (6'-ArCH), 124.08 (3'-ArCH), 120.61 (5-C); SMILES S=C(NC(/C1=C/C2=C([N+]([O-])=O)C=CC=C2)=O)NC1=O.

5-(2-Nitrobenzylidene)pyrimidine-2,4,6(1*H*,3*H*,5*H*)-trione (6b)

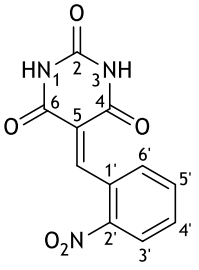

From barbituric acid **(5h)** (1.00 mmol, 131 mg) and 2-nitrobenzaldehyde; Yield 97%; white solid; mp 274-275 ºC (lit.[87] 274-276 ºC); FTIR υ_{max} (cm^{-1})[27] 3230 (N-H), 3070, 2849, 1739 (C=O), 1676 (C=O), 1597, 1516 (N-O), 1434, 1368 (N-O), 1341, 1312, 1218, 848, 791, 803, 735, 710; ^{1}H-NMR (400 MHz, DMSO-d_6) δ (ppm)[27] 11.49 (s, 1H, NH), 11.24 (s, 1H, NH), 8.60 (s, 1H, 5-CCH), 8.23 (d, *J* = 7.9 Hz, 1H, 3'-ArCH), 7.79 (t, *J* = 7.4 Hz, 1H, 5'-ArCH), 7.68 (t, *J* = 7.7 Hz, 1H, 4'-ArCH), 7.57 (d, *J* = 7.7 Hz, 1H, 6'-ArCH); ^{13}C-NMR (101 MHz, DMSO-d_6) δ (ppm)[27] 162.38 (CO), 161.20 (CO), 152.45 (5-CCH), 150.26 (2-CO), 146.28 (2'-ArC), 133.76 (5'-ArCH), 131.72 (1'-ArC), 130.41 (4'-ArCH), 130.16 (6'-ArCH), 124.06 (3'-ArCH), 120.54 (5-C); SMILES O=C(/C(C(N1)=O)=C/C2=C([N+]([O-])=O)C=CC=C2)NC1=O.

5-(2-Nitrobenzylidene)-1,3-diphenyl-2-thioxodihydropyrimidine-4,6(1*H*,5*H*)-dione (6c)

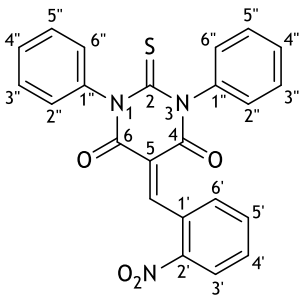

From 1,3-diphenylthiobarbituric acid **(5a)** (1.00 mmol, 296 mg) and 2-nitrobenzaldehyde; Yield 90%; pale orange solid; mp 235-236 ºC decomposes (lit.[88] 232 ºC); FTIR υ_{max} (cm^{-1})[27] 3032, 1717 (C=O), 1691 (C=O), 1624, 1607, 1591, 1520 (N-O), 1486, 1353 (N-O), 1325, 1265, 1189, 1156, 788, 781, 752, 722, 692; ^{1}H-NMR (400 MHz, DMSO-d_6) δ (ppm)[27] 8.80 (s, 1H, 5-CCH), 8.19 (d, *J* = 8.2 Hz, 1H), 7.71 (t, *J* = 7.5 Hz, 1H, ArCH), 7.59 (t, *J* = 7.9 Hz, 2H, ArCH), 7.45 (t, *J* = 7.6 Hz, 2H, ArCH), 7.40-7.28 (m, 6H, ArCH), 7.20 (d, *J* = 7.7 Hz, 2H, ArCH); ^{13}C-NMR (101 MHz, DMSO-d_6) δ (ppm)[27] 181.43 (2-CS), 160.28 (CO), 158.81 (CO), 155.03 (5-CCH), 146.20 (2'-ArC), 140.02 (ArC), 139.72 (ArC), 134.04 (5'-ArCH), 131.76 (1'-ArC), 130.40 (4'-ArCH), 130.16 (6'-ArCH), 129.05 (ArCH), 128.88 (ArCH),128.85 (ArCH),128.83 (ArCH),128.28 (ArCH), 128.10 (ArCH), 124.12 (3'-ArCH), 121.30 (5-C); SMILES S=C(N(C1=CC=CC=C1)C(/C2=C/C3=C([N+]([O-])=O)C=CC=C3)=O)N (C4=CC=CC=C4)C2=O.

1,3-Dimethyl-5-(2-nitrobenzylidene)pyrimidine-2,4,6(1*H*,3*H*,5*H*)-trione (6d)

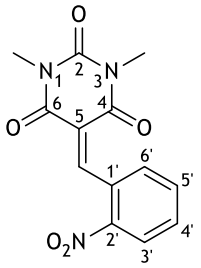

From 1,3-dimethylbarbituric acid **(5i)** (1.00 mmol, 159 mg) and 2-nitrobenzaldehyde; Yield 97%; white solid; mp 158-159 ºC (lit.[88] 159-161 ºC); FTIR υ_{max} (cm^{-1})[27] 3028, 2950, 1663 (C=O), 1603, 1518 (N-O), 1457, 1415, 1377 (N-O), 1342, 1323, 1161, 1092, 1057, 787, 754, 737, 692; ^{1}H-NMR (400 MHz, DMSO-d_6) δ (ppm)[27] 8.71 (s, 1H, 5-CC<u>H</u>), 8.26 (dd, *J* = 8.3 and 1.2 Hz, 1H, 3'-ArC<u>H</u>), 7.80 (td, *J* = 7.6 and 1.3 Hz, 1H, 5'-ArC<u>H</u>), 7.69 (t, J = 7.7 Hz, 1H, 4'-ArC<u>H</u>), 7.53 (d, *J* = 7.8 Hz, 1H, 6'-ArC<u>H</u>), 3.25 (s, 3H, NC<u>H</u>$_3$), 3.06 (s, 3H, NC<u>H</u>$_3$); ^{13}C-NMR (101 MHz, DMSO-d_6) δ (ppm)[27] 161.20 (<u>C</u>O), 159.96 (<u>C</u>O), 153.65 (5-C<u>C</u>H), 151.10 (2-<u>C</u>O), 146.15 (2'-Ar<u>C</u>), 133.90 (5'-Ar<u>C</u>H), 132.01 (1'-Ar<u>C</u>), 130.09 (4'-Ar<u>C</u>H), 130.02 (6'-Ar<u>C</u>H), 124.06 (3'-Ar<u>C</u>H), 120.14 (5-<u>C</u>), 28.44 (N-<u>C</u>H$_3$), 27.82 (N-<u>C</u>H$_3$); SMILES O=C(N(C)C(/C1=C/C2=C([N+]([O-])=O)C=CC=C2)=O)N(C)C1=O.

5-(2-Nitrobenzylidene)-1,3-diphenylpyrimidine-2,4,6(1*H*,3*H*,5*H*)-trione (6e)

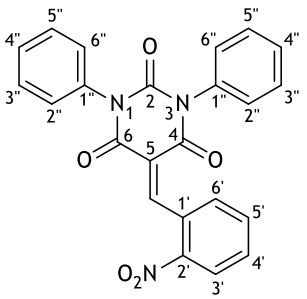

From 1,3-diphenylbarbituric acid **(5b)** (1.00 mmol, 280 mg) and 2-nitrobenzaldehyde; Yield 82%; white solid; mp 239-240 ºC; FTIR υ_{max} (cm^{-1}) 3028, 1746 (C=O), 1681 (C=O), 1627, 1608, 1574, 1519 (N-O), 1491, 1404, 1355 (N-O), 1325, 1247, 1210, 1185, 1169, 942, 794, 762, 750, 735, 709, 695, 671, 558, 545; ^{1}H-NMR (400 MHz, DMSO-d_6) δ (ppm) 8.82 (s, 1H, 5-CC<u>H</u>), 8.25 (dd, *J* = 8.2 and 1.2 Hz, 1H, 3'-ArC<u>H</u>), 7.82 (td, *J* = 7.6 and 1.2 Hz, 1H, 5'-ArC<u>H</u>), 7.71-7.61 (m, 2H, ArC<u>H</u>), 7.57-7.50 (m, 2H, ArC<u>H</u>), 7.49-7.36 (m, 6H, ArC<u>H</u>), 7.34-7.27 (m, 2H, ArC<u>H</u>); ^{13}C-NMR (101 MHz, DMSO-d_6) δ (ppm) 161.86 (<u>C</u>=O), 160.63 (<u>C</u>=O), 154.56 (5-C<u>C</u>H), 151.05 (2-<u>C</u>O), 146.67 (2'-Ar<u>C</u>), 135.98 (Ar<u>C</u>), 135.62 (Ar<u>C</u>), 134.49 (5'-Ar<u>C</u>H), 132.36 (1'-Ar<u>C</u>), 130.69 (4'-Ar<u>C</u>H), 130.54 (6'-Ar<u>C</u>H), 129.42 (Ar<u>C</u>H), 129.32 (Ar<u>C</u>H), 129.25 (Ar<u>C</u>H), 129.02 (Ar<u>C</u>H), 128.86 (Ar<u>C</u>H), 124.58 (3'-Ar<u>C</u>H), 121.45 (5-<u>C</u>); SMILES O=C(N(C1=CC=CC=C1)C(/C2=C/C3=C([N+]([O-])=O)C=CC=C3)=O)N(C4=CC=CC=C4)C2=O.

1,3-Dimethyl-5-(2-nitrobenzylidene)-2-thioxodihydropyrimidine-4,6(1*H*,5*H*)-dione (6f)

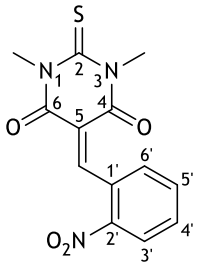

From 1,3-dimethylthiobarbituric acid **(5f)** (1.00 mmol, 172 mg) and 2-nitrobenzaldehyde; Yield 83%; light brown solid; mp 161-162 ºC; FTIR υ_{max} (cm^{-1}) 3061, 2952, 1705 (C=O), 1678 (C=O), 1632, 1599, 1570, 1518 (N-O), 1442, 1359, 1342 (N-O), 1322, 1244 (C=S), 1171, 1115, 1093, 1046, 859, 787, 730, 672, 631; ^{1}H-NMR (400 MHz, DMSO-d_6) δ (ppm) 8.78 (s, 1H, 5-CC<u>H</u>), 8.28 (d, *J* = 8.3 Hz, 1H, 3'-ArC<u>H</u>), 7.83 (t, *J* = 7.5 Hz, 1H, 5'-ArC<u>H</u>), 7.72 (t, *J* =

7.9 Hz, 1H, 4'-ArCH), 7.60 (d, *J* = 7.7 Hz, 1H, 6'-ArCH), 3,67 (s, 3H, NCH_3), 3,48 (s, 3H, NCH_3); ^{13}C-NMR (101 MHz, DMSO-d_6) δ (ppm) 180.92 (2-CS), 160.10 (CO), 158.60 (CO), 155.78 (5-CCH), 146.14 (2'-ArC), 134.00 (5'-ArCH), 131.97 (1'-ArC), 130.36 (4'-ArCH), 130.04 (6'-ArCH), 124.12 (3'-ArCH), 120.47 (5-C), 35.54 (N-CH_3), 34.96 (N-CH_3); SMILES S=C(N(C)C(/C1=C/C2=C([N+]([O-])=O)C=CC=C2)=O)N(C)C1=O.

1-(4-Chlorophenyl)-5-(2-nitrobenzylidene)-3-phenyl-2-thioxodihydropyrimidine-4,6(1*H*, 5*H*)-dione (6g)

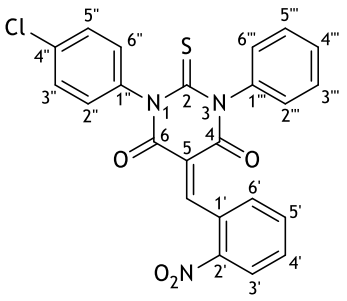

From 1-(4-chlorophenyl)-3-phenyl-2-thioxodihydropyrimidine-4,6(1*H*,5*H*)-dione **(5c)** (1.00 mmol, 331 mg) and 2-nitrobenzaldehyde; Yield 91%; beige solid; mp 238-239 ºC; FTIR υ_{max} (cm^{-1}) 3029, 1717 (C=O), 1690 (C=O), 1623, 1605, 1592, 1570, 1519 (N-O), 1488, 1454, 1393 (N-O), 1351, 1323, 1266, 1189, 1156, 1093, 1017, 922, 846, 826, 787, 775, 732, 697, 689; ^{1}H-NMR (400 MHz, DMSO-d_6) δ (ppm) 8.82 (s, 1H, 5-CCH), 8.25 (d, *J* = 8.2 Hz, 1H, 3'-ArCH), 7.98 – 7.16 (m, 12H, ArCH); ^{13}C-NMR (101 MHz, DMSO-d_6) δ (ppm) 181.34 (2-CS), 160.29 and 160.26 (CO), 158.81 and 158.79 (CO), 155.26 (5-CCH), 146.22 (2'-ArC), 139.92 and 139.62, 138.90 and 138.62, 134.08 (5'-ArCH), 132.90 and 132.76, 131.71 and 131.70 (1'-ArCH), 130.84 and 130.81, 130.50 and 130.48, 130.20 (4'-ArCH), 130.11 (6'-ArCH), 129.22, 129.12, 129.05, 128.95, 128.79, 128.36, 128.19, 124.16 (3'-ArC), 121.20 and 121.18 (5-C); SMILES S=C(N(C1=CC=C(Cl)C=C1)C(/C2=C/C3=C([N+]([O-])=O)C=CC=C3)=O)N(C4=CC=CC=C4)C2=O.

1-(4-Fluorophenyl)-5-(2-nitrobenzylidene)-3-phenyl-2-thioxodihydropyrimidine-4,6(1*H*, 5*H*)-dione (6h)

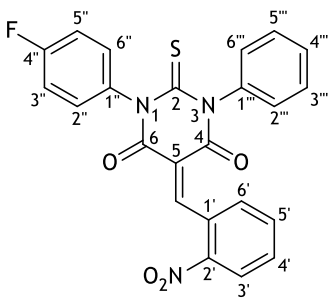

From 1-(4-fluorophenyl)-3-phenyl-2-thioxodihydropyrimidine-4,6(1*H*,5*H*)-dione **(5d)** (1.00 mmol, 314 mg) and 2-nitrobenzaldehyde; Yield 91%; beige solid; mp 249-250 ºC; FTIR υ_{max} (cm^{-1}) 3066, 1716 (C=O), 1690 (C=O), 1625, 1606, 68, 1570, 1520 (N-O), 1505, 1543, 1394 (N-O), 1351, 1325, 1268, 1222, 1189, 1152, 1090, 1071, 1016, 846, 834, 816, 787, 781, 730, 710, 689, 688; ^{1}H-NMR (400 MHz, DMSO-d_6) δ (ppm) 8.83 (s, 1H, 5-CCH), 8.26 (d, *J* = 8.3 Hz, 1H, 3'-ArCH), 7.76 (dt, *J* = 7.6 Hz, 4H, 5'-ArCH), 7.56 – 7.19 (m, 8H, ArCH); ^{13}C-NMR (101 MHz, DMSO-d_6) δ (ppm) 181.55 (2-CS), 160.37 and 160.31 (CO), 158.90 and 158.83 (CO), 155.21 (5-CCH), 146.22 (2'-ArC), 140.02 and 139.71, 136.24 and 135.94, 134.28 and 134.21, 134.09 (5'-ArCH), 131.74 (1'-ArCH), 131.02 and 130.93, 130.48 and 130.46, 130.20

(4'-ArCH), 130.12 (6'-ArCH), 129.86, 129.11, 128.94, 128.81, 128.80, 128.34, 128.17, 124.16 (3'-ArC), 121.25 and 121.22 (5-C); SMILES S=C(N(C1=CC=C(F)C=C1)C(/C2=C/C3=C([N+]([O-])=O)C=CC=C3)=O)N(C4=CC=CC=C4)C2=O.

1-(4-Iodophenyl)-5-(2-nitrobenzylidene)-3-phenyl-2-thioxodihydropyrimidine-4,6(1*H*,5*H*)-dione (6i)

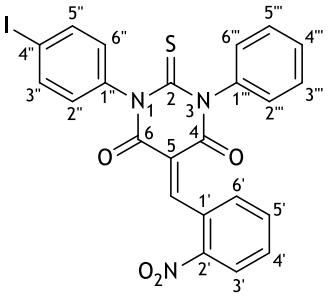

From 1-(4-iodophenyl)-3-phenyl-2-thioxodihydropyrimidine-4,6(1*H*,5*H*)-dione **(5e)** (1.00 mmol, 422 mg) and 2-nitrobenzaldehyde; Yield 93%; light brown solid; mp 193-194 ºC; FTIR υ_{max} (cm^{-1}) 3061, 1715 (C=O), 1688 (C=O), 1624, 1605, 1568, 1518 (N-O), 1480, 1392 (N-O), 1351, 1321, 1265, 1190, 1155, 1092, 1074, 1055, 1030, 1011, 921, 844, 785, 772, 733, 694; ^{1}H-NMR (400 MHz, DMSO-d_6) δ (ppm) 8.81 (s, 1H, 5-CCH), 8.25 (d, *J* = 8.0 Hz, 1H, 3'-ArCH), 7.96 – 7.08 (m, 12H, ArCH); ^{13}C-NMR (101 MHz, DMSO-d_6) δ (ppm) 181.24 (2-CS), 160.29 (CO), 158.82 (CO), 155.26 (5-CCH), 146.23 (2'-ArC), 139.93 and 139.89, 139.62 and 139.59, 138.08, 137.93, 134.30 and 134.23, 134.09 (5'-ArCH), 131.73 and 131.71 (1'-ArCH), 131.27 and 131.25, 130.52 and 130.50, 130.20 (4'-ArCH), 130.14 (6'-ArCH), 129.89, 129.14, 128.97, 128.82, 128.67, 128.39, 128.22, 124.35 (3'-ArC), 121.21 (5-C); SMILES S=C(N(C1=CC=C(I)C=C1)C(/C2=C/C3=C([N+]([O-])=O)C=CC=C3)=O)N(C4=CC=CC=C4)C2=O.

5.1.1.4. 5-(Benzisoxazol-3-ylidene)pyrimidines

To a solution of 5-(2-nitrobenzylidene)pyrimidine **6** (1.00 mmol) and tin chloride dihydrate (1.00 mmol, 226 mg) in THF (20 mL), concentrated hydrochloride acid (1 mL) was added and refluxed for 15 minutes. After cooling, the solid was filtered and washed with diethyl ether to give the following 5-(benzisoxazol-3-ylidene)pyrimidines:

5-(benzo[*c*]isoxazol-3(1*H*)-ylidene)-2-thioxodihydropyrimidine-4,6(1*H*,5*H*)-dione (7a)

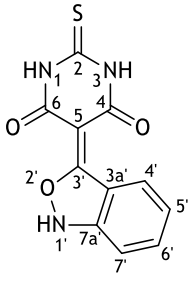

From 5-(2-nitrobenzylidene)-2-thioxodihydropyrimidine-4,6(1*H*,5*H*)-dione **(6a)** (1.00 mmol, 277 mg); Yield 87%; yellow solid; mp 207-208 ºC (lit.[37] 207-208 ºC). FTIR υ_{max} (cm^{-1})[37] 3381 (N-H), 2879, 2709, 1664 (C=O), 1607, 1506, 1466, 1357 (N-O), 1282, 1251, 1164, 1005, 939, 907, 785, 754, 714; ^{1}H-NMR (400 MHz, DMSO-d_6) δ (ppm)[37] 11.05 (s, 2H, 1- and 3-NH), 7.88 (d, *J* = 8.8 Hz, 1H, 4'-ArCH), 7.34 (d, *J* = 9.0 Hz, 1H, 7'-ArCH), 7.22 (dd, *J* = 9.0 and 6.3 Hz, 1H, 6'-ArCH), 6.73 (dd, *J* = 8.8 and 6.3 Hz, 1H, 5'-ArCH); ^{13}C-NMR (101 MHz, DMSO-d_6) δ (ppm)[37] 174.58 (2-CS), 166.10 (3'-C), 161.02 (4 and 6-CO), 156.35 (7a'-ArC), 130.32

(6'-ArCH), 125.43 (4'-ArCH), 119.34 (5'-ArCH), 114.25 (3a'-C), 113.16 (7'-ArCH), 85.07 (5-C); SMILES S=C(NC(/C1=C2ONC3=C\2C=CC=C3) =O)NC1=O.

5-(benzo[*c*]isoxazol-3(1*H*)-ylidene)pyrimidine-2,4,6(1*H*,3*H*,5*H*)-trione (7b)

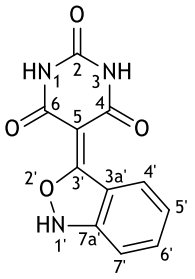

From 5-(2-nitrobenzylidene)pyrimidine-2,4,6(1*H*,3*H*,5*H*)-trione **(6b)** (1.00 mmol, 261 mg); Yield 87%; yellow solid; mp 267-268 ºC (lit.[37] 266-268 ºC); FTIR υ_{max} (cm^{-1})[37] 3174 (N-H), 2960, 2813, 1722 (C=O), 1666 (C=O), 1648, 1601, 1440, 1403, 1360 (N-O), 1320, 1286, 1238, 1142, 906, 841, 766, 752; ^{1}H-NMR (400 MHz, DMSO-d_6) δ (ppm)[37] 10.69 (s, 2H, 1- and 3-NH), 7.77 (dt, *J* = 8.8 and 1.7 Hz, 1H, 4'-ArCH), 7.46 (dt, *J* = 9.1 and 1.7 Hz, 1H, 7'-ArCH), 7.32 (ddd, *J* = 9.1, 6.4, and 0.8 Hz, 1H, 6'-ArCH), 6.89 (ddd, *J* = 8.8, 6.4, and 0.8 Hz, 1H, 5'-ArCH); ^{13}C-NMR (101 MHz, DMSO-d_6) δ (ppm)[37] 163.68 (3'-C), 162.71 (4 and 6-CO), 156.40 (7a'-ArC), 150.82 (2-CO), 131.82 (6'-ArCH), 124.15 (4'-ArCH), 122.01 (5'-ArCH), 116.21 (3a'-C), 113.76 (7'-ArCH), 82.71 (5-C); SMILES O=C(NC(/C1=C2ONC3=C\2C=CC=C3)=O) NC1=O.

5-(benzo[*c*]isoxazol-3(1*H*)-ylidene)-1,3-diphenyl-2-thioxodihydropyrimidine-4,6(1*H*,5*H*)-dione (7c)

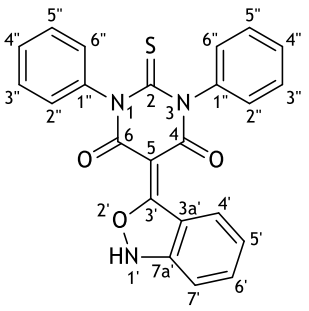

From 5-(2-nitrobenzylidene)-1,3-diphenyl-2-thioxodihydropyrimidine-4,6(1*H*,5*H*)-dione **(6c)** (1.00 mmol, 429 mg); Yield 73%; yellow solid; mp 254-255 ºC (lit.[37] 255-256 ºC); FTIR υ_{max} (cm^{-1})[37] 3141 (N-H), 2791, 2718, 1684 (C=O), 1614, 1592, 1467, 1412, 1347 (N-O), 1297, 1246, 1183, 955, 902, 764, 741, 684, 603; ^{1}H-NMR (400 MHz, DMSO-d_6) δ (ppm)[37] 7.80 (d, *J* = 8.8 Hz, 1H, 4'-ArCH), 7.40 (t, *J* = 7.7 Hz, 4H, 3''- and 5''-ArCH), 7.35 (d, *J* = 8.9 Hz, 1H, 7'-ArCH), 7.29 (t, *J* = 7.4 Hz, 2H, 4''-ArCH), 7.24-7.19 (m, 5H, 2''-, 6''- and 6'-ArCH), 6.71 (dd, *J* = 8.9 and 6.2 Hz, 1H, 5'-ArCH); ^{13}C-NMR (101 MHz, DMSO-d_6) δ (ppm)[37] 178.64 (2-CS), 166.33 (3'-C), 159.62 (4 and 6-CO), 156.11 (7a'-ArC), 141.85 (1''-ArC), 130.28 (6'-ArCH), 129.63 (2''- and 6''-ArCH), 128.42 (3''- and 5''-ArCH), 126.91 (4''-ArCH), 125.32 (4'-ArCH), 119.39 (5'-ArCH), 114.39 (3a'-ArC), 113.13 (7'-ArCH), 85.44 (5-C); SMILES S=C(N(C(/C(C1=O) =C2ONC3=C\2C=CC=C3)=O)C4=CC=CC=C4)N1C5=CC=CC=C5.

5-(benzo[*c*]isoxazol-3(1*H*)-ylidene)-1,3-dimethylpyrimidine-2,4,6(1*H*,3*H*,5*H*)-trione (7d)

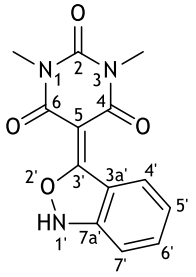

From 1,3-dimethyl-5-(2-nitrobenzylidene)pyrimidine-2,4,6(1*H*,3*H*,5*H*)-trione **(6d)** (1.00 mmol, 289 mg); Yield 84%; yellow solid; mp 212-213 ºC (lit.[37] 211-213 ºC); FTIR υ_{max} (cm^{-1})[37] 3195 (N-H), 2922, 2852, 2715, 1707 (C=O), 1644 (C=O), 1604, 1445, 1353 (N-O), 1230, 1175, 1142, 1068, 899, 760, 749, 683; ^{1}H-NMR (400 MHz, DMSO-d_6) δ (ppm)[37] 7.90 (dt, *J* = 8.8 and 1.1 Hz, 1H, 4'-ArC<u>H</u>), 7.37 (dt, *J* = 8.9 and 1.0 Hz, 1H, 7'-ArC<u>H</u>), 7.29 (ddd, *J* = 8.9, 6.2, and 1.1 Hz, 1H, 6'-ArC<u>H</u>), 6.80 (ddd, *J* = 8.8, 6.3, and 0.9 Hz, 1H, 5'-ArC<u>H</u>), 3.17 (s, 6H, 1- and 3-NC<u>H</u>$_3$); ^{13}C-NMR (101 MHz, DMSO-d_6) δ (ppm)[37] 167.45 (3'-<u>C</u>), 160.91 (4- and 6-<u>C</u>O), 155.93 (7a'-Ar<u>C</u>), 152.37 (2-<u>C</u>O), 131.15 (6'-Ar<u>C</u>H), 125.51 (4'-Ar<u>C</u>H), 120.01 (5'-Ar<u>C</u>H), 114.92 (3a'-<u>C</u>), 112.92 (7'-Ar<u>C</u>H), 82.54 (5-<u>C</u>), 27.75 (1 and 3-N<u>C</u>H$_3$); SMILES O=C(N(C(/C(C1=O)=C2ONC3=C\2C=CC=C3)=O)C)N1C.

5-(benzo[*c*]isoxazol-3(1*H*)-ylidene)-1,3-diphenylpyrimidine-2,4,6(1*H*,3*H*,5*H*)-trione (7e)

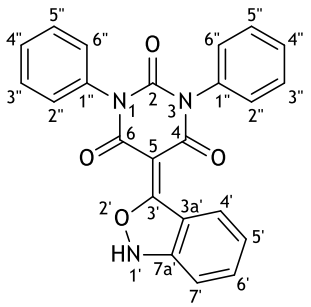

From 5-(2-nitrobenzylidene)-1,3-diphenyl-2-thioxodihydropyrimidine-4,6(1*H*,5*H*)-dione **(6e)** (1.00 mmol, 413 mg); Yield 70%; yellow solid; mp 264-265 ºC; FTIR υ_{max} (cm^{-1}) 3133 (N-H), 2945, 2784, 2708, 1719(C=O) , 1656 (C=O), 1609, 1474, 1454, 1419, 1356 (N-O), 1325, 1293, 1268, 1246, 1165, 1088, 1073, 979, 903, 804, 785, 762, 750, 737, 696, 633, 594, 583; ^{1}H-NMR (400 MHz, DMSO-d_6) δ (ppm) 7.83 (d, *J* = 8.8 Hz, 1H, 4'-ArC<u>H</u>), 7.42 (dd, *J* = 8.3 and 6.9 Hz, 4H, 3''- and 5''-ArC<u>H</u>), 7.36-7.26 (m, 7H, 7'-, 2''-, 4''- and 6''-ArC<u>H</u>), 7.21 (dd, *J* = 8.9 and 6.3 Hz, 1H, 6'-ArC<u>H</u>), 6.70 (dd, *J* = 8.8 and 6.2 Hz, 1H, 5'-ArC<u>H</u>); ^{13}C-NMR (101 MHz, DMSO-d_6) δ (ppm) 167.79 (3'-<u>C</u>), 161.23 (4 and 6-<u>C</u>O), 156.52 (7ª'-Ar<u>C</u>), 152.17 (2-<u>C</u>O), 137.84 (1''-Ar<u>C</u>), 130.81 (6'-Ar<u>C</u>H), 130.13 (2''- and 6''-Ar<u>C</u>H), 128.79 (3''- and 5''-Ar<u>C</u>H), 127.60 (4''-Ar<u>C</u>H), 126.01 (4'-Ar<u>C</u>H), 119.43 (5'-Ar<u>C</u>H), 114.49 (3a'-Ar<u>C</u>), 113.30 (7'-Ar<u>C</u>H), 85.33 (5-<u>C</u>); SMILES O=C(N(C1=CC=CC=C1)C(/C2=C3ONC4=C\3C=CC=C4)=O)N(C5=CC=CC=C5)C2=O.

5-(benzo[*c*]isoxazol-3(1*H*)-ylidene)-1,3-dimethyl-2-thioxodihydropyrimidine-4,6(1*H*,5*H*)-dione (7f)

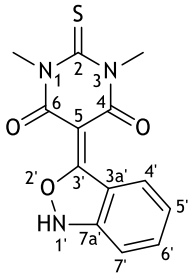

From 1,3-dimethyl-5-(2-nitrobenzylidene)-2-thioxodihydropyrimidine-4,6(1*H*,5*H*)-dione **(6f)** (1.00 mmol, 305 mg); Yield 84%; yellow solid; mp 218-219 ºC; FTIR υ_{max} (cm^{-1}) 3142 (N-H), 2947, 2788, 2718, 1667 (C=O), 1606 (C=O), 1566, 1520, 1478, 1447 (N-O), 1367, 1310, 1246, 1226, 1179, 1138, 1100, 1068, 929, 899, 778, 755, 740, 680, 635; ^{1}H-NMR (400 MHz, DMSO-d_6) δ (ppm) 7.77 (dt, *J* = 8.8 and 1.1 Hz, 1H, 4'-ArC<u>H</u>), 7.38 (dt, *J* = 9.0 and 1.0 Hz, 1H, 7'-ArC<u>H</u>), 7.24 (ddd, *J* = 9.0, 6.3 and 1.1 Hz, 1H, 6'-ArC<u>H</u>), 6.77 (ddd, *J* = 8.8, 6.3 and 0.9 Hz, 1H, 5'-ArC<u>H</u>), 3.62 (s, 6H, 1- and 3-NC<u>H</u>$_3$); ^{13}C-NMR (101 MHz, DMSO-d_6) δ (ppm) 177.12 (2-<u>C</u>S), 166.53 (3'-<u>C</u>), 159.21 (4- and 6-CO), 156.19 (7a'-Ar<u>C</u>), 130.42 (6'-ArCH), 125.06 (4'-ArCH), 119.77 (5'-ArCH), 114.78 (3a'-C), 113.32 (7'-ArCH), 84.69 (5-C), 34.86 (1- and 3-NCH_3); SMILES S=C(N(C)C(/C1=C2ONC3=C\2C=CC=C3)=O)N(C)C1=O.

5-(Benzo[*c*]isoxazol-3(1*H*)-ylidene)-1-(4-chlorophenyl)-3-phenyl-2-thioxodihydropyrimidine-4,6(1*H*,5*H*)-dione (7g)

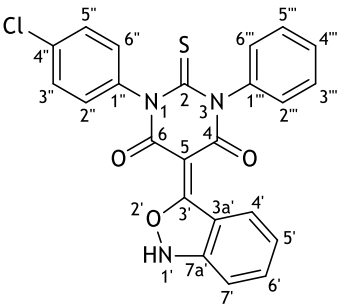

From 1-(4-chlorophenyl)-5-(2-nitrobenzylidene)-3-phenyl-2-thioxodihydropyrimidine-4,6(1*H*,5*H*)-dione **(6g)** (1.00 mmol, 464 mg); Yield 67%; yellow solid; mp 248-249 ºC; FTIR υ_{max} (cm^{-1}) 3143 (N-H), 2810, 1682 (C=O), 1621, 1510, 1466, 1404, 1344 (N-O), 1280, 1187, 1126, 1089, 1017, 957, 901, 761, 734, 698; ^{1}H-NMR (400 MHz, DMSO-d_6) δ (ppm) 7.78 (dt, *J* = 8.8, 1.1 Hz, 1H, 4'-ArC<u>H</u>), 7.48 – 7.36 (m, 4H), 7.34 (d, *J* = 9.0 Hz, 1H, 7'-ArC<u>H</u>), 7.32 – 7.24 (m, 3H), 7.24 – 7.17 (m, 3H), 6.71 (dd, *J* = 8.9, 6.2 Hz, 1H, 5'-ArC<u>H</u>); ^{13}C-NMR (101 MHz, DMSO-d_6) δ (ppm) 178.45 (2-<u>C</u>S), 166.09 (3'-<u>C</u>), 159.55 (<u>C</u>O), 159.43 (<u>C</u>O), 156.14 (7a'-Ar<u>C</u>), 141.73 (Ar<u>C</u>), 140.78 (Ar<u>C</u>), 131.56 (Ar<u>C</u>H), 131.50 (Ar<u>C</u>H), 130.27 (6'-Ar<u>C</u>H), 129.53 (Ar<u>C</u>H), 128.49 (Ar<u>C</u>H), 128.44 (4''-Ar<u>C</u>), 127.00 (Ar<u>C</u>H), 125.29 (4'-Ar<u>C</u>H), 119.36 (5'-Ar<u>C</u>H), 114.30 (3a'-Ar<u>C</u>), 113.14 (7'-Ar<u>C</u>H), 85.33 (5-<u>C</u>); SMILES S=C(N(C(/C(C1=O)=C2ONC3=C\2C=CC=C3)=O)C4=CC=C (Cl)C=C4)N1C5=CC=CC=C5.

5-(Benzo[*c*]isoxazol-3(1*H*)-ylidene)-1-(4-fluorophenyl)-3-phenyl-2-thioxodihydropyrimidine-4,6(1*H*,5*H*)-dione (7h)

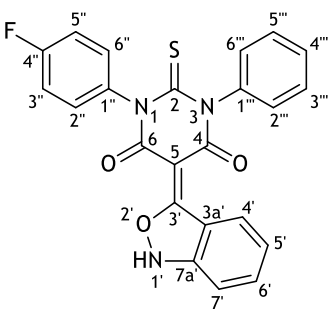

From 1-(4-fluorophenyl)-5-(2-nitrobenzylidene)-3-phenyl-2-thioxodihydropyrimidine-4,6(1*H*,5*H*)-dione **(6h)** (1.00 mmol, 447 mg); Yield 65%; yellow solid; mp 249-250 ºC; FTIR υ_{max} (cm^{-1}) 3145 (N-H), 2807, 1682 (C=O), 1622, 1596, 1506, 1466, 1350 (N-O), 1300, 1283, 1221, 1184, 1152, 1125, 1099, 1017, 957, 902, 846, 832, 781, 765, 730, 687, 656; ^{1}H-NMR (400 MHz, DMSO-d_6) δ (ppm) 7.78 (d, *J* = 8.8 Hz, 1H, 4'-ArC<u>H</u>), 7.39 (t, *J* = 7.6 Hz, 2H), 7.37 – 7.15 (m, 9H); 6.71 (dd, *J* = 8.9, 6.3 Hz, 1H, 5'-ArC<u>H</u>); ^{13}C-NMR (101 MHz, DMSO-d_6) δ (ppm) 178.76 (2-<u>C</u>S), 166.26 (3'-<u>C</u>), 162.20 (4''-Ar<u>C</u>), 159.79 (<u>C</u>O), 159.63 (<u>C</u>O), 156.10 (7a'-Ar<u>C</u>), 141.84 (Ar<u>C</u>), 138.07 (Ar<u>C</u>), 131.58 (Ar<u>C</u>H), 131.50 (Ar<u>C</u>H), 130.43 (6'-Ar<u>C</u>H), 129.56 (Ar<u>C</u>H), 128.49 (Ar<u>C</u>H), 127.03 (Ar<u>C</u>H), 125.38 (4'-Ar<u>C</u>H), 119.48 (5'-Ar<u>C</u>H), 115.36 (Ar<u>C</u>H), 115.14 (Ar<u>C</u>H), 114.39 (3a'-Ar<u>C</u>), 113.11 (7'-Ar<u>C</u>H), 85.49 (5-<u>C</u>); SMILES S=C(N(C(/C(C1=O)=C2ONC3=C\2C=CC =C3)=O)C4=CC=C(F)C=C4)N1C5=CC=CC=C5.

5-(Benzo[*c*]isoxazol-3(1*H*)-ylidene)-1-(4-iodophenyl)-3-phenyl-2-thioxodihydropyrimidine-4,6(1*H*,5*H*)-dione (7i)

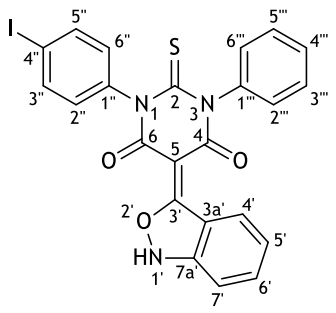

From 1-(4-fluorophenyl)-5-(2-nitrobenzylidene)-3-phenyl-2-thioxodihydropyrimidine-4,6(1*H*,5*H*)-dione **(6i)** (1.00 mmol, 555 mg); Yield 60%; yellow solid; mp 258-259 ºC; FTIR υ_{max} (cm^{-1}) 3141 (N-H), 2807, 1683 (C=O), 1623, 1513, 1623, 1463, 1346 (N-O), 1292, 1186, 1146, 1125, 1098, 1055, 1013, 1001, 956902, 833, 799, 783, 731, 693, 657; ^{1}H-NMR (400 MHz, DMSO-d_6) δ (ppm) 7.75 (t, *J* = 9.4 Hz, 3H), 7.39 (t, *J* = 7.5 Hz, 2H), 7.32 (dd, *J* = 15.8, 8.1 Hz, 2H), 7.21 (d, *J* = 7.5 Hz, 3H), 7.05 (d, *J* = 8.0 Hz, 2H), 6.71 (t, *J* = 7.5 Hz, 1H, 5'-ArC<u>H</u>); ^{13}C-NMR (101 MHz, DMSO-d_6) δ (ppm) 178.30 (2-<u>C</u>S), 166.05 (3'-<u>C</u>), 159.52 (<u>C</u>O), 159.35 (<u>C</u>O), 156.14 (7a'-Ar<u>C</u>), 141.76 (Ar<u>C</u>), 141.71 (Ar<u>C</u>), 137.35 (Ar<u>C</u>H), 132.11 (Ar<u>C</u>H), 130.22 (6'-Ar<u>C</u>H), 129.52 (Ar<u>C</u>H), 128.42 (Ar<u>C</u>H), 126.98 (Ar<u>C</u>H), 125.27 (4'-Ar<u>C</u>H), 119.31 (5'-Ar<u>C</u>H), 114.27 (3a'-Ar<u>C</u>), 113.14 (7'-Ar<u>C</u>H), 92.89 (4''-Ar<u>C</u>), 85.28 (5-<u>C</u>); SMILES S=C(N(C(/C(C1=O)=C2ONC3=C\2C=CC=C3)=O)C4=CC=C(I)C=C4)N1C5=CC=CC=C5.

5.1.2. Spiroindolin-3-one(thio)barbiturates

The spiroindolin-3-one(thio)barbiturates were obtained by the following conditions:

Condition A: A suspension of 5-(benzisoxazol-3-ylidene)pyrimidine **7** (100 mg) in DMF (1 mL), was heated at 100°C. The reaction was followed by TLC (DCM/MeOH 10%). Once completed, the DMF was removed at reduced pressure and the product was extracted with EtOAc (10 mL). The solvent was evaporated, and at the obtained oil, 10 mL of water was added. The solid precipitated was filtered, washed with water (5 mL) and diethyl ether (5 mL).

Condition B: 5-(Benzisoxazol-3-ylidene)pyrimidines **7** (100 mg) was heated at 210 ºC for 5 minutes. The product was extracted with EtOAc (10 mL). The solvent was evaporated, and at the obtained oil, 10 mL of water was added. The solid precipitated was filtered, washed with water (5 mL) and diethyl ether (5 mL).

Condition C: A suspension of 5-(benzisoxazol-3-ylidene)pyrimidines **7** (100 mg) in DMF (1 mL) was irradiated with light at a temperature of 50°C. The reaction was followed by TLC (DCM/MeOH 10%). Once completed, the DMF was removed at reduced pressure and the product was extracted with EtOAc (10 mL). The solvent was evaporated, and at the obtained oil, 10 mL of water was added. The solid precipitated was filtered, washed with water (5 mL) and diethyl ether (5 mL).

Condition D: At a suspension of 5-(benzisoxazol-3-ylidene)pyrimidines (100 mg) in DMF (1 mL), mws were irradiated at a temperature of 100°C. The reaction was followed by TLC (DCM/MeOH 10%). Once completed, the DMF was removed at reduced pressure and the product was extracted with EtOAc (10 mL). The solvent was evaporated, and at the obtained oil, 10 mL of water was added. The solid precipitated was filtered, washed with water (5 mL) and diethyl ether (5 mL).

2'-Thioxo-2',3'-dihydro-4'*H*-spiro[indoline-2,5'-pyrimidine]-3,4',6'(1'*H*)-trione (8a)

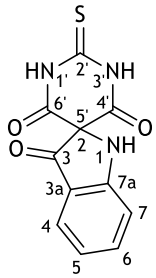

From 5-(benzo[*c*]isoxazol-3(1*H*)-ylidene)-2-thioxodihydropyrimidine-4,6(1*H*,5*H*)-dione **(7a)**; Condition A, yield 70%; Condition B, yield 10%; Condition C, yield 40%; Condition D, yield 85%; light yellow solid; mp 219-220 ºC; FTIR υ_{max} (cm^{-1}) 3508 (N-H), 3355 (N-H), 3201, 2887, 1700 (C=O), 1608, 1591, 1528, 1484, 1466, 1434, 1382, 1347, 1318, 1261, 1210, 1187, 1144, 1131, 1102, 929, 891, 852, 740, 695; ^{1}H-NMR (400 MHz, DMSO-d_6) δ (ppm) 12.63 (s, 2H, 1'- and 3'-N<u>H</u>), 7.57 (ddd, *J* = 8.4, 7.0 and 1.3 Hz, 1H, 6-ArC<u>H</u>), 7.47 (s, 1H, 1-N<u>H</u>), 7.42 (dt, *J* = 7.9 and 0.7 Hz, 1H, 4-ArC<u>H</u>), 7.17 (dt, *J* = 8.3 and 0.9 Hz, 1H, 7-ArC<u>H</u>), 6.81 (ddd, *J* =7.8, 7.0 and 0.9 Hz, 1H, 5-ArC<u>H</u>); ^{13}C-NMR (101 MHz, DMSO-d_6) δ (ppm) 189.32 (3-<u>C</u>O), 179.66 (2'-<u>C</u>S), 164.99

(7a-Ar<u>C</u>), 162.42 (4'- and 6'-<u>C</u>O), 138.94 (6-Ar<u>C</u>H), 125.35 (4-ArCH), 119.07 (5-Ar<u>C</u>H), 114.27 (3a-Ar<u>C</u>), 113.18 (7-Ar<u>C</u>H), 78.33 (2,5'-<u>C</u>); SMILES S=C(NC(C12C(C(C=CC=C3)=C3N2)=O)=O)NC1=O.

2'*H*-Spiro[indoline-2,5'-pyrimidine]-2',3,4',6'(1'*H*,3'*H*)-tetraone (8b)

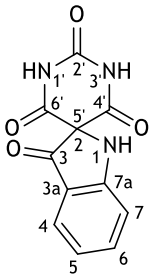

From 5-(benzo[*c*]isoxazol-3(1*H*)-ylidene)pyrimidine-2,4,6(1*H*,3*H*,5*H*)-trione **(7b)**; Condition D, Yield 70%; light yellow solid; mp 198-199 ºC; FTIR υ_{max} (cm^{-1}) 3391 (N-H), 3081 (N-H), 2861, 1762 (C=O), 1693 (C=O), 1609, 1589, 1486, 1464, 1367, 1325, 1267, 1243, 1192, 1141, 1102, 1046, 951, 899, 846, 750, 668; ^{1}H-NMR (400 MHz, DMSO-d_6) δ (ppm) 11.62 (s, 2H, 1' and 3'-N<u>H</u>), 7.57 (ddd, *J* = 8.5, 7.2 and 1.4 Hz, 1H, 6-Ar<u>C</u>H), 7.50 (s, 1H, 1-N<u>H</u>), 7.42 (d, *J* = 7.8 Hz, 1H, 4-Ar<u>C</u>H), 7.16 (d, *J* = 8.3 Hz, 1H, 7-Ar<u>C</u>H), 6.80 (t, *J* = 7.4 Hz, 1H, 5-Ar<u>C</u>H); ^{13}C-NMR (101 MHz, DMSO-d_6) δ (ppm) 189.63 (3-CO), 165.10 (7a-Ar<u>C</u>), 164.02 (4'- and 6'-<u>C</u>O), 150.51 (2'-<u>C</u>O), 138.91 (6-Ar<u>C</u>H), 125.34 (4-Ar<u>C</u>H), 119.00 (5-Ar<u>C</u>H), 114.45 (3a-Ar<u>C</u>), 113.14 (7-Ar<u>C</u>H), 78.05 (2,5'-<u>C</u>); SMILES O=C(NC(C12C(C(C=CC=C3)=C3N2)=O)=O)NC1=O.

1',3'-Diphenyl-2'-thioxo-2',3'-dihydro-4'*H*-spiro[indoline-2,5'-pyrimidine]-3,4',6'(1'*H*)-trione (8c)

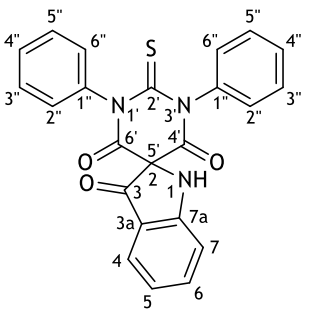

From 5-(benzo[*c*]isoxazol-3(1*H*)-ylidene)-1,3-diphenyl-2-thioxo-dihydropyrimidine-4,6(1*H*,5*H*)-dione **(7c)**; Condition D, Yield 78%; mp 170-171 ºC; brown solid; FTIR υ_{max} (cm^{-1}) 3351 (N-H), 3063, 1698 (C=O), 1609, 1592, 1488, 1467, 1455, 1346, 1323, 1282, 1260, 1195, 1170, 1149, 1131, 1103, 1071, 961, 905, 877, 749, 724, 692; ^{1}H-NMR (400 MHz, DMSO-d_6) δ (ppm) 8.04 (s, 1H, 1-N<u>H</u>), 7.64 (ddd, *J* = 8.4, 7.0 and 1.4 Hz, 1H, 6-Ar<u>C</u>H), 7.58 – 7.38 (m, 7H, Ar<u>C</u>H), 7.34 (dt, *J* = 8.0 and 1.6 Hz, 2H, Ar<u>C</u>H), 7.22 (d, *J* = 8.3 and 0.9 Hz, 1H, 7-ArCH), 7.06 (dt, *J* = 7.8 and 1.7 Hz, 2H, Ar<u>C</u>H), 6.89 (t , *J* = 8.0 and 1.6 Hz, 1H, 5-ArCH); ^{13}C-NMR (101 MHz, DMSO-d_6) δ (ppm) 188.61 (3-<u>C</u>O), 182.20 (2'-<u>C</u>S), 165.28 (7a-Ar<u>C</u>), 161.87 (4' and 6'-<u>C</u>O), 140.00 (6-Ar<u>C</u>H), 139.90 (1''-Ar<u>C</u>), 129.89 (Ar<u>C</u>H), 129.76 (Ar<u>C</u>H), 129.48 (Ar<u>C</u>H), 129.07 (Ar<u>C</u>H), 128.48 (Ar<u>C</u>H), 126.29 (4-Ar<u>C</u>H), 120.11 (5-Ar<u>C</u>H), 114.17 (3a-Ar<u>C</u>), 113.95 (7-Ar<u>C</u>H), 80.30 (2,5'-<u>C</u>); SMILES S=C(N(C1=CC=CC=C1)C(C23C(C(C=CC=C4)=C4N3)=O)=O)N(C5=CC=CC=C5)C2=O.

1',3'-Dimethyl-2'*H*-spiro[indoline-2,5'-pyrimidine]-2',3,4',6'(1'*H*,3'*H*)-tetraone (8d)

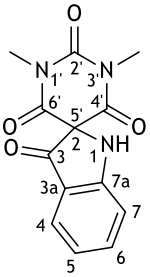

From 5-(benzo[*c*]isoxazol-3(1*H*)-ylidene)-1,3-dimethylpyrimidine-2,4,6(1*H*,3*H*,5*H*)-trione **(7d)**; Condition D, Yield 75 %; light yellow solid; mp 222-223C; FTIR υ_{max} (cm^{-1}) 3356 (N-H), 2958, 1748, 1720 (C=O), 1669 (C=O), 1608, 1589, 1487, 1466, 1438, 1418, 1370, 1327, 1285, 1259, 1223, 1197, 1148, 1116, 1102, 1065, 978, 929, 892, 751, 670; ^{1}H-NMR (400 MHz, DMSO-d_6) δ (ppm) 7.79 (s, 1H, 1-NH), 7.60 (ddd, *J* = 8.4, 6.9 and 1.4 Hz, 1H, 6-ArCH), 7.41 (d, *J* = 7.8 Hz, 1H, 4-ArCH), 7.18 (d, *J* = 8.4 Hz, 1H, 7-ArCH), 6.82 (t, *J* =7.4 Hz, 1H, 5-ArCH), 3.19 (s, 6H, 1'- and 3'-NCH_3); ^{13}C-NMR (101 MHz, DMSO-d_6) δ (ppm) 188.90 (3-CO), 165.13 (7a-ArC), 162.88 (4' and 6'-CO), 151.46 (2'-CO), 139.22 (6-ArCH), 125.51 (4-ArCH), 119.25 (5-ArCH), 113.91 (3a-ArC), 113.24 (7-ArCH), 78.35 (2,5'-C), 29.11 (1'- and 3'-NCH3); SMILES O=C(N(C)C(C12C(C(C=CC=C3)=C3N2)=O)=O)N(C)C1=O.

1',3'-Diphenyl-2'*H*-spiro[indoline-2,5'-pyrimidine]-2',3,4',6'(1'*H*,3'*H*)-tetraone (8e)

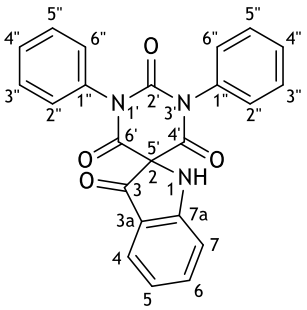

From 5-(benzo[*c*]isoxazol-3(1*H*)-ylidene)-1,3-diphenylpyrimidine-2,4,6(1*H*,3*H*,5*H*)-trione **(7e)**; Condition D, Yield 80%; mp 188-189 ºC; light yellow solid; FTIR υ_{max} (cm^{-1}) 3398 (N-H), 3065, 2929, 1688 (C=O), 1660 (C=O), 1609, 1488, 1469, 1455, 1375, 1326, 1284, 1257, 1198, 1150, 1092, 971, 913, 887, 739, 693, 664, 611, 571; ^{1}H-NMR (400 MHz, DMSO-d_6) δ (ppm) 8.06 (s, 1H, 1-NH), 7.64 (ddd, *J* = 8.3, 7.0 and 1.3 Hz, 1H, 6-ArCH), 7.59 – 7.42 (m, 7H, ArCH), 7.26 (d, *J* = 7.5 Hz, 4H, ArCH), 7.22 (d, *J* = 8.3 Hz, 1H, 7-ArCH), 6.89 (ddd, *J* = 7.8, 7.0 and 0.8 Hz, 1H, 5-ArCH); ^{13}C-NMR (101 MHz, DMSO-d_6) δ (ppm) 188.57 (3-CO), 165.10 (7a-ArC), 162.58 (4' and 6'-CO), 150.92 (2'-CO), 139.58 (6-ArCH), 135.05 (1''-ArC), 129.38 (ArCH), 128.98 (ArCH), 128.49 (ArCH), 125.87 (4-ArCH), 119.65 (5-ArCH), 113.87 (3a-ArC), 113.52 (7-ArCH), 79.48 (2,5'-C); SMILES O=C(N(C1=CC=CC=C1)C(C23C(C(C=CC=C4)=C4N3)=O)=O)N(C5=CC=CC=C5)C2=O.

1',3'-Dimethyl-2'-thioxo-2',3'-dihydro-4'*H*-spiro[indoline-2,5'-pyrimidine]-3,4',6'(1'*H*)-trione (8f)

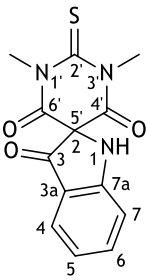

From 5-(benzo[*c*]isoxazol-3(1*H*)-ylidene)-1,3-dimethyl-2-thioxodihydropyrimidine-4,6(1*H*,5*H*)-dione **(7f)**; Condition D, Yield 85%; light yellow solid; mp 212-213 ºC; FTIR υ_{max} (cm^{-1}) 3391 (N-H), 1693 (C=O), 1608, 1586, 1484, 1464, 1430, 1352, 1324, 1291, 1281, 1245, 1220, 1193, 1144, 1064, 970, 907, 880, 750, 728, 690; ^{1}H-NMR (400 MHz, DMSO-d_6) δ (ppm) 7.82 (s, 1H, 1-NH), 7.61 (t, 1H, *J* = 7.7 Hz, 6-ArCH), 7.41 (d, 1H, *J* = 7.9 Hz, 4-ArCH), 7.20 (d, 1H, *J* = 8.4 Hz, 7-ArCH), 6.83 (t, 1H, *J* =7.4, 5-ArCH), 3.59 (s, 6H, 1'- and 3'-NCH_3); ^{13}C-NMR (101 MHz, DMSO-

d$_6$) δ (ppm) 188.24 (3-CO), 181.48 (2'-CS), 164.92 (7a-ArC), 161.84 (4' and 6'-CO), 139.37 (6-ArCH), 125.62 (4-ArCH), 119.38 (5-ArCH), 113.67 (3a-ArC), 113.30 (7-ArCH), 79.12 (2,5'-C), 36.07 (1'- and 3'-NCH$_3$); SMILES S=C(N(C)C(C12C(C(C=CC=C3)=C3N2)=O)=O)N(C)C1=O.

1'-(4-Chlorophenyl)-3'-phenyl-2'-thioxo-2',3'-dihydro-4'*H*-spiro[indoline-2,5'-pyrimidine]-3,4',6'(1'*H*)-trione (8g)

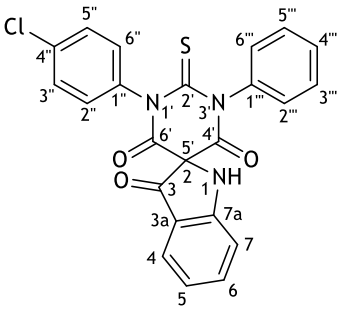

From 5-(Benzo[*c*]isoxazol-3(1*H*)-ylidene)-1-(4-chlorophenyl)-3-phenyl-2-thioxodihydropyrimidine-4,6(1*H*,5*H*)-dione **(7g)**; Condition D, yield 77%; yellow solid; mp 180-181 ºC; FTIR υ_{max} (cm^{-1}) 3350 (N-H), 3063, 1704 (C=O), 1608, 1518, 1487, 1467, 1346, 1323, 1264, 1196, 1149, 1087, 1018, 960, 879, 838, 807, 750; ^{1}H-NMR (400 MHz, DMSO-*d*$_6$) δ (ppm) 8.09 (s, 1H, 1-NH), 7.77 – 7.28 (m, 8H), 7.21 (d, *J* = 8.3 Hz, 1H, 7-ArCH), 7.15 – 7.01 (m, 2H), 6.89 (t , *J* = 8.0, 1H, 5-ArCH); ^{13}C-NMR (101 MHz, DMSO-*d*$_6$) δ (ppm) 188.00 (3-CO), 181.60 (2'-CS), 164.84 (7a-ArC), 161.35 (4' and 6'-CO), 139.58 (6-ArCH), 139.33 (ArC), 138.24 (ArC), 133.22 (4''-ArC), 131.55 (ArCH), 130.96 (ArCH), 130.05 (ArCH), 129.52 (ArCH), 129.34 (ArCH), 128.98 (ArCH), 128.67 (ArCH), 128.46 (ArCH), 127.95 (ArCH), 125.85 (4-ArCH), 119.70 (5-ArCH), 113.66 (3a-ArC), 113.52 (7-ArCH), 79.86 (2,5'-C); SMILES S=C(N(C1=CC=C(Cl)C=C1)C(C23C(C(C=CC=C4)=C4N3)=O)=O)N(C5=CC=CC=C5)C2=O.

1'-(4-Fluorophenyl)-3'-phenyl-2'-thioxo-2',3'-dihydro-4'*H*-spiro[indoline-2,5'-pyrimidine]-3,4',6'(1'*H*)-trione (8h)

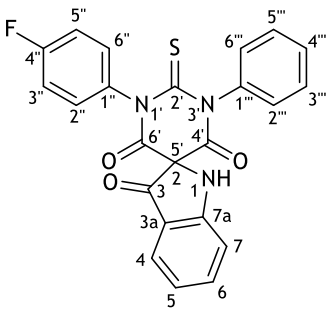

From 5-(Benzo[*c*]isoxazol-3(1*H*)-ylidene)-1-(4-fluorophenyl)-3-phenyl-2-thioxodihydropyrimidine-4,6(1*H*,5*H*)-dione **(7h)**; Condition D, yield 74%; yellow solid; mp 179-180 ºC; FTIR υ_{max} (cm^{-1}) 3354 (N-H), 3066, 1704 (C=O), 1608, 1505, 1467, 1347, 1323, 1263, 1219, 1150, 1131, 1103, 1071, 1017, 959, 906, 879, 842, 800, 778, 750, 697, 687; ^{1}H-NMR (400 MHz, DMSO-*d*$_6$) δ (ppm) 8.07 (s, 1H, 1-NH), 7.63 (t, *J* = 7.8 Hz, 1H, 6-ArCH), 7.58 – 7.25 (m, 8H), 7.21 (d, *J* = 8.3 Hz, 1H, 7-ArCH), 7.13 – 7.02 (m, 2H), 6.88 (t, *J* = 7.5 Hz, 1H, 5-ArCH); ^{13}C-NMR (101 MHz, DMSO-*d*$_6$) δ (ppm) 188.05 (3-CO), 181.82 (2'-CS), 164.84 (7a-ArC), 161.38 (4' and 6'-CO), 160.43 (4''-ArC), 139.57 (6-ArCH), 139.42, (ArC), 135.61 (ArC), 135, 58 (ArCH), 131.21 (ArCH), 131.12 (ArCH), 130.21 (ArCH), 129.46 (ArCH), 129.32 (ArCH), 128.99 (ArCH), 128.64 (ArCH), 127.97 (ArCH), 125.85 (4-ArCH), 119.67 (5-ArCH), 113.68 (3a-ArC), 113.52 (7-ArCH), 79.86 (2,5'-C); SMILES S=C(N(C1=CC=C(F)C=C1)C(C23C(C(C=CC=C4)=C4N3)=O)=O)N(C5=CC=CC=C5)C2=O.

1'-(4-Iodophenyl)-3'-phenyl-2'-thioxo-2',3'-dihydro-4'*H*-spiro[indoline-2,5'-pyrimidine]-3,4',6'(1'*H*)-trione (8i)

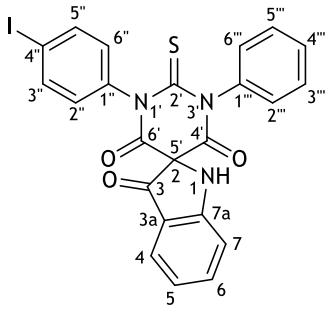

From 5-(Benzo[*c*]isoxazol-3(1*H*)-ylidene)-1-(4-chlorophenyl)-3-phenyl-2-thioxodihydropyrimidine-4,6(1*H*,5*H*)-dione **(7i)**; Condition D, yield 81%; yellow solid; mp 208-209 ºC; FTIR υ_{max} (cm^{-1}) 3358 (N-H), 3062, 1704 (C=O), 1607, 1482, 1466, 1393, 1347, 1323, 1263, 1196, 1173, 1131, 1102, 1006, 960, 878, 750, 732, 695, 638; ^{1}H-NMR (400 MHz, DMSO-d_6) δ (ppm) 8.09 (s, 1H, 1-NH), 7.86 (dd, *J* = 17.7, 8.4 Hz, 2H, 3''- and 5''-ArCH), 7.63 (t, *J* = 7.8 Hz, 1H, 6-ArCH), 7.58 – 7.28 (m, 6H), 7.21 (d, *J* = 8.3 Hz, 1H, 7-ArCH), 7.10 – 6.98 (m, 2H), 6.87 (t, *J* = 7.5 Hz, 1H, 5-ArCH); ^{13}C-NMR (101 MHz, DMSO-d_6) δ (ppm) 188.01 (3-CO), 181.50 (2'-CS), 164.84 (7a-ArC), 161.34 (4' and 6'-CO), 139.59 (6-ArCH), 139.27, (ArC), 138.38 (ArC), 132.12 (ArCH), 131.33 (ArCH), 130.38 (ArCH), 129.47 (ArCH), 129.34 (ArCH), 128.98 (ArCH), 128.67 (ArCH), 128.42 (ArCH), 127.96 (ArCH), 125.86 (4-ArCH), 119.67 (5-ArCH), 113.66 (3a-ArC), 113.53 (7-ArCH), 95.04 (4''-ArC), 79.84 (2,5'-C); SMILES S=C(N(C1=CC=C(I)C=C1)C(C23C(C(C=CC=C4)=C4N3)=O)=O)N(C5=CC=CC=C5)C2=O.

5.1.2. Nitrene trapping – Aziridines derivatives

At a suspension of 5-(benzisoxazol-3-ylidene)pyrimidine **7a** (1 mmol, 261 mg) in DMF (2.6 mL), an alkene (10 mmol) was added and mws were irradiated at a temperature of 100°C.

2-thioxo-5-(2-(2,2,3-trimethylaziridin-1-yl)benzoyl)dihydropyrimidine-4,6(1*H*,5*H*)-dione (10a)

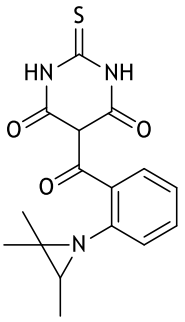

From 5-(2-nitrobenzylidene)-2-thioxodihydropyrimidine-4,6(1*H*,5*H*)-dione **(7a)** and 2-methylbut-2-ene (**9a)** (10 mmol, 700 mg). No reaction was observed by TLC.

5-(2-(2-(2-bromoethyl)aziridin-1-yl)benzoyl)-2-thioxodihydropyrimidine-4,6(1*H*,5*H*)-dione (10b)

From 5-(2-nitrobenzylidene)-2-thioxodihydropyrimidine-4,6(1*H*,5*H*)-dione **(7a)** and 4-bromobut-1-ene (**9b)** (10 mmol, 1,35 g). No reaction was observed by TLC.

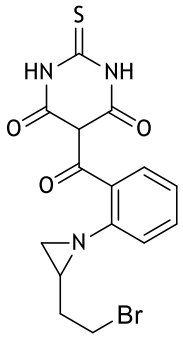

5-(2-(2-(hydroxymethyl)aziridin-1-yl)benzoyl)-2-thioxodihydropyrimidine-4,6(1*H*,5*H*)-dione (10c)

From 5-(2-nitrobenzylidene)-2-thioxodihydropyrimidine-4,6(1*H*,5*H*)-dione **(7a)** and allyl alcohol (**9c)** (10 mmol, 580 mg). No reaction was observed by TLC.

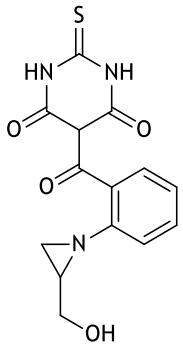

5-(2-(7-azabicyclo[4.1.0]heptan-7-yl)benzoyl)-2-thioxodihydropyrimidine-4,6(1*H*,5*H*)-dione (10d)

From 5-(2-nitrobenzylidene)-2-thioxodihydropyrimidine-4,6(1*H*,5*H*)-dione **(7a)** and cyclohexene (**9d)** (10 mmol, 820 mg). No reaction was observed by TLC.

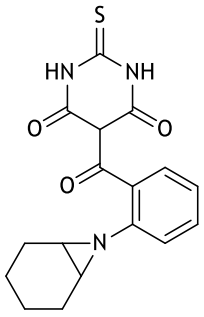

5.2. Biological evaluation

The evaluation of the biological activity of the synthetized compounds was only performed for the spiroindolin-3-one(thio)barbiturates 8**a-f**, which were pure and characterized by ^{1}H and ^{13}C-NMR.

In the cell viability assays, 96-well culture plates (Nunc, Apo-gent, Denmark) were used, while in the enzymatic studies, 96-well enzyme-linked immunosorbent assay (ELISA) plates were used.

Absorbance readings were recorded on a Bio-Rad xMark™ microplate spectrophotometer.

5.2.1. Cell viability assays

In order to evaluate the effects on cell proliferation, the compounds in study were compared with 5-FU as the positive control. The cell lines used were NHDF and MCF-7, and their culture mediums were changed every 2 to 3 days. These cells were obtained from American Type Culture Collection (ATCC), while culture media, reagents and supplements were purchased from Sigma-Aldrich.

5.2.1.1. Cells cultures

The cells were maintained in an incubator at 37 ºC in a humidified atmosphere containing 5% of CO_2. NHDF cells were cultured in Roswell Park Memorial Institute (RPMI) medium supplemented with 10% fetal bovine serum (FBS), *L*-glutamine (2 mM), 4-(2-hydroxyethyl)-1-piperazineethanesulfonic acid (HEPES) (10 mM), sodium pyruvate (1 mM) and 1% antibiotic/antimycotic (10,000 units/mL penicillin, 10 mg/mL streptomycin and 25 µg/mL amphotericin B). MCF-7 cells were cultured in high-glucose Dulbecco's modified Eagle's medium (DMEM) supplemented with 10% FBS and 1% antibiotic/antimycotic (10,000 units/mL penicillin, 10 mg/mL streptomycin and 25 µg/mL amphotericin B). These cells were used in passages P+8 to P+12 (NHDF) and P+38 (MCF-7).

5.2.1.2. Preparation of samples solutions

All the tested compounds were dissolved in DMSO in a concentration of 10 mM and stored at 4 °C. From this mother solution, several dilutions were prepared with the respective complete culture medium before each experiment. For the initial screening a concentration of 30 µM was guaranteed in each well, while for the concentration-response curves, concentrations of 0.1,

1, 10, 30, 50 and 100 μM, were used. The maximum DMSO concentration in the studies was 1% (v/v), a concentration with no significant effect on cell proliferation (data not shown).

5.2.1.3. MTT assay

The cell proliferation was evaluated by quantifying the extent of the reduction of MTT as described in Figueiredo *et al.*[27] Cells were seeded in 96-well plates (2×10^4 cells/mL) in the respective culture medium. After 48 hours of adherence they were incubated at 37 ºC with the compounds, in the different concentrations for 72 h. Untreated cells were used as negative control where 5-FU was used as positive control. At the end of incubation, the medium was removed, and the cells were washed with phosphate-buffered saline (PBS) solution (NaCl 137 mM, KCl 2.7 mM, Na_2HPO_4 10 mM and KH_2PO_4 1.8 mM (pH 7.4)), and further incubated for 4 hours with MTT solution (5 mg/mL) in PBS and incomplete culture medium. Lastly, the medium containing MTT was removed and formazan crystals were dissolved with DMSO followed by absorbance readings at 570 nm. The cytotoxicity was expressed as the relative cell proliferation in percentage in comparison with the negative control cells.

5.2.2. Xanthine Oxidase inhibitory activity assay

In order to evaluate the XO inhibitory activity, the compounds in study were compared with ALO as the positive control. The XO used was of bovine origin and was purchased from Sigma-Aldrich, as well as other reagents and supplements in the experiment.

5.2.1.1. Preparation of samples solutions

All the tested compounds were dissolved in DMSO in a concentration of 10 mM and stored at 4 °C. From these solutions, several dilutions were prepared in 50 mM dihydrogen phosphate buffer (pH 7.4) before each experiment. For the initial screening a concentration of 30 μM of each compound was guaranteed in the wells, while for the concentration-response curves, concentrations of 0.01, 0.1, 1, 7.5, 15 and 30 μM were used. The maximum DMSO concentration in the studies was 1% (v/v), a concentration with no significant effect on the enzyme activity (data not shown). Additionally, a 10 mM solution of xanthine was prepared in 25 mM aqueous solution of NaOH and was diluted to 0.42 mM with the buffer. The solution of XO (0.1 U/mL) was prepared with a dilution with buffer of the XO commercialized (4 U/mL).

5.2.1.2. Experimental procedure

The XO inhibitory activity was spectrophotometrically determined by quantifying the uric acid formation from xanthine as described in Figueiredo *et al.*[27] For each assay, 50 µL of test solution and 50 µL of a XO bovine serum suspension (0.1 U/mL) in each well of a 96-well plate was pre-incubated at 37 °C for 5 minutes. The enzymatic reaction started after the addition of 150 µL of xanthine (0.42 mM) and further incubation at 37 °C during 10 min. The absorbances readings were performed every minute at 295 nm, with 20 seconds of a constant and automatic slow stirring before each one. Dihydrogen phosphate buffer (50 mM, pH 7.4) was used as negative control, where and ALO was used as a positive control. In order to discount the absorbance of each compound, a blank assay containing 50 µL of test solution and 200 µL of buffer was performed. Two independent experiments, each one in triplicate, were performed. The percentage of enzyme inhibition for each compound was calculated according to the following formula:

$$\% \text{ of inhibition} = [1 - (Abs_{sample} - Abs_{blank\ of\ sample}) / Abs_{negative\ control}] \times 100$$

5.2.3. Statistics

The results of the cell viability assays in NHDF are representative of two independent experiments, and in the MCF-7 is represented the only experiment realized. In the XO inhibitory activity assay, the results are representative of one independent experiment. These results are expressed as mean values ± standard error of the mean (SEM). The difference between groups was considered statistically significant at $p<0.05$ (Student's *t*-test). The IC_{50} values were calculated by sigmoidal fitting analysis considering a 95% confidence interval.

5.3. *In silico* studies

5.3.1. Molecular docking

The molecular docking was performed between the compound for validation of the method, allopurinol, the spiroindolin-3-one(thio)barbiturates biologically evaluated, and the XO, at its active site.

The two-dimensional structures were drawn, and the minimization of 3D energies was performed using the drawing software CamBridgeSoft's ChemOffice v14.0. The crystallized structure of XO was obtained through the Protein Data Bank code 1VDV (1.98 Å resolution).[92] Protein and ligand (Y-700) were isolated using Chimera 1.10.2 software. AutoDock Tools 1.5.6

software was used to prepare the molecules for docking, to set the docking parameters and analyze results. All docking calculations were obtained using the AutoDock 4.0 software. The interactions between the ligand and the active site of the protein were visualized through the Discovery Studio Visualizer v16.1 software.

The protein was prepared by removing the water molecules, adding protons, Gasteiger charges and removing the non-polar hydrogens. The ligand parameters were maintained unchanged. The validation of the method was performed with the re-docking of the XO with the Y-700. The grid box was used with the dimensions of 60 x 60 x 60 Å with a spacing of 0.300 Å around the center of the co-crystallized ligand, ensuring that the docking is realized in the active site of the enzyme. For the execution of the grid the parameter library filename "AD4_Parameters.dat" was added (Attachment 1). The Lamarckian Genetic algorithm was used as the docking research method and 10 different conformations were generated.

5.3.2. ADMET properties predictions

Pharmacokinetic properties predictions were performed for the spiroindolin-3-one(thio)barbiturates synthesized by online pkCSM software at http://structure.bioc.cam.ac.uk/pkcsm/prediction, in order to predict the ADMET profile of these molecules.

Chapter 6 - References

1. Lombardino, J. G., Lowe III, J. A., The role of the medicinal chemist in drug discovery - then and now. *Nature Reviews Drug Discovery*, 3 (2004), 853-862.

2. Lemke, T. L., Williams, D. A., Roche, V. F., Zito, S. W., *Foye's Principles of Medicinal Chemistry: Seventh Edition*. 2013, pages 1-10.

3. Schmitz, R., Friedrich Wilhelm Serturner and the Discovery of Morphine. *Pharmacy in History,* 27 (1985), 61-74.

4. Dias, D. A., Urban, S., Roessner, U., A Historical Overview of Natural Products in Drug Discovery. *Metabolites*, 2 (2012), 303-336.

5. Trescot, A. M., Datta, S., Lee, M., Hans, H., Opioid pharmacology. *Pain Physician*, 11 (2008), S133-S153.

6. Patil, S. A., Role of Medicinal Chemist in the Modern Drug Discovery and Development. *Organic Chemestry: Current Research,* 1 (2012), 1-2.

7. Gupta, M., Sharma, R., Kumar, A., Docking techniques in pharmacology: How much promising? *Computational Biology and Chemistry,* 76 (2018), 210-217.

8. Pires, D. E. V., Blundell, T. L., Ascher, D. B., pkCSM: Predicting Small-Molecule Pharmacokinetic and Toxicity Properties Using Graph-Based Signatures. *Journal of Medicinal Chemistry*, 58 (2015), 4066-4072.

9. Suvarna, V., Phase IV of Drug Development. *Perspectives in Clinical Research,* 1 (2010), 57-60.

10. Kitchen, D. B., Decornez, H., Furr, J. R., Bajorath, J., Docking and scoring in virtual screening for drug discovery: methods and applications. *Nature Reviews Drug Discovery*, 3 (2004), 935-949.

11. Nantasenamat, C., Isarankura-Na-Ayudhya, C., Naenna, T., Prachayasittikul, V., A practical overview of quantitative structure-activity relationship. *Experimental and Clinical Sciences,* 8 (2009), 74-88.

12. Lipinski, C. A., Lombardo, F., Dominy, B. W., Feeney, P. J., Experimental and computational approaches to estimate solubility and permeability in drug discovery and development settings. *Advanced Drug Delivery Reviews,* 23 (1997), 3–25.

13. Lipinski, C. A., Lead- and drug-like compounds: the rule-of-five revolution. *Drug Discovery Today: Technologies,* 1 (2004), 337-341.

14. Veber, D. F., Johnson, S. R., Cheng, H. Y., Smith, B. R., Ward, K. W., Kopple, K. D., Molecular Properties That Influence the Oral Bioavailability of Drug Candidates. *Journal of Medicinal Chemistry,* 45 (2002), 2615-2623.

15. Campbell, I. B., Macdonald, S. J. F., Procopiou, P. A., Medicinal chemistry in drug discovery in big pharma: past, present and future. *Drug Discovery Today,* 23 (2018), 219-234.

16. Mitscher, L. A., Aubé, J., Dutta, A., Golden, J. E., Combinatorial Chemistry and Multiple Parallel Synthesis. *Burger's medicinal chemistry and drug discovery*, 2 (2003), 1-35.

17. Szostak, J. W., Introduction: Combinatorial Chemistry. *Chemical Reviews,* 97 (1997), 347-348.

18. Kappe, C. O., High-speed combinatorial synthesis utilizing microwave irradiation. *Current Opinion in Chemical Biology,* 6 (2002, 314-320.

19. Lidström, P., Tierney, J., Wathey, B., Westman, J., Microwave assisted organic synthesis—a review. *Tetrahedron,* 57 (2001), 9225-9283.

20. Sawada, T., Yamada, T., Microwave-specific effect on enantioselective reactions. *Journal of the Japan Petroleum Institute,* 61 (2018), 121-128.

21. Allen, D. D., Caviedes, R., Cárdenas, A. M., Shimahara, T., Segura-Aguilar, J., Caviedes, P. A., Cell lines as *in vitro* models for drug screening and toxicity studies. *Drug development and industrial pharmacy,* 31 (2005), 757-768.

22. Mosmann, T., Rapid colorimetric assay for cellular growth and survival: Application to proliferation and cytotoxicity assays. *Journal of Immunological Methods,* 65 (1983), 55-63.

23. Šmelcerović, A., Tomović, K., Šmelcerović, Ž., Petronijević, Ž., Kocić, G., Tomašič, T., Jakopin, Ž., Anderluh, M., Xanthine oxidase inhibitors beyond allopurinol and febuxostat, an overview and selection of potential leads based on *in silico* calculated physico-chemical properties, predicted pharmacokinetics and toxicity. *European Journal of Medicinal Chemistry,* 135 (2017), 491-516.

24. Kumar, R., Darpan, Sharma, S., Singh, R., Xanthine oxidase inhibitors: a patent survey. *Expert Opinion on Therapeutic Patents,* 21 (2011), 1071-1108.

25. Pacher, P., Nivorozhkin, A., Szabó, C., Therapeutic Effects of Xanthine Oxidase Inhibitors: Renaissance Half a Century after the Discovery of Allopurinol. *Pharmacological Reviews,* 58 (2006), 87-114.

26. Kuang-Hui, Y., Febuxostat: A Novel Non-Purine Selective Inhibitor of Xanthine Oxidase for the Treatment of Hyperuricemia in Gout. *Recent Patents on Inflammation & Allergy Drug Discovery,* 1 (2007), 69-75.

27. Figueiredo, J., Serrano, J. L., Cavalheiro, E., Keurulainen, L., Yli-Kauhaluoma, J., Moreira, V. M., Ferreira, S., Domingues, F. C., Silvestre, S., Almeida, P., Trisubstituted barbiturates and thiobarbiturates: Synthesis and biological evaluation as xanthine oxidase inhibitors, antioxidants, antibacterial and anti-proliferative agents. *European Journal of Medicinal Chemistry,* 143 (2018), 829-842.

28. Gupta, S., Rodrigues, L. M., Esteves, A. P., Oliveira-Campos, A. M. F., Nascimento, M. S. J., Nazareth, N., Cidade, H., Neves, M. P., Fernandes, E., Pinto, M., Cerqueira, N. M. F. S. A., Brás, N., Synthesis of N-aryl-5-amino-4-cyanopyrazole derivatives as potent xanthine oxidase inhibitors. *European Journal of Medicinal Chemistry,* 43 (2008), 771-780.

29. Baeyer, A., Mittheilungen aus dem organischen Laboratorium des Gewerbeinstitutes in Berlin: Untersuchungen über die Harnsäuregruppe. *Justus Liebigs Annalen der Chemie,* 130 (1864), 129-175.

30. Dundee, J. W., McIlroy, P. D. A., The history of the barbiturates. *Anaesthesia,* 37 (1982), 726-734.

31. López-Muñoz, F., Ucha-Udabe, R., Alamo, C., The history of barbiturates a century after their clinical introduction. *Neuropsychiatric Disease and Treatment,* 1 (2005), 329-343.

32. Mohammadi Ziarani, G., Aleali, F., Lashgari, N., Recent applications of barbituric acid in multicomponent reactions. *Royal Society of Chemestry Advances,* 6 (2016), 895-922.

33. Drews, J., Drug discovery: a historical perspective. *Science,* 287 (2000), 1960-1964.

34. Kwan, P., Brodie, M. J., Phenobarbital for the Treatment of Epilepsy in the 21st Century: A Critical Review. *Epilepsia,* 45 (2004), 1141-1149.

35. Chang, A., Kim, K., Glick, J., Anderson, T., Karp, D., Johnson, D., Phase II study of taxol, merbarone, and piroxantrone in stage IV non-small-cell lung cancer: The Eastern Cooperative Oncology Group Results. *Journal of the National Cancer Institute,* 85 (1993), 388-394.

36. Neumann, D. M., Cammarata, A., Backes, G., Palmer, G. E., Jursic, B. S., Synthesis and antifungal activity of substituted 2,4,6-pyrimidinetrione carbaldehyde hydrazones. *Bioorganic & Medicinal Chemistry,* 22 (2014), 813-826.

37. Serrano, J. L., Cavalheiro, E., Barroso, S., Romão, M. J., Silvestre, S., Almeida, P., A synthetic route to novel 3-substituted-2,1-benzisoxazoles from 5-(2-nitrobenzylidene)(thio)barbiturates. *Comptes Rendus Chimie,* 20 (2017), 990-995.

38. Dyachenko, V., Tkachev, R., Functionally-substituted alkoxyethylenes in reactions with nucleophiles: Part 2. Synthesis of noncyclic structures, benzene derivatives, 5-, 7-membered, and macroheterocycles. *Russian journal of organic chemistry,* 42 (2006), 149-171.

39. Moirangthem, N. D., Laitonjam, W. S., A new and facile synthetic approach to substituted 2-thioxoquinazolin-4-ones by the annulation of a pyrimidine derivative. *Beilstein journal of organic chemistry,* 6 (2010), 1056-1060.

40. Pati, A., Majumdar, P., Garnayak, S., Behera, A. K., Behera, R. K., Regiospecific ring closure reactions of 1, 3-diphenylthiobarbituric acid and dimedone: Formation of spiro vs fused heterocycles. *Indian Journal of Chemistry,* 53 (2014), 384-391.

41. Khan, K. M., Khan, M., Karim, A., Taha, M., Ambreen, N., Gojayev, A., Perveen, S., Choudhary, M. I., Xanthine oxidase inhibition by 5-aryledene N,N'-dimethylbarbituric acid derivatives. *Journal of the Chemical Society of Pakistan,* 35 (2013), 495-498.

42. Khan, K. M., Khan, M., Ahmad, A., Irshad, A., Kardono, L. B. S., Rahim, F., Haider, S. M., Ahmed, S., Parveen, S., Antibacterial and antifungal activities of 5-arylidene-N,N-

dimethylbarbiturates derivatives. *Journal of the Chemical Society of Pakistan,* 36 (2015), 1153-1157.

43. Jursic, B. S., A simple method for knoevenagel condensation of α,β-conjugated and aromatic aldehydes with barbituric acid. *Journal of Heterocyclic Chemistry,* 38 (2009), 655-657.

44. Yoshikazu, U., 1, 2-Benzisoxazole: A Privileged Structure with a Potential for Polypharmacology. *Current Pharmaceutical Design,* 22 (2016), 3201-3211.

45. Biton, V., Zonisamide: newer antiepileptic agent with multiple mechanisms of action. *Expert Review of Neurotherapeutics,* 6 (2014), 935-943.

46. Scott, L. J., Dhillon, S., Risperidone. *Pediatric Drugs,* 9 (2007), 343-354.

47. Friedländer, P., Henriques, R., Zur Reduktion des Orthonitrobenzaldehyds. *Berichte der deutschen chemischen Gesellschaft,* 15 (1882), 2105-2110.

48. Więcław, M., Bobin, M., Kwast, A., Bujok, R., Wróbel, Z., Wojciechowski, K., General synthesis of 2,1-benzisoxazoles (anthranils) from nitroarenes and benzylic C–H acids in aprotic media promoted by combination of strong bases and silylating agents. *Molecular Diversity,* 19 (2015), 807-816.

49. Budruev, A. V., Dzhons, D. Y., Synthesis of 2, 1-benzisoxazoles (microreview). *Chemistry of Heterocyclic Compounds,* 52 (2016), 441-443.

50. Coe, P. L., Jukes, A. E., Tatlow, J. C., Aromatic polyfluoro-compounds. Part XXXIII. The synthesis of some derivatives of 1,2,3,4-tetrafluoroacridine. *Journal of the Chemical Society,* 1 (1966), 2020-2025.

51. Hawkins, D. G., Meth-Cohn, O., An in-depth study of the azidobenzophenone-anthranil-acridone transformation. *Journal of the Chemical Society,* 1 (1983), 2077-2087.

52. Maki, Y., Hosokami, T., Suzuki, M., Reduction of N-acetyl-2-nitrodiphenylamines by triethyl phosphite: formation of dihydrophenazines involving a novel aromatic rearrangement. *Tetrahedron Letters,* 12 (1971), 3509-3512.

53. Saraswat, P., Jeyabalan, G., Hassan, M. Z., Rahman, M. U., Nyola, N. K., Review of synthesis and various biological activities of spiro heterocyclic compounds comprising oxindole and pyrrolidine moities. *Synthetic Communications,* 46 (2016), 643-1664.

54. Zheng, Y., Tice, C. M., Singh, S. B., The use of spirocyclic scaffolds in drug discovery. *Bioorganic & Medicinal Chemistry Letters,* 24 (2014), 3673-3682.

55. Bariwal, J., Voskressensky, L. G., Van der Eycken, E. V., Recent advances in spirocyclization of indole derivatives. *Chemical Society Reviews,* 47 (2018), 3831-3848.

56. Song, J. C., White, C. M., Clinical Pharmacokinetics and Selective Pharmacodynamics of New Angiotensin Converting Enzyme Inhibitors. *Clinical Pharmacokinetics,* 41 (2002), 207-224.

57. Matsumura, Y., Yokota, M., Yoshioka, H., Shibata, S., Ida, S., Takiguchi, Y., Acute Effects of Griseofulvin on the Pharmacokinetics and Pharmacodynamics of Warfarin in Rats. *Journal of International Medical Research,* 27 (1999), 167-175.

58. Płusa, T., Ochwat, A., Fenspiride in patients with acute bronchitis. *Polski merkuriusz lekarski: organ Polskiego Towarzystwa Lekarskiego,* 19 (2005), 32-36.

59. Rottmann, M., McNamara, C., Yeung, B. K., Lee, M. C., Zou, B., Russell, B., Seitz, P., Plouffe, D. M., Dharia, N. V., Tan, J., Spiroindolones, a potent compound class for the treatment of malaria. *Science,* 329 (2010), 1175-1180.

60. Kohlhoff, S. A., Huband, M. D., Hammerschlag, M. R., *In vitro* activity of AZD0914, a novel DNA gyrase inhibitor, against Chlamydia trachomatis and Chlamydia pneumoniae. *Antimicrobial agents and chemotherapy,* 58 (2014), 7595-7596.

61. Guo, C., Schedler, M., Daniliuc, C. G., Glorius, F., N-Heterocyclic Carbene Catalyzed Formal [3+2] Annulation Reaction of Enals: An Efficient Enantioselective Access to Spiro-Heterocycles. *Angewandte Chemie International Edition,* 53 (2014), 10232-10236.

62. Kong, L., Wang, M., Zhang, F., Xu, M., Li, Y., Copper-Catalyzed Oxidative Dearomatization / Spirocyclization of Indole-2-Carboxamides: Synthesis of 2-Spiro-pseudoindoxyls. *Organic Letters,* 18 (2016), 6124-6127.

63. Zhang, X., Zhou, G., Zhang, Y., Zhang-Negrerie, D., Du, Y., Zhao, K., Ring-Contraction Disproportionation/Spirocyclization Cascade Reaction of Isochromeno[4,3-b]indol-5(11*H*)-ones: Synthesis of N-Unsubstituted Spirocycles. *The Journal of Organic Chemistry,* 81 (2016), 11397-11403.

64. Chen, H., Shang, H., Liu, Y., Guo, R., Lin, W., Development of a Unique Class of Spiro-Type Two-Photon Functional Fluorescent Dyes and Their Applications for Sensing and Bioimaging. *Advanced Functional Materials,* 26 (2016), 8128-8136.

65. Marien, N., Brigou, B., Pinter, B., De Proft, F., Verniest, G., Synthesis of 2-Spiropseudoindoxyls via an Intramolecular Nitroalkyne Redox–Dipolar Cycloaddition Cascade. *Organic Letters,* 17 (2015), 270-273.

66. Zhang, B., Zhang, X., Hu, B., Sun, D., Wang, S., Zhang-Negrerie, D., Du, Y., PhI(OCOCF3)2-Mediated Construction of a 2-Spiropseudoindoxyl Skeleton via Cascade Annulation of 2-Sulfonamido-N-phenylpropiolamide Derivatives. *Organic Letters,* 19 (2017), 902-905.

67. Mu, D., Wang, X., Chen, G., He, G., Iridium-Catalyzed ortho-C(sp2)–H Amidation of Benzaldehydes with Organic Azides. *The Journal of Organic Chemistry,* 82 (2017), 4497-4503.

68. Serrano, J. L., Novos espiro(tio)barbituratos: Síntese, caracterização estrutural e avaliação biológica. Universidade da Beira Interior: 2016.

69. Lu, A., Wang, Z., Zhou, Z., Chen, J., Wang, Q., Application of “hydrogen bonding interaction” in new drug development: Design, synthesis, antiviral activity, and SARs of thiourea derivatives. *Journal of agricultural and food chemistry,* 63 (2015), 1378-1384.

70. Padiya, K. J., Gavade, S., Kardile, B., Tiwari, M., Bajare, S., Mane, M., Gaware, V., Varghese, S., Harel, D., Kurhade, S., Unprecedented “In Water” Imidazole Carbonylation: Paradigm Shift for Preparation of Urea and Carbamate. *Organic Letters,* 14 (2012), 2814-2817.

71. Wang, F., Zhao, P., Xi, C., Copper-catalyzed one-pot synthesis of 2-thioxo-2, 3-dihydroquinazolin-4 (1H)-ones from ortho-bromobenzamides and isothiocyanates. *Tetrahedron letters,* 52 (2011), 231-235.

72. Gonçalves, I. L., Davi, L., Rockenbach, L., das Neves, G. M., Kagami, L. P., Canto, R. F. S., Figueiró, F., Battastini, A. M. O., Eifler-Lima, V. L., Versatility of the Biginelli reaction: Synthesis of new biphenyl dihydropyrimidin-2-thiones using different ketones as building blocks. *Tetrahedron Letters,* 59 (2018), 2759-2762.

73. Lourenço, A. L., Saito, M. S., Dorneles, L. E. G., Viana, G. M., Sathler, P. C., Aguiar, L. C. d. S., de Pádula, M., Domingos, T. F. S., Fraga, A. G. M., Rodrigues, C. R., Synthesis and antiplatelet activity of antithrombotic thiourea compounds: biological and structure-activity relationship studies. *Molecules,* 20 (2015), 7174-7200.

74. Li, Z., Chen, Y., Yin, Y., Wang, Z., Sun, X., Convenient synthesis of unsymmetrical N, N'-disubstituted thioureas in water. *Journal of Chemical Research,* 40 (2016), 670-673.

75. Abdel-Sattar, N. E., El-Naggar, A. M., Abdel-Mottaleb, M., Novel Thiazole Derivatives of Medicinal Potential: Synthesis and Modeling. *Journal of Chemistry,* 1 (2017), 1-11.

76. Khan, K. M., Naz, F., Taha, M., Khan, A., Perveen, S., Choudhary, M. I., Voelter, W., Synthesis and *in vitro* urease inhibitory activity of *N,N′*-disubstituted thioureas. *European Journal of Medicinal Chemistry,* 74 (2014), 314-323.

77. Begum, S., Choudhary, M. I., Khan, K. M., Synthesis, phytotoxic, cytotoxic, acetylcholinesterase and butrylcholinesterase activities of *N,N′*-diaryl unsymmetrically substituted thioureas. *Natural Product Research,* 23 (2009), 1719-1730.

78. Singh, K., Sharma, S., An isocyanide based multi-component reaction under catalyst- and solvent-free conditions for the synthesis of unsymmetrical thioureas. *Tetrahedron Letters,* 58 (2017), 197-201.

79. Koshti, V. S., Thorat, S. H., Gote, R. P., Chikkali, S. H., Gonnade, R. G., The impact of modular substitution on crystal packing: the tale of two ureas. *CrystEngComm,* 18 (2016), 7078-7094.

80. Walter, W., Rueß, K.-P., Über die Struktur der Thioamide und ihrer Derivate, XIV1). Konfiguration 1.3-disubstituierter Thioharnstoffe. *Justus Liebigs Annalen der Chemie,* 746 (1971), 54-64.

81. Mohammadi, L., Zolfigol, M. A., Khazaei, A., Yarie, M., Ansari, S., Azizian, S., Khosravi, M., Synthesis of nanomagnetic supported thiourea–copper(I) catalyst and its application in the synthesis of triazoles and benzamides. *Applied Organometallic Chemistry,* 32 (2018), 1-13.

82. Schulte, H., Über die Kondensation des NN'-Diphenylthioharnstoffes mit Malonylchlorid. *Chemische Berichte,* 87 (1954), 820-824.

83. Whiteley, M. A. 3-Diphenylbarbituric acid and some coloured derivatives. *Journal of the Chemical Society,* 91 (1907), 1330-1350.

84. Botsi, S., Tsolomitis, A., One or two step acid mediated cyclocondensation process for the preparation of 5-carbethoxy-2-thiouracils from diethyl ethoxymethylenemalonate and thioureas. *Heterocyclic Communications,* 13 (2007), 229-234.

85. Manick, A.-D., Berhal, F., Prestat, G., Development of a One-Pot Four C–C Bond-Forming Sequence Based on Palladium/Ruthenium Tandem Catalysis. *Organic Letters,* 20 (2018), 194-197.

86. Kuanar, M., Mishra, B., Applicability of Williams-Norrington model for quantitative structure spectra relationship. *The National Institute of Science Communication and Information Resources,* 34 (1995), 721-723.

87. Haldar, M. K., Scott, M. D., Sule, N., Srivastava, D. K., Mallik, S., Synthesis of barbiturate-based methionine aminopeptidase-1 inhibitors. *Bioorganic & Medicinal Chemistry Letters,* 18 (2018), 2373-2376.

88. Seyyedi, N., Shirini, F., Langarudi, M. S. N., DABCO-based ionic liquids: green and recyclable catalysts for the synthesis of barbituric and thiobarbituric acid derivatives in aqueous media. *Royal Society of Chemestry Advances,* 6 (2016), 44630-44640.

89. Atkinson, R. S., 3-Acetoxyaminoquinazolinones (QNHOAc) as aziridinating agents: ring-opening of N-(Q)-substituted aziridines. *Tetrahedron,* 55 (1999), 1519-1559.

90. Sweeney, J. B., Aziridines: epoxides' ugly cousins? *Chemical Society Reviews,* 31 (2002), 247-258.

91. Shi, D. H., Huang, W., Li, C., Liu, Y.-W., Wang, S.-F., Design, synthesis and molecular modeling of aloe-emodin derivatives as potent xanthine oxidase inhibitors. *European Journal of Medicinal Chemistry,* 75 (2014), 289-296.

92. Fukunari, A., Okamoto, K., Nishino, T., Eger, B. T., Pai, E. F., Kamezawa, M., Yamada, I., Kato, N., Y-700 [1-[3-Cyano-4-(2,2-dimethylpropoxy)phenyl]-1*H*-pyrazole-4-carboxylic acid]: a potent xanthine oxidoreductase inhibitor with hepatic excretion. *Journal of Pharmacology and Experimental Therapeutics,* 311 (2004), 519-528.

93. B-Rao, C., Kulkarni-Almeida, A., Katkar, K. V., Khanna, S., Ghosh, U., Keche, A., Shah, P., Srivastava, A., Korde, V., Nemmani, K. V. S., Deshmukh, N. J., Dixit, A., Brahma, M. K., Bahirat, U., Doshi, L., Sharma, R., Sivaramakrishnan, H., Identification of novel isocytosine

derivatives as xanthine oxidase inhibitors from a set of virtual screening hits. *Bioorganic & Medicinal Chemistry,* 20 (2012), 2930-2939.

94. Kikuchi, H., Fujisaki, H., Furuta, T., Okamoto, K., Leimkühler, S., Nishino, T., Different inhibitory potency of febuxostat towards mammalian and bacterial xanthine oxidoreductases: insight from molecular dynamics. *Scientific Reports,* 2 (2012), 331-339.

Chapter 7 – Publications

Oral communication fulfilled within this dissertation

Soeiro P., Serrano J. L., Figueiredo J., Silvestre S., Almeida P., Boto R. E. F., Alternative microwave improved preparation of new spiroindolin-3-one(thio)barbiturate derivatives., Abstract book of the XIII Annual CICS-UBI Symposium (Attachment 2).

Panel communication fulfilled within this dissertation

Soeiro P., Serrano J. L., Silvestre S., Almeida P., Boto R. E. F., Synthesis of new spiroindolin-3-one (thio)barbiturate derivatives. A microwave optimized method., Abstract book of the VI ENEQUI (Attachment 3).

Scientific articles in international journals peer-reviewed referred in Journal Citation Reports (JCR) of ISI Wed of Knowledge and/or SciVerse Scopus

Serrano J. L., Soeiro P. F., Reis M. A., Silvestre S., Boto R. E. F. and Almeida P., The synthesis and process optimization of symmetric and asymmetric 3-substituted 2,1-benzisoxazoles from 5-(2-nitrobenzylidene)(thio)barbiturates., *Tetrahedron Letters* (2018) (submitted) (Attachment 4).

Chapter 8 – Attachments

Attachment 1 - "AD4_Parameters.dat" file

Provided by Dr. Renjith Raveendran Pillai of the TKM College of Arts and Science, India.

```
# $Id: AD4_parameters.dat,v 1.4 2005/10/31 18:36:45 rhuey Exp $
# AutoDock Parameters - Version 1.0

#
# AutoDock 4 coefficient with respect to original (AD2) parameters
#

FE_coeff_vdW 0.1560
FE_coeff_hbond 0.0974
FE_coeff_estat 0.1465
FE_coeff_desolv 0.1159
FE_coeff_tors 0.2744

# - Unweighted vdW and Unweighted hbond Well Depths
#
# - To obtain the Rij value for non H-bonding atoms, calculate the
# arithmetic mean of the Rii values for the two atom types.
#
# - To obtain the epsij value for non H-bonding atoms, calculate the
# geometric mean of the epsii values for the two atom types.
#
# - Note that the Rij_hb value is non-zero for heteroatoms only, and
zero for H atoms;
# to obtain the Rij_hb for an H-bond, look up for the heteroatom only;
# do not combine Rij_hb values between heteroatoms and hydrogens;
# Similarly, for epsij_hb values.
#
# For example, the Rij_hb for OA-HD H-bonds will be 1.9 Angstrom,
# and epsij_hb will be 5.0 kcal/mol .
#
# Rii Rij_hb rec_index
# Atom epsii solpar epsij_hb map_index
# Type vol hbond bond_index
# -- ---- ----- ------- -------- --- --- - -- -- --
atom_par C 4.00 0.150 33.5103 -0.00143 0.0 0.0 0 -1 -1 0 # Non H-bonding
atom_par A 4.00 0.150 33.5103 -0.00052 0.0 0.0 0 -1 -1 0 # Non H-bonding
atom_par N 3.50 0.160 22.4493 -0.00162 0.0 0.0 0 -1 -1 1 # Non H-bonding
atom_par NA 3.50 0.160 22.4493 -0.00162 1.9 5.0 4 -1 -1 1 # Acceptor 1 H-bond
atom_par NS 3.50 0.160 22.4493 -0.00162 1.9 5.0 3 -1 -1 1 # Acceptor S Spherical
atom_par OA 3.20 0.200 17.1573 -0.00251 1.9 5.0 3 -1 -1 2 # Acceptor 2 H-bonds
atom_par OS 3.20 0.200 17.1573 -0.00251 1.9 5.0 3 -1 -1 2 # Acceptor S Spherical
atom_par SA 4.00 0.200 33.5103 -0.00214 2.5 1.0 5 -1 -1 6 # Acceptor 2 H-bonds
atom_par S 4.00 0.200 33.5103 -0.00214 0.0 0.0 0 -1 -1 6 # Non H-bonding
atom_par H 2.00 0.020 0.0000 0.00051 0.0 0.0 0 -1 -1 3 # Non H-bonding
atom_par HD 2.00 0.020 0.0000 0.00051 0.0 0.0 2 -1 -1 3 # Donor 1 H-bond
atom_par HS 2.00 0.020 0.0000 0.00051 0.0 0.0 1 -1 -1 3 # Donor S Spherical
atom_par P 4.20 0.200 38.7924 -0.00110 0.0 0.0 0 -1 -1 5 # Non H-bonding
atom_par Br 4.33 0.389 42.5661 -0.00110 0.0 0.0 0 -1 -1 4 # Non H-bonding
atom_par BR 4.33 0.389 42.5661 -0.00110 0.0 0.0 0 -1 -1 4 # Non H-bonding
atom_par Ca 1.98 0.550 2.7700 -0.00110 0.0 0.0 0 -1 -1 4 # Non H-bonding
atom_par CA 1.98 0.550 2.7700 -0.00110 0.0 0.0 0 -1 -1 4 # Non H-bonding
atom_par Cl 4.09 0.276 35.8235 -0.00110 0.0 0.0 0 -1 -1 4 # Non H-binding
atom_par CL 4.09 0.276 35.8235 -0.00110 0.0 0.0 0 -1 -1 4 # Non H-binding
atom_par F 3.09 0.080 15.4480 -0.00110 0.0 0.0 0 -1 -1 4 # Non H-binding
atom_par Fe 1.30 0.010 1.8400 -0.00110 0.0 0.0 0 -1 -1 4 # Non H-bonding
atom_par FE 1.30 0.010 1.8400 -0.00110 0.0 0.0 0 -1 -1 4 # Non H-bonding
atom_par I 4.72 0.550 55.0585 -0.00110 0.0 0.0 0 -1 -1 4 # Non H-binding
atom_par Mg 1.30 0.875 1.5600 -0.00110 0.0 0.0 0 -1 -1 4 # Non H-bonding
atom_par MG 1.30 0.875 1.5600 -0.00110 0.0 0.0 0 -1 -1 4 # Non H-bonding
atom_par Mn 1.30 0.875 2.1400 -0.00110 0.0 0.0 0 -1 -1 4 # Non H-bonding
```

```
atom_par MN 1.30 0.875 2.1400 -0.00110 0.0 0.0 0 -1 -1 4 # Non H-bonding
atom_par Zn 1.48 0.550 1.7000 -0.00110 0.0 0.0 0 -1 -1 4 # Non H-bonding
atom_par ZN 1.48 0.550 1.7000 -0.00110 0.0 0.0 0 -1 -1 4 # Non H-bonding
atom_par He 2.36 0.056 15.240 -0.00110 0.0 0.0 0 -1 -1 0 # Non H-bonding
atom_par Li 2.45 0.025 12.000 -0.00110 0.0 0.0 0 -1 -1 1 # Non H-bonding
atom_par Be 2.76 0.085 12.000 -0.00110 0.0 0.0 0 -1 -1 1 # Non H-bonding
atom_par B 4.08 0.180 12.052 -0.00110 0.0 0.0 0 -1 -1 0 # Non H-bonding
atom_par Ne 3.24 0.042 15.440 -0.00110 0.0 0.0 0 -1 -1 0 # Non H-bonding
atom_par Na 3.98 0.030 12.000 -0.00110 0.0 0.0 0 -1 -1 1 # Non H-bonding
atom_par Al 4.49 0.505 11.278 -0.00110 0.0 0.0 0 -1 -1 1 # Non H-bonding
atom_par Si 4.30 0.402 12.175 -0.00110 0.0 0.0 0 -1 -1 1 # Non H-bonding
atom_par K 3.81 0.035 12.000 -0.00110 0.0 0.0 0 -1 -1 1 # Non H-bonding
atom_par Sc 3.30 0.019 12.000 -0.00110 0.0 0.0 0 -1 -1 1 # Non H-bonding
atom_par Ti 3.18 0.017 12.000 -0.00110 0.0 0.0 0 -1 -1 1 # Non H-bonding
atom_par V 3.14 0.016 12.000 -0.00110 0.0 0.0 0 -1 -1 1 # Non H-bonding
atom_par Co 2.87 0.014 12.000 -0.00110 0.0 0.0 0 -1 -1 1 # Non H-bonding
atom_par Ni 2.83 0.015 12.000 -0.00110 0.0 0.0 0 -1 -1 1 # Non H-bonding
atom_par Cu 3.50 0.005 12.000 -0.00110 0.0 0.0 0 -1 -1 1 # Non H-bonding
atom_par Ga 4.38 0.415 11.000 -0.00110 0.0 0.0 0 -1 -1 1 # Non H-bonding
atom_par Ge 4.28 0.379 12.000 -0.00110 0.0 0.0 0 -1 -1 1 # Non H-bonding
atom_par As 4.23 0.309 13.000 -0.00110 0.0 0.0 0 -1 -1 1 # Non H-bonding
atom_par Se 4.21 0.291 14.000 -0.00110 0.0 0.0 0 -1 -1 1 # Non H-bonding
atom_par Kr 4.14 0.220 16.000 -0.00110 0.0 0.0 0 -1 -1 1 # Non H-bonding
atom_par Rb 4.11 0.040 12.000 -0.00110 0.0 0.0 0 -1 -1 2 # Non H-bonding
atom_par Sr 3.64 0.235 12.000 -0.00110 0.0 0.0 0 -1 -1 2 # Non H-bonding
atom_par Y 3.35 0.072 12.000 -0.00110 0.0 0.0 0 -1 -1 1 # Non H-bonding
atom_par Zr 3.12 0.069 12.000 -0.00110 0.0 0.0 0 -1 -1 1 # Non H-bonding
atom_par Nb 3.17 0.059 12.000 -0.00110 0.0 0.0 0 -1 -1 1 # Non H-bonding
atom_par Mo 3.05 0.056 12.000 -0.00110 0.0 0.0 0 -1 -1 1 # Non H-bonding
atom_par Tc 3.00 0.048 12.000 -0.00110 0.0 0.0 0 -1 -1 1 # Non H-bonding
atom_par Ru 2.96 0.056 12.000 -0.00110 0.0 0.0 0 -1 -1 1 # Non H-bonding
atom_par Rh 2.93 0.053 12.000 -0.00110 0.0 0.0 0 -1 -1 1 # Non H-bonding
atom_par Pd 1.34 0.048 12.000 -0.00110 0.0 0.0 0 -1 -1 1 # Non H-bonding
atom_par Ag 3.15 0.036 12.000 -0.00110 0.0 0.0 0 -1 -1 1 # Non H-bonding
atom_par Cd 2.85 0.228 12.000 -0.00110 0.0 0.0 0 -1 -1 1 # Non H-bonding
atom_par In 4.46 0.599 11.000 -0.00110 0.0 0.0 0 -1 -1 1 # Non H-bonding
atom_par Sn 4.39 0.567 12.000 -0.00110 0.0 0.0 0 -1 -1 1 # Non H-bonding
atom_par Sb 4.42 0.449 13.000 -0.00110 0.0 0.0 0 -1 -1 1 # Non H-bonding
atom_par Te 4.47 0.398 14.000 -0.00110 0.0 0.0 0 -1 -1 1 # Non H-bonding
atom_par Xe 4.40 0.332 12.000 -0.00110 0.0 0.0 0 -1 -1 1 # Non H-bonding
atom_par Cs 4.52 0.045 12.000 -0.00110 0.0 0.0 0 -1 -1 2 # Non H-bonding
atom_par Ba 3.70 0.364 12.000 -0.00110 0.0 0.0 0 -1 -1 2 # Non H-bonding
atom_par La 3.52 0.017 12.000 -0.00110 0.0 0.0 0 -1 -1 1 # Non H-bonding
atom_par Ce 3.56 0.013 12.000 -0.00110 0.0 0.0 0 -1 -1 1 # Non H-bonding
atom_par Pr 3.61 0.010 12.000 -0.00110 0.0 0.0 0 -1 -1 1 # Non H-bonding
atom_par Nd 3.58 0.010 12.000 -0.00110 0.0 0.0 0 -1 -1 1 # Non H-bonding
atom_par Pm 3.55 0.009 12.000 -0.00110 0.0 0.0 0 -1 -1 1 # Non H-bonding
atom_par Sm 3.52 0.008 12.000 -0.00110 0.0 0.0 0 -1 -1 1 # Non H-bonding
atom_par Eu 3.49 0.008 12.000 -0.00110 0.0 0.0 0 -1 -1 1 # Non H-bonding
atom_par Gd 3.37 0.009 12.000 -0.00110 0.0 0.0 0 -1 -1 1 # Non H-bonding
atom_par Tb 3.45 0.007 12.000 -0.00110 0.0 0.0 0 -1 -1 1 # Non H-bonding
atom_par Dy 3.43 0.007 12.000 -0.00110 0.0 0.0 0 -1 -1 1 # Non H-bonding
atom_par Ho 3.41 0.007 12.000 -0.00110 0.0 0.0 0 -1 -1 1 # Non H-bonding
atom_par Er 3.39 0.007 12.000 -0.00110 0.0 0.0 0 -1 -1 1 # Non H-bonding
atom_par Tm 3.37 0.006 12.000 -0.00110 0.0 0.0 0 -1 -1 1 # Non H-bonding
atom_par Yb 3.36 0.228 12.000 -0.00110 0.0 0.0 0 -1 -1 1 # Non H-bonding
atom_par Lu 3.64 0.041 12.000 -0.00110 0.0 0.0 0 -1 -1 1 # Non H-bonding
atom_par Hf 3.41 0.072 12.000 -0.00110 0.0 0.0 0 -1 -1 1 # Non H-bonding
atom_par Ta 3.71 0.081 12.000 -0.00110 0.0 0.0 0 -1 -1 1 # Non H-bonding
atom_par W 3.07 0.067 12.000 -0.00110 0.0 0.0 0 -1 -1 1 # Non H-bonding
```

```
atom_par Re 2.95 0.066 12.000 -0.00110 0.0 0.0 0 -1 -1 1 # Non H-bonding
atom_par Os 3.12 0.120 12.000 -0.00110 0.0 0.0 0 -1 -1 1 # Non H-bonding
atom_par Ir 2.84 0.073 12.000 -0.00110 0.0 0.0 0 -1 -1 1 # Non H-bonding
atom_par Pt 2.75 0.080 12.000 -0.00110 0.0 0.0 0 -1 -1 1 # Non H-bonding
atom_par Au 3.29 0.039 12.000 -0.00110 0.0 0.0 0 -1 -1 1 # Non H-bonding
atom_par Hg 2.71 0.385 12.000 -0.00110 0.0 0.0 0 -1 -1 1 # Non H-bonding
atom_par Tl 4.35 0.680 11.000 -0.00110 0.0 0.0 0 -1 -1 1 # Non H-bonding
atom_par Pb 4.30 0.663 12.000 -0.00110 0.0 0.0 0 -1 -1 1 # Non H-bonding
atom_par Bi 4.37 0.518 13.000 -0.00110 0.0 0.0 0 -1 -1 1 # Non H-bonding
atom_par Po 4.71 0.325 14.000 -0.00110 0.0 0.0 0 -1 -1 1 # Non H-bonding
atom_par At 4.75 0.284 15.000 -0.00110 0.0 0.0 0 -1 -1 1 # Non H-bonding
atom_par Rn 4.77 0.248 16.000 -0.00110 0.0 0.0 0 -1 -1 1 # Non H-bonding
atom_par Fr 4.90 0.050 12.000 -0.00110 0.0 0.0 0 -1 -1 2 # Non H-bonding
atom_par Ra 3.68 0.404 12.000 -0.00110 0.0 0.0 0 -1 -1 2 # Non H-bonding
atom_par Ac 3.48 0.033 12.000 -0.00110 0.0 0.0 0 -1 -1 1 # Non H-bonding
atom_par Th 3.40 0.026 12.000 -0.00110 0.0 0.0 0 -1 -1 1 # Non H-bonding
atom_par Pa 3.42 0.022 12.000 -0.00110 0.0 0.0 0 -1 -1 1 # Non H-bonding
atom_par U 3.40 0.022 12.000 -0.00110 0.0 0.0 0 -1 -1 1 # Non H-bonding
atom_par Np 3.42 0.019 12.000 -0.00110 0.0 0.0 0 -1 -1 1 # Non H-bonding
atom_par Pu 3.42 0.016 12.000 -0.00110 0.0 0.0 0 -1 -1 1 # Non H-bonding
atom_par Am 3.38 0.014 12.000 -0.00110 0.0 0.0 0 -1 -1 1 # Non H-bonding
atom_par Cm 3.33 0.014 12.000 -0.00110 0.0 0.0 0 -1 -1 1 # Non H-bonding
atom_par Bk 3.34 0.013 12.000 -0.00110 0.0 0.0 0 -1 -1 1 # Non H-bonding
atom_par Cf 3.31 0.013 12.000 -0.00110 0.0 0.0 0 -1 -1 1 # Non H-bonding
atom_par E 3.30 0.012 12.000 -0.00110 0.0 0.0 0 -1 -1 1 # Non H-bonding
atom_par Fm 3.29 0.012 12.000 -0.00110 0.0 0.0 0 -1 -1 1 # Non H-bonding
```

Attachment 2 – Abstract of oral communication fulfilled within this dissertation

Alternative microwave improved preparation of new spiroindolin-3-one(thio)barbiturate derivatives.

Soeiro P.[1,2(*)], Serrano J. L.[1,2], Figueiredo J.[1,2], Silvestre S.[2,3], Almeida P.[1,2], Boto R. E. F.[1,2]

[1] Chemistry Department, Faculty of Sciences, University of Beira Interior, Covilhã, Portugal.
[2] CICS-UBI, Faculty of Health Science, University of Beira Interior, Covilhã, Portugal.
[3] CNC, University of Coimbra, Coimbra, Portugal.
(*)*Email:* pedroafsoeiro@gmail.com

ABSTRACT

Barbiturates constitute a relevant class of compounds due to their wide range of biological activities and structural versatility [1].
Recently, the interest of our research group in the synthesis and biological evaluation of new (thio)barbiturate derivatives led to the development of a new method for the synthesis of 3-substituted-2,1-benzisoxazoles [2]. In the course of this work, a structural rearrangement of these 2,1-benzisoxazoles promoted by heating at the dimethylformamide (DMF) reflux temperature was observed. An O-N bond cleavage to originate an electrophilic nitrene like key intermediate followed by the intramolecular attack by a barbiturate enolate to afford the spiroindolin-3-ones **2**. The optimization of this new method allowed the preparation of new spiroindolin-3-one (thio)barbiturates **2** from **1** in 5 to 10 minutes using DMF as solvent and microwave irradiation at 100ºC instead of conventional heating as previously reported [3].
All spiroindolin-3-one(thio)barbiturates **2** were synthetized with very good yields (75-85%) and were structurally characterized by uni- and bidimentional nuclear magnetic resonance. Further *in silico* and *in vitro* studies were realized to predict several pharmacokinetic and toxicity properties, and better understanding of the structural activity relation of the prepared compounds, respectively.

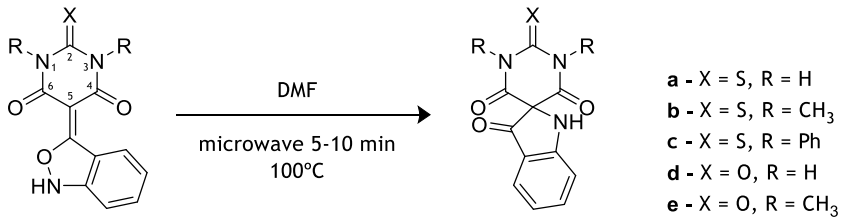

Keywords: Spiroindolin-3-one(thio)barbiturates, microwave synthesis, structural characterization, biological activity.

Acknowledgements: This work is supported by FEDER funds through the POCI - COMPETE 2020 - Operational Program Competitiveness and Internationalization in Axis I - Strengthening research, technological development and innovation (Project POCI- 01-0145-FEDER-007491) and National Funds by FCT - Foundation for Science and Technology (Project UID/Multi /00709/2013). J. L. Serrano and J. Figueiredo acknowledge a fellowship from Santander-Totta/UBI (BID/ICI-UID FC/Santander Universidades-UBI/2017).

References: [1] Figueiredo, J. *et al*. Eur. J. Med. Chem. 143 (2018) 829-842.; [2] Serrano, J. *et al*. C. R. Chimie. 20 (2017) 990-995. [3] Serrano J, *et al*. XII Annual CICS-UBI Symposium Covilhã, 2017.

Attachment 3 – Abstract of panel communication fulfilled within this dissertation

Synthesis of new spiroindolin-3-one (thio)barbiturate derivatives. A microwave optimized method

Soeiro P.[1], Serrano J. L.[1], Silvestre S.[1,2], Almeida P.[1], Boto R. E. F.[1]
[1]CICS-UBI – Health Sciences Research Centre, University of Beira Interior, Av. Infante D. Henrique, 6200-506 Covilhã, Portugal;
[2]CNC – Center for Neuroscience and Cell Biology, University of Coimbra, Rua Larga, 3400-517 Coimbra, Portugal.

Email: pedroafsoeiro@gmail.com

Barbiturates constitute a relevant class of compounds due to their wide range of biological activities and structural versatility. Although barbituric acid itself lacks pharmacological effects, additions and/or substitutions in its backbone yields compounds with a more desirable outcome, being the positions N1, C2, N3 and C5 the most explored, especially the latter, which can be mono- or disubstituted or forming a spiro structure condensed with other types of heterocycles [1].

Recently, the interest of our research group in the synthesis and biological evaluation of new (thio)barbiturate derivatives led to the development of a new method for the synthesis of 3-substituted-2,1-benzisoxazoles [2]. In the course of this work, a structural rearrangement of these 2,1-benzisoxazoles promoted by heating at the dimethylformamide (DMF) reflux temperature was observed. An O-N bond cleavage to originate an electrophilic nitrene like key intermediate followed by the intramolecular attack by a barbiturate enolate to afford the spiroindolin-3-ones **2**. The optimization of this new method allowed the preparation of new spiroindolin-3-one (thio)barbiturates **2** from **1** in 5 to 10 minutes also using DMF as solvent and microwave irradiation at 100ºC instead of conventional heating.

All spiroindolin-3-one (thio)barbiturates **2** were synthetized with high yields (75-85%) and were structurally characterized by uni- and bidimentional nuclear magnetic resonance. Additionally, the structure of **2a** was unequivocally confirmed by X-ray analysis.

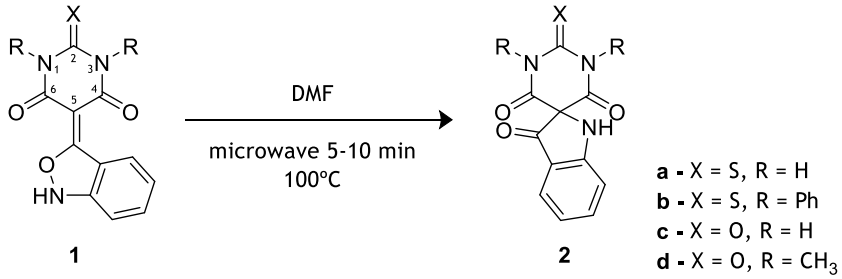

Acknowledgements:
This work is supported by FEDER funds through the POCI - COMPETE 2020 - Operational Program Competitiveness and Internationalization in Axis I - Strengthening research, technological development and innovation (Project POCI- 01-0145-FEDER-007491) and National Funds by FCT - Foundation for Science and Technology (Project UID/Multi /00709/2013). J. L. Serrano acknowledge a fellowship from Santander-Totta/UBI (BID/ICI-UID FC/Santander Universidades-UBI/2017).

References:
[1] Figueiredo, J. et al. *Eur. J. Med. Chem.* 143 (2018) 829-842.
[2] Serrano, J. et al. C. R. Chimie. 20 (2017) 990-995.

Attachment 4 – Scientific articles in international journals peer-reviewed referred in Journal Citation Reports (JCR) of ISI Wed of Knowledge and/or SciVerse Scopus

Tetrahedron
journal homepage: www.elsevier.com

The synthesis and process optimization of symmetric and asymmetric 3-substituted 2,1-benzisoxazoles from 5-(2-nitrobenzylidene)(thio)barbiturates

João L. Serrano[a, b, ‡], Pedro F. Soeiro[a, b, ‡], Melani A. Reis[a, b], Samuel Silvestre[a, c], Renato E. F. Boto[a, b] and Paulo Almeida[a, b] *

[a] CICS-UBI - Health Sciences Research Center, University of Beira Interior, Av. Infante D. Henrique, 6201-506 Covilhã, Portugal
[b] Department of Chemistry, University of Beira Interior, Rua Marquês D'Ávila e Bolama, 6201-001 Covilhã, Portugal
[c] CNC - Center for Neuroscience and Cell Biology, University of Coimbra, Rua Larga, 3004-517 Coimbra, Portugal

ARTICLE INFO

Article history:

Received

Received in revised form

Accepted

Available online

Keywords:

2,1-Benzisoxazoles

Anthranils

Barbituric Acid Derivatives

Process Optimization

ABSTRACT

Benzisoxazoles represent an important pharmacophore in medicinal chemistry. Recently, an unexpected formation of symmetric 3-substituted 2,1-benzisoxazoles from the reduction of 5-(2-nitrobenzylidene)barbiturates have been described by a reductive intramolecular heterocyclisation involving a nitroso intermediary. As part of our efforts to improve the previous reactional conditions, herein is reported the optimization study of the synthesis of 3-substituted 2,1-benzisoxazoles, where the nature of the reducing agent and additives, time and solvents were explored. In addition, using the optimized conditions several 2,1-benzisoxazoles were prepared in 40-87 % yield. From this set, six compounds have never been described, where the asymmetric nature of the (thio)barbituric acid moiety was for the first time explored. For this, the total synthesis starting from the respective urea or thiourea was successfully performed, where some thiobarbiturates and benzylidenebarbiturate and thiobarbiturate precursors are for the first time described. All the novel compounds showed spectral data, including HRMS, fully consistent with the assigned structures.

* Corresponding author. Tel.: +351 275329174; fax: +351 275319056; e-mail: paulo.almeida@ubi.pt
‡ These authors contributed equally to this work

1. Introduction

Heterocycles are known to possess a very broad biological activity spectrum and therefore have been found to be a structural key in drugs for varied diseases [1]. As a relevant example, barbituric and thiobarbituric acid derivatives have become progressively attractive to medicinal chemists due to their wide range of biological activities, in addition to their most important and classical use as sedative hypnotics. In fact, functionalized barbiturates and thiobarbiturates have been described as xanthine oxidase inhibitors, antioxidants, antibacterial agents and as anti-proliferative compounds. Classically, these compounds are prepared from the condensation of ureas or thioureas with malonate derivatives [2].

Benzisoxazoles constitute another important pharmacophore in medicinal chemistry. Their wide spectrum of pharmacological activities justifies the presence of this structure in different biologically active compounds in many therapeutic areas [3]. As representative examples, these heterocyclic compounds are present in clinically used antipsychotics (e.g. risperidone, figure 1) and anticonvulsants (e.g. zonisamide, figure 1) [3a]. Benzisoxazoles can be divided into 1,2-benzisoxazoles (indoxazene) and 2,1-benzisoxazoles (anthranils). The first one has been mainly studied from a pharmacological perspective by itself, while the latter is well-known in the preparation of some another biologically active compounds. In fact, 2,1-benzisoxazoles can be used in the preparation of quinazolines and benzodiazepines comprising aminoarylketone intermediates or in the direct preparation of quinolines and acridines [4].

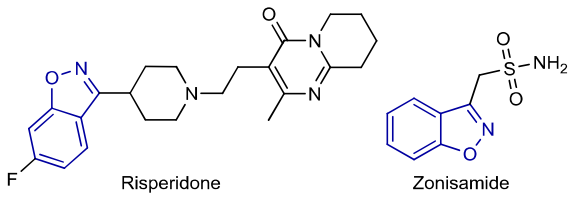

Figure 1 – Example of benzisoxazoles used in the clinic.

After the first anthranil described synthesis by Friedlander and Henriques in 1882 [5], several other methods to prepare this nucleus have been described [4, 6]. Recently, aiming to develop new bioactive barbiturates [2d], we reported the unexpected formation of symmetric 3-substituted 2,1-benzisoxazoles **4** from the reduction of 5-(2-nitrobenzylidene)barbiturates **3** (last step, scheme 1). 2,1-Benzisoxazoles **4** were obtained by a reductive intramolecular heterocyclisation with tin(II) chloride dihydrate in methanol and hydrochloric acid, from moderate to good yields [4a].

As part of our efforts to optimize the previous reactional conditions, herein is reported the optimization study of the process to prepare the 3-substituted 2,1-benzisoxazoles 4. For this, the nature of the reducing agent and additives, temperature, reaction time and solvents were explored. In addition, ten 2,1-benzisoxazoles were prepared using the herein described optimized conditions in 40-87 % yield. From this set of ten, six were not previously described, and the asymmetric nature of the (thio)barbituric acid moiety was for the first time explored. For this, the total synthesis starting from the respective symmetric or asymmetric urea or thiourea is also described, where five thiobarbiturates and six benzylidene barbiturate and thiobarbiturate precursors are, to the best of our knowledge, for the first time described.

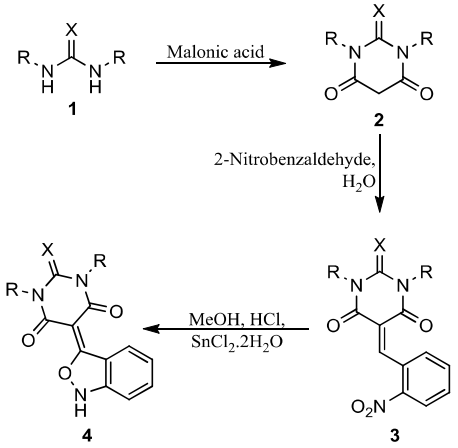

Scheme 1. Preparation of symmetric 3-substituted 2,1-benzisoxazole (thio)barbiturate derivatives **4** [4a]. X = O, S; R = H, CH_3, C_6H_5.

2. Results and discussion

Initially, we aimed to optimize the reaction conditions previously established by our group to obtain 3-substituted 2,1-benzisoxazoles from 5-(2-nitrobenzylidene)(thio)barbiturates [4a]. For this, 2,1-benzisoxazole **4b** (table 1) was used as a model and several variables were explored, namely the nature of the reducing agent, additives, temperature, reaction time and solvents. As expected all of these variables affected the yield of **4b** preparation.

Table 1. Reducer and additive optimization screening on the formation of 3-substituted 2,1-benzisoxazole **4b**.

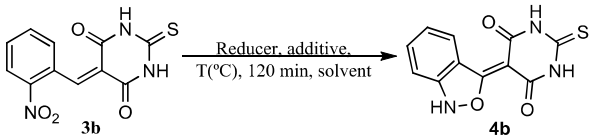

Entry	Reducer	Additive	T (ºC)	Solvent	Yield (%)[a]
1	**$N_2H_4 \cdot H_2O$** [7a]	Raney Nickel	0	EtOH/ DCM	np[b]
2	**KBH_4** [7b]	$BiCl_3$	rt[c]	EtOH/ H_2O	np[b]
3	**Zn** [7c]	NH_4Cl/ H_2O	70	MeOH	np[b]
4	**Zn** [7d]	HCl	Reflux	MeOH	traces
5	**$Na_2S \cdot 9H_2O$** [7e]	-	80	Dioxane/ H_2O	35
6	**Sn**	HCl	Reflux	MeOH	39
7	**$SnCl_2$**	HCl	Reflux	MeOH	70
8	**$SnCl_2 \cdot 2H_2O$** [4a]	**HCl**	Reflux	MeOH	**82**
9	$SnCl_2 \cdot 2H_2O$	**AcOH**	Reflux	MeOH	62
10	$SnCl_2 \cdot 2H_2O$	**$NaHCO_3$/ H_2O**	Reflux	MeOH	np[b]
11	$SnCl_2 \cdot 2H_2O$	**NaOH/ H_2O**	Reflux	MeOH	np[b]

[a] Isolated yields with the pure product; [b] np: no product detected, by NMR analysis after total solvent evaporation; [c] rt: room temperature.

From the selected nitro reducer agents with different strengths [7], tin(II) chloride dihydrate (entry 8, table 1) proved to be the most effective, even when compared to its dehydrated equivalent (entry 7, table 1). A rough analysis of the results involving the variation of the metallic reducer (entries 1-8, table 1) suggests that the yield seems to decrease with the strength of the reductant (more negative electric potential). This result can be understood, regarding the postulated nitrous intermediate involved in this heterocyclisation [4a] whose formation is favored by weaker nitro reducers and therefore their use is expectable to increase the yield of the final benzisoxazoles. The use of hydrazine hydrate and Raney nickel (entry 1, table 1) [7a], potassium borohydride and bismuth trichloride (entry 2, table 1) [7b] or zinc in ammonium chloride (entry 3, table 1) [7c] has been described for the selective reduction of nitroarenes to their hydroxylamine derivatives. However, in our hands, the use of these reducers did not promote the formation of the desired product **4b**, even after 120 minutes of reaction. Once again, this result points to a nitroso rather than a hydroxylamine as the most probable key intermediate in this reaction. On the other hand, the formation of the 2,1-benzisoxazole **4b** appears to occur exclusively in acidic medium (entries 8-9 *vs* entries 10-11, table 1). Within the two acids explored, hydrochloric acid proved to be most effective than acetic acid. The alternative use of a basic medium ($NaHCO_3$ or NaOH), which can decrease the velocity of nitro to amine reduction, revealed to not well succeed after 120 minutes of reaction (entry 10-11, table 1). Thus, the combination of tin(II) chloride dihydrate and hydrochloric acid previously described [4a] showed to be the most effective reductant and additive, respectively, in this reductive heterocyclization.

Subsequently, the temperature, reaction time and solvent effects on 5-(2-nitrobenzylidene)(thio)barbiturate **3b** reduction to afford 2,1-benzisoxazole **4b** using the best reductive conditions [4a] herein supported were analyzed (table 2). Generally, the nature of the solvents and the temperature influenced the yield of **4b** (table 2). In fact, by using methanol as solvent, as previously described [4a], it was observed that the yield increased as the temperature increase until refluxing conditions (entries 1-3, table 2). Interestingly, methanol, ethanol or tetrahydrofuran (THF) at reflux temperatures leads to the highest similar yields, ranging from 80 to 85 % (entries 3, 4 and 8, table 2). However, the use of THF instead of methanol allows shortening the reaction time from 120 to 15 minutes and any advantage was observed when extending the time longer than 15 minutes (entries 8-13, table 2). Thus, using THF at reflux temperature has shown to be the best reaction condition to afford **4b**. In fact, this compound could be obtained in the highest yield (85 %) after 15 min (entry 11, table 2). In addition, the use of this solvent simplifies the isolation procedure since at room temperature the starting material **3b** and the reducer tin(II) chloride dihydrate are soluble, unlike the product **4b**. This allows an easy and direct isolation by filtration of the intended 3-substituted 2,1-benzisoxazole **4b**.

Finally, the effect of the number of equivalents of tin(II) chloride dihydrate and hydrochloric acid on 5-(2-nitrobenzylidene) (thio)barbiturate **3b** reduction to produce 3-substituted 2,1-benzisoxazole **4b** was investigated (table 3) using the best conditions already established. Remarkably, the yield of benzisoxazole **4b** varied to a different extent depending on the ratio of tin(II) chloride dihydrate and hydrochloric acid. In the range between 0.5 to 5.0 equivalents of tin(II) chloride dihydrate in the presence of 15.0 equivalents of HCl (entries 1-5, table 3), the use of 1.0 or 2.0 equivalents of the reducer demonstrated to be the most effective, affording an 85 % yield (entries 2-3, table 3). Considering these results and taking in mind the cost of the reducer, the use of one equivalent of tin(II) chloride dihydrate (entry 2, table 3) was selected to further analyze the influence of hydrochloric acid in the range between 0.0 to 50.0 equivalents (entries 2 and 6-11, table 3).

Table 2. Temperature, reaction time and solvent optimization on the formation of 3-substituted 2,1-benzisoxazole **4b**.

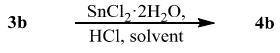

Entry	T (ºC)	Time (min)	Solvent	Yield (%)
1	**rt**	120	MeOH	43
2	**50**	120	MeOH	61
3	**Reflux**	120	**MeOH**	**82**
4	Reflux	120	**EtOH**	80
5	Reflux	120	**H_2O**	55
6	Reflux	120	**BuOH**	57
7	Reflux	120	**1,4-Dioxane**	61
8	Reflux	**120**	**THF**	**85**
9	Reflux	**240**	THF	82
10	Reflux	**30**	THF	85
11	Reflux	**15**	THF	**85**
12	Reflux	**10**	THF	83
13	Reflux	**5**	THF	80

The presence of hydrochloric acid revealed to be crucial for the success of the reaction regarding the poor 5 % of yield obtained in the absence of hydrochloric acid (entry 6, table 3). In fact, this yield significantly increased as the hydrochloric acid number of equivalents rises until an excellent 87 % yield when ten equivalents were used (entry 10, table 3). Apparently, a further increase to fifty equivalents of hydrochloric acid did not present any advantage since the yield decay from 87 to 85 and 72 % (entries 2 and 10-11, table 3).

Table 3. Tin(II) chloride dihydrate and hydrochloric acid equivalents optimization on the formation of 3-substituted 2,1-benzisoxazole **4b**.

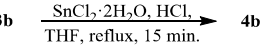

Entry	$SnCl_2·2H_2O$ (equivalents)	HCl (equivalents)	Yield (%)
1	**0.5**	15.0	40
2	**1.0**	15.0	**85**
3	**2.0**	15.0	85
4	**3.0**	15.0	62
5	**5.0**	15.0	26
6	1.0	**0.0**	5
7	1.0	**0.1**	12
8	1.0	**1.0**	18
9	1.0	**5.0**	75
10	**1.0**	**10.0**	**87**
11	1.0	**50.0**	72

By applying the optimized reactional conditions above described, we then extended the reaction scope to a set of ten 3-substituted 2,1-benzisoxazoles **4a-j**, six of them (**4d-e** and **4g-j**) were never been described, where the asymmetric nature of the (thio)barbituric acid moiety was for the first time explored (table 4).

Table 4 – Scope of 3-substituted 2,1-benzisoxazoles **4**.

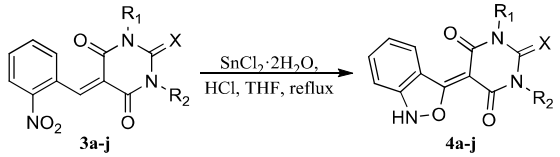

Entry	4	X	R_1	R_2	Yield (%)
1	**a**	O	H	H	87 (79)[a]
2	**b**	S	H	H	87 (82)[a]
3	**c**	O	Me	Me	84 (51)[a]
4	**d**	S	Me	Me	84
5	**e**	O	Ph	Ph	70
6	**f**	S	Ph	Ph	73 (67)[a]
7	**g**	S	Ph	3-ClC_6H_4	40
8	**h**	S	Ph	4-ClC_6H_4	67
9	**i**	S	Ph	4-FC_6H_4	65
10	**j**	S	Ph	4-IC_6H_4	60

[a] Previously described obtained by previous no optimized method [4a].

For this purpose, the starting materials *N*,*N*-disubstituted thioureas **1a-d** and 1,3-diphenylurea (**1e**) were prepared as already described in the literature [4a, 8]. Then, by condensation with malonic acid in the presence of phosphoryl chloride [9] or acetyl chloride [4a], the starting barbituric and thiobarbituric acids **2d-j** were obtained (table 5).

Table 5. Scope of barbituric and thiobarbituric acids **2** and 5-(2-nitrobenzylidene) barbiturates and thiobarbiturates **3**.

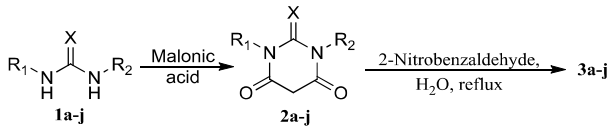

Entry	2 and 3a-j	X	R_1	R_2	Yield of 2 (%)	Yield of 3 (%)
1	**a**	O	H	H	[a]	97
2	**b**	S	H	H	[a]	90
3	**c**	O	Me	Me	[a]	97
4	**d**	S	Me	Me	70	83
5	**e**	O	Ph	Ph	65	82
6	**f**	S	Ph	Ph	95	90
7	**g**	S	Ph	3-ClC_6H_4	60	48
8	**h**	S	Ph	4-ClC_6H_4	78	91
9	**i**	S	Ph	4-FC_6H_4	71	91
10	**j**	S	Ph	4-IC_6H_4	68	93

[a] Purchased from commercially sources.

To the best of our knowledge, the 1,3-dissubstituted thiobarbituric acids **2d** and **2g-j** have not been reported to date. These were successfully synthesized with good yields (60-78 %) after ethanol recrystallization. Afterwards, (thio)barbiturates **2a-j** were subjected to a Knoevenagel condensation with 2-nitrobenzaldehyde in water [4a] to afford ten 5-(2-nitrobenzylidene)(thio)barbiturates **3a-j** (table 5), six of them (**3d-e** and **3g-j**) are new, in very good yields from 82 to 97 %, with exception of the asymmetric derivative 3-chlorine **3g** (48 % yield).

Finally, the 5-(2-nitrobenzylidene)(thio)barbiturates **3a-j** were submitted to reductive heterocyclizaton using the optimized reactional conditions presented above to afford compounds **4a-j** (table 4). Interestingly, the 3-substituted 2,1-benzisoxazoles **4a-c** and **4f** previously described were obtained in higher yields than before [4a], concretely from 51-82 % to 73-87 % (entries 1-3 and 6, table 4). The remaining new 2,1-benzisoxazoles 4**d-e** and **4g-j** were synthesized in moderate to good yields, between 40 and 84 % (entries 4-5 and 7-10, table 4).

In general, the yields of 2,1-benzisoxazoles **4** resulting from the reduction of the 5-(2-nitrobenzylidene)(thio)barbiturates **3** seem to be more dependent on the R_1 and R_2 nature than of the chalcogen X nature (table 4). However, some more examples must be analyzed in order to take stronger conclusions depicted below. As representative examples, the yields of symmetric benzisoxazoles (entries 1-6, table 4) are almost the same within each serial where the chalcogen differed from oxygen to sulphur (**4a-b**, 87 %; **4c-d**, 84 %; **4e** and **4f**, 73 and 70 %, table 4). Contrariwise, the yields seem to be steric hindrance dependent and therefore favored when the substituents R_1 and R_2 groups are smaller. In fact, the 87 and 84 % better yields were obtained when hydrogen or methyl group were present (entries 1-2 and 3-4, table 4) when compared to 73 and 70 % obtained for phenyl group cases (entries 5 and 6, table 4). Besides, asymmetric 3-substituted 2,1-benzisoxazoles **4** were generally obtained in lower yields, ranging from 40 to 67 % (entries 7-10, table 4). While the nature of the halogen in the phenyl substituent seems to not influence the yields (entries 8-10, table 4), the substitution in the *para* position (67%; entry 8, table 4) seems to be favored in relation to their *meta* congener (40%; entry 9, table 4).

3. Conclusion

Several symmetric and asymmetric 3-substituted 2,1-benzisoxazoles from 5-(2-nitrobenzylidene)(thio)barbiturates were successfully synthetized and some of them are described for the first time. The reactional conditions for their synthesis were optimized and involved the reflux for 15 minutes of a stirred mixture containing tin(II) chloride dihydrate (1,0 equivalent), concentrated hydrochloride acid (1,0 equivalent) and starting 5-(2-nitro-benzylidene)pyrimidines in THF (20 mL). The work-up was very simple and involved the filtration and washing the product so formed with diethyl ether and after cooling the final yields ranged from 40 to 87%. In general, the yields of these 2,1-benzisoxazoles seems to be more dependent on the R1 and R2 nature of the pyrimidine system than of the chalcogen X nature.

As 2,1-benzisoxazoles are relevant synthetic precursors and are associated to relevant bioactivities, this procedure can find large interest in the future in organic and medicinal chemistry fields.

4. Experimental section

4.1. General experimental details

Reagents and solvents were purchased from standard sources and used without purification. All reactions were performed in the one mmol scale and were monitored by thin-layer chromatography (TLC) on Macherey-Nagel 60 G/UV_{254} (0.2 mm) plates which were visualized by ultra-violet (UV) light detection (254 nm). Melting points (mp) were measured in open capillary tubes in a Büchi B-540 apparatus and were uncorrected. NMR spectra were acquired at room temperature on a Brüker Avance III 400 MHz spectrometer (^{1}H NMR at 400.13 MHz and ^{13}C NMR at 100.62 MHz) and were processed with the software MestReNova 11.0.3 (trial). Deuterated dimethylsulfoxide (DMSO-d_6) and chloroform ($CDCl_3$) were used as solvents and as an internal standard (DMSO-d_6: δ_H = 2.50 and δ_C = 39.52, or $CDCl_3$: δ_H = 7.26 and δ_C = 77.16). The chemical shift (δ) values are given in parts per million (ppm), and the coupling constants (*J*) are given in Hertz (Hz). The ^{1}H and ^{13}C spectra of all new 2,1-benzisoxazoles **4d-e** and **4-g-j** were present on Supplementary Material. High resolution mass spectrometry (HRMS) was performed for new compounds at CACTI services, University of Vigo, Spain.

*4.2. Synthesis of 1,3-disubstitutedthioureas **1f-j***

As already described [4a], to a stirred solution of phenylisothiocyanate (1.0 mmol, 137.9 mg, 121.9 µL) in dichloromethane (0.5 mL) at room temperature, was added dropwise a solution of the respective aniline (1.0 mmol) in dichloromethane (0.5 mL). The reaction was followed by TLC (dichloromethane). The suspension so formed was filtered and washed with ethyl ether to afford the corresponding 1,3-disubstitutedthioureas.

*4.2.1. 1,3-Diphenylthiourea (**1f**)*

From aniline (1.0 mmol, 93.1 mg, 91.3 µL); white crystals (223.7 mg, 95 %); mp 142-144 ºC (lit. 140-142 ºC [10]); ^{1}H NMR and ^{13}C NMR spectral data of the product were compared to those of authentic sample [4a].

*4.2.2. 1-(3-chlorophenyl)-3-phenylthiourea (**1g**)*

From 3-chloroaniline (1.0 mmol, 127.6 mg, 105.8 µL); white solid (126.1 mg, 97 %); mp 100-101 ºC (lit. 104 ºC [11]); ^{1}H NMR and ^{13}C NMR spectral data of the product were compared to those of authentic sample [11].

*4.2.3. 1-(4-chlorophenyl)-3-phenylthiourea (**1h**)*

From 4-chloroaniline (1.0 mmol, 130.2 mg); white solid (254.9 mg, 97 %); mp 156-157 ºC (lit. 150 ºC [11]); ^{1}H NMR and ^{13}C NMR spectral data of the product were compared to those of authentic sample [11].

*4.2.4. 1-(4-fluorophenyl)-3-phenylthiourea (**1i**)*

From 4-fluoroaniline (1.0 mmol, 112.3 mg, 95.7 µL); white solid (220.8 mg, 90 %); mp 171-172 ºC (lit. 173-174 ºC [11]); ^{1}H NMR and ^{13}C NMR spectral data of the product were compared to those of authentic sample [11].

*4.2.5. 1-(4-iodophenyl)-3-phenylthiourea (**1j**)*

From 4-iodoaniline (1.0 mmol, 223.5 mg); white solid (336.5 mg, 95 %); 168-169 ºC (lit. 170 ºC [12]); ^{1}H NMR and ^{13}C NMR spectral data of the product were compared to those of authentic sample [12].

*4.3. Synthesis of 1,3-diphenylurea (**1e**)*

Adapted from the method already described [8]. To a suspension of aniline (2.0 mmol; 187.2 mg; 183.2 µL) in water (5 mL) at room temperature, carbonyldiimidazole (1 mmol; 167.2 mg) was added. The reaction was followed by TLC (dichloromethane) and completed in 4 h. The resulting suspension was filtered and washed with diethyl ether to yield the title compound as a white solid (180.4 mg, 85 %); mp 239-240 ºC (lit. 250-255 ºC [13]); ^{1}H NMR and ^{13}C NMR spectral data of the product were compared to those of authentic sample [13].

4.4. Synthesis of 1,3-disubstituted(thio)barbituric acids ***2d-j***

According to the already described methods A [9] or B [4a]:

Method A: To a solution of respective 1,3-disubstituted(thio)urea (1.00 mmol) and malonic acid (1.0 mmol, 105.1 mg) in chloroform (5ml), phosphoryl chloride (2.0 mmol, 309.8 mg, 188.3 µL) was added dropwise. The solution was heated at 50 ºC and the reaction was followed by TLC (dichloromethane). The solvent was removed at reduced pressure, water was added (10 mL) and solid obtained was filtered, dried and recrystallized from ethanol.

Method B: A stirred solution of respective 1,3-disubstituted(thio)urea (1.0 mmol), malonic acid (1.3 mmol, 136.6 mg) and acetyl chloride (3.0 mmol, 240.3 mg, 217.7 µL) was heated at 60 ºC and the reaction was followed by TLC (dichloromethane). Water was added to the obtained mixture and the solid was filtered, washed with water and recrystallized from ethanol.

*4.4.1. 1,3-Dimethylthiobarbituric acid (**2d**)*

From 1,3-dimethylthiourea (1.0 mmol, 105.2 mg) by method A; yellow solid (120.5 mg, 70 %); mp 193-194 ºC; ^{1}H NMR (400 MHz, $CDCl_3$) δ (ppm) (s, 2H), 3.67 (s, 6H).; ^{13}C NMR (101 MHz, $CDCl_3$) δ (ppm) 181.6, 163.6, 40.4, 35.5.

*4.4.2. 1,3-Diphenylbarbituric acid (**2e**)*

From **1e** (1.0 mmol, 212.3 mg) by method A; yellow solid (182.2 mg, 65 %); mp 241-242 ºC (lit. 222-223 °C [14]); ^{1}H NMR and ^{13}C NMR spectral data of the product were compared to those of authentic sample [14].

*4.4.3. 1,3-Diphenylthiobarbituric acid (**2f**)*

From **1f** (1.0 mmol, 228.3 mg) by method B; yellow needles (281.5 mg, 95 %); mp 252-253 ºC (lit. 258-259 ºC [15]); ^{1}H NMR and ^{13}C NMR spectral data of the product were compared to those of authentic sample [4a].

*4.4.4. 1-(3-chlorophenyl)-3-phenylthiobarbituric acid (**2g**)*

From **1g** (1.0 mmol, 262.8 mg) by method B; beige solid (199.0 mg, 60%); mp 205-207 ºC; ^{1}H NMR (400 MHz, $CDCl_3$) δ (ppm) 7.56 – 7.38 (m, 5H), 7.24 (s, 2H), 7.24 – 7.18 (m, 2H), 4.11 (s, 2H); ^{13}C NMR (101 MHz, DMSO-d_6) δ (ppm) 181.2, 163.1, 139.6, 138.6, 135.3, 130.6, 129.8, 129.6, 129.4, 129.3, 128.7, 127.2, 41.2.

*4.4.5. 1-(4-chlorophenyl)-3-phenylthiobarbituric acid (**2h**)*

From **1h** (1.0 mmol, 292.8 mg) by method B; light yellow solid (258.0 mg, 78 %); mp 259-260 ºC; ^{1}H NMR (400 MHz, $CDCl_3$) δ (ppm) 7.52 – 7.44 (m, 5H), 7.21 (d, J = 8.0 Hz, 2H), 7.16 (d, J = 8.6 Hz, 2H), 4.11 (s, 2H); ^{13}C NMR (101 MHz, $CDCl_3$) δ (ppm) 181.4, 163.2, 163.1, 138.7, 137.1, 135.3, 130.1, 130.1, 129.8, 129.3, 128.6, 41.2.

*4.4.6. 1-(4-fluorophenyl)-3-phenylthiobarbituric acid (**2i**)*

From **1i** (1.0 mmol, 246.3 mg) by method B; light yellow solid (223.2 mg, 71 %); mp 238-239 ºC; ^{1}H NMR (400 MHz, $CDCl_3$) δ (ppm) 7.55 – 7.44 (m, 3H), 7.24 – 7.15 (m, 6H), 4.11 (s, 2H); ^{13}C NMR (101 MHz, $CDCl_3$) δ (ppm) 181.7, 163.4, 163.2, 138.7, 130.6, 130.5, 129.8, 129.3, 128.6, 117.0, 116.7, 41.2.

*4.4.7. 1-(4-iodophenyl)-3-phenylthiobarbituric acid (**2j**)*

From **1j** (1.0 mmol, 354.2 mg) by method B; beige solid (287.1 mg, 68 %); mp 230-231 ºC; ^{1}H NMR (400 MHz, $CDCl_3$) δ (ppm) 7.84 (dd, J = 16.7, 8.6 Hz, 2H), 7.59 – 7.44 (m, 3H), 7.24 (dd, J = 24.5, 7.9 Hz, 2H), 6.99 (dd, J = 24.5, 8.6 Hz, 2H), 4.12 (d, J = 5.8 Hz, 2H); ^{13}C NMR (101 MHz, $CDCl_3$) δ (ppm) 181.3, 163.2, 163.1, 139.0, 130.6, 129.8, 129.8, 129.8, 129.3, 128.6, 128.6, 41.2.

4.5. 5-(2-Nitro-benzylidene)pyrimidines ***3a-j***

A stirred mixture of respective (thio)barbituric acid **2a-j** (1.0 mmol) and 2-nitrobenzaldehyde (1.0 mmol, 154.2 mg) in water (5 mL) was refluxed for 2 hours. The product so formed after cooling was filtered, washed with water, ethanol and ethyl ether to afford the following 5-(2-nitro-benzylidene)pyrimidines:

*4.5.1. 5-(2-Nitrobenzylidene)pyrimidine-2,4,6(1H,3H,5H)-trione (**3a**)*

From barbituric acid (1.0 mmol, 130.7 mg, **1a**); white solid (253.3 mg, 97 %); mp 274-275 ºC (literature 274-276 ºC) [19]. ^{1}H NMR and ^{13}C NMR spectral data of the product were compared to those of authentic sample [4a].

*4.5.2. 5-(2-Nitrobenzylidene)-2-thioxodihydropyrimidine-4,6(1H,5H)-dione (**3b**)*

From thiobarbituric acid (1.0 mmol, 147.1 mg, **2b**); pale yellow solid (249.5 mg, 90 %); mp 239-241 ºC (literature 246-250 ºC [17]). ^{1}H NMR and ^{13}C NMR spectral data of the product were compared to those of authentic sample [4a].

*4.5.3. 1,3-dimethyl-5-(2-nitrobenzylidene)dihydropyrimidine-2,4,6(1H,3H,5H)-trione (**3c**)*

From 1,3-dimethylbarbituric acid (1.0 mmol, 159.3 mg, **2c**); white solid (280.6 mg, 97 %); mp 158-159 ºC (literature 159-161 ºC [18]). ^{1}H NMR and ^{13}C NMR spectral data of the product were compared to those of authentic sample [4a].

*4.5.4. 1,3-dimethyl-5-(2-nitrobenzylidene)-2-thioxodihydropyrimidine-4,6(1H,5H)-dione (**3d**)*

From **2d** (1.0 mmol, 172.2 mg); light brown solid (253.4 mg, 83 %); mp 161-162 ºC; ^{1}H NMR (400 MHz, DMSO-d_6) δ (ppm) 8.78 (s, 1H), 8.28 (d, J = 8.3 Hz, 1H), 7.83 (t, J = 7.5 Hz, 1H), 7.72 (t, J = 7.9 Hz, 1H), 7.60 (d, J = 7.7 Hz, 1H), 3.67 (s, 3H), 3.48 (s, 3H); ^{13}C NMR (101 MHz, DMSO-d_6) δ (ppm) 180.9, 160.1, 158.6, 155.8, 146.14, 134.0, 132.0, 130.4, 130.0, 124.1, 120.5, 35.5, 35.0.

*4.5.5. 5-(2-nitrobenzylidene)-1,3-diphenylpyrimidine-2,4,6(1H,3H,5H)-trione (**3e**)*

From **2e** (1.0 mmol, 280.3 mg); white solid (338.9 mg, 82 %); mp 239-240 ºC; ^{1}H NMR (400 MHz, DMSO-d_6) δ (ppm) 8.82 (s, 1H), 8.25 (dd, J = 8.2 and 1.2 Hz, 1H), 7.82 (td, J = 7.6 and 1.2 Hz, 1H), 7.71-7.61 (m, 2H), 7.57-7.50 (m, 2H), 7.49-7.36 (m, 6H), 7.34-7.27 (m, 2H); ^{13}C NMR (101 MHz, DMSO-d_6) δ (ppm) 161.9, 160.6, 154.6, 151.1, 146.7, 136.0, 135.6, 134.5, 132.4, 130.7, 130.5, 129.4, 129.3, 129.3, 129.0, 128.9, 124.6, 121.5.

*4.5.6. 5-(2-Nitrobenzylidene)-1,3-diphenyl-2-thioxodihydropyrimidine-4,6(1H,5H)-dione (**3f**)*

From **2f** (1.0 mmol, 296.4 mg); pale orange solid (386.5 mg, 90%); mp 235 ºC decomposes (literature 232ºC [18]). ^{1}H NMR and ^{13}C NMR spectral data of the product were compared to those of authentic sample [4a].

*4.5.7. 1-(3-chlorophenyl)-5-(2-nitrobenzylidene)-3-phenyl-2-thioxodihydropyrimidine-4,6(1H,5H)-dione (**3g**)*

From **2g** (1.0 mmol, 330.8 mg); orange solid (222.8 mg, 48 %); mp 227-229 ºC; ^{1}H NMR (400 MHz, DMSO-d_6) δ (ppm)

8.84 (s, 1H), 8.25 (dd, *J* = 8.1, 2.8 Hz, 1H), 7.86 – 7.78 (m, 1H), 7.74 – 7.62 (m, 2H), 7.56 – 7.48 (m, 2H), 7.47 – 7.30 (m, 6H), 7.31 – 7.20 (m, 2H); ^{13}C NMR (101 MHz, DMSO-d_6) δ (ppm) 181.2, 160.3, 160.2, 158.8, 158.7, 155.5, 155.4, 146.2, 146.2, 141.2, 140.9, 139.8, 139.5, 134.1, 133.1, 132.9, 131.7, 130.5, 130.5, 130.2, 130.0, 129.1, 129.0, 128.8, 128.5, 128.4, 128.3, 128.2, 127.9, 124.2, 121.1, 121.0.

*4.5.8. 1-(4-chlorophenyl)-5-(2-nitrobenzylidene)-3-phenyl-2-thioxodihydropyrimidine-4,6(1H,5H)-dione (**3h**)*

From **2h** (1.0 mmol, 330.8 mg); beige solid (422.2 mg, 91 %); mp 238-239 ºC; ^{1}H NMR (400 MHz, DMSO-d_6) δ (ppm) 8.82 (s, 1H), 8.25 (d, *J* = 8.2 Hz, 1H), 7.81 (t, *J* = 7.6 Hz, 1H), 7.68 (t, *J* = 9.1 Hz, 2H), 7.58 (d, *J* = 8.1 Hz, 1H), 7.54 – 7.45 (m, 2H), 7.45 – 7.20 (m, 7H); ^{13}C NMR (101 MHz, DMSO-d_6) δ (ppm) 181.3, 160.3, 160.3, 158.8, 158.8, 155.3, 146.2, 139.9, 139.6, 138.9, 138.6, 134.1, 132.9, 132.8, 131.7, 131.7, 130.8, 130.8, 130.5, 130.5, 130.2, 130.1, 129.2, 129.1, 129.1, 129.0, 128.8, 128.4, 128.2, 124.2, 121.2, 121.2.

*4.5.9. 1-(4-fluorophenyl)-5-(2-nitrobenzylidene)-3-phenyl-2-thioxodihydropyrimidine-4,6(1H,5H)-dione (**3i**)*

From **2i** (1.0 mmol, 314.4 mg); beige solid (407.2 mg, 91 %); mp 249-250 ºC; ^{1}H NMR (400 MHz, DMSO-d_6) δ (ppm) 8.82 (s, 1H), 8.25 (d, *J* = 8.3 Hz, 1H), 7.81 (t, *J* = 7.6 Hz, 1H), 7.68 (t, *J* = 8.7 Hz, 2H), 7.50 (t, *J* = 7.6 Hz, 1H), 7.45 – 7.20 (m, 9H); ^{13}C NMR (101 MHz, DMSO-d_6) δ (ppm) 181.6, 160.4, 160.3, 158.9, 158.8, 155.2, 146.2, 140.0, 139.7, 136.3, 136.2, 136.0, 135.9, 134.1, 131.7, 131.0, 131.0, 130.9, 130.9, 130.5, 130.5, 130.2, 130.1, 129.1, 128.9, 128.8, 128.3, 128.2, 124.2, 121.2, 121.2, 116.1, 115.9, 115.9, 115.7.

*4.5.10. 1-(4-iodophenyl)-5-(2-nitrobenzylidene)-3-phenyl-2-thioxodihydropyrimidine-4,6(1H,5H)-dione (**3j**)*

From **2j** (1.0 mmol, 422.3 mg); light brown solid (516.5 mg, 93 %); mp 193-194 ºC; ^{1}H NMR (400 MHz, DMSO-d_6) δ (ppm) δ 8.82 (s, 1H), 8.28 – 8.22 (m, 1H), 7.89 – 7.86 (m, 1H), 7.85 – 7.63 (m, 5H), 7.61 – 7.31 (m, 4H), 7.28 – 7.16 (m, 2H), 7.11 – 7.02 (m, 1H); ^{13}C NMR (101 MHz, DMSO-d_6) δ (ppm) 181.2, 160.3, 158.8, 155.3, 146.2, 139.9, 139.6, 138.1, 137.9, 134.1, 131.3, 130.2, 129.1, 129.0, 128.8, 128.4, 128.2, 124.2, 121.2.

*4.6. 5-(Benzisoxazol-3-ylidene)pyrimidines **4a-j***

To a solution of appropriated 5-(2-nitrobenzylidene)pyrimidine **3a-j** (1.0 mmol) and tin(II) chloride dihydrate (1.0 mmol, 225.9 mg) in THF (20 mL), concentrated hydrochloride acid (10.0 mmol, 974.2 mg, 811.8 µL) was added and refluxed for 15 minutes. After cooling, the solid was filtered and washed with diethyl ether to give the following 5-(benzisoxazol-3-ylidene)pyrimidines:

*4.6.1. 5-(benzo[c]isoxazol-3(1H)-ylidene)pyrimidine-2,4,6(1H,3H,5H)-trione (**4a**)*

From **3a** (1.0 mmol, 261.2 mg); yellow solid (213.3 mg, 87 %); mp 266-268 ºC decomposes; ^{1}H NMR and ^{13}C NMR spectral data of the product were compared to those of authentic sample [4a].

*4.6.2. 5-(benzo[c]isoxazol-3(1H)-ylidene)-2-thioxodihydropyrimidine-4,6(1H,5H)-dione (**4b**)*

From **3b** (1.0 mmol, 277.3 mg); yellow solid (227.3 mg, 87 %); mp 207-208 ºC decomposes; ^{1}H NMR and ^{13}C NMR spectral data of the product were compared to those of authentic sample [4a].

*4.6.3. 5-(benzo[c]isoxazol-3(1H)-ylidene)-1,3-dimethylpyrimidine-2,4,6(1H,3H,5H)-trione (**4c**)*

From **3c** (1.0 mmol, 289.3 mg); yellow solid (229.5 mg, 84 %); mp 211-213 ºC; ^{1}H NMR and ^{13}C NMR spectral data of the product were compared to those of authentic sample [4a].

*4.6.4. 5-(benzo[c]isoxazol-3(1H)-ylidene)-1,3-dimethyl-2-thioxodihydropyrimidine-4,6(1H,5H)-dione (**4d**)*

From **3d** (1.0 mmol, 305.3 mg); yellow solid (243.1 mg, 84 %); mp 218-219 ºC; ^{1}H NMR (400 MHz, DMSO-d_6) δ (ppm) 7.76 (dt, *J* = 8.8, 1.1 Hz, 1H), 7.38 (dt, *J* = 9.0, 1.0 Hz, 1H), 7.23 (ddd, *J* = 9.0, 6.3, 1.1 Hz, 1H), 6.76 (ddd, *J* = 8.8, 6.3, 0.9 Hz, 1H), 3.61 (s, 6H); ^{13}C NMR (101 MHz, DMSO-d_6) δ (ppm) 177.1, 166.5, 159.2, 156.2, 130.4, 125.1, 119.8, 114.8, 113.3, 84.7, 34.9; HRMS (EI-TOF): calcd. for $C_{13}H_{11}N_3O_3S$ $[M]^+$ 289.0521; found 289.0528.

*4.6.5. 5-(benzo[c]isoxazol-3(1H)-ylidene)-1,3-diphenylpyrimidine-2,4,6(1H,3H,5H)-trione (**4e**)*

From **3e** (1.0 mmol, 413.4 mg); yellow solid (278.2 mg, 70 %); mp 264-265 ºC; ^{1}H NMR (400 MHz, DMSO-d_6) δ (ppm 7.83 (d, *J* = 8.8 Hz, 1H), 7.41 (t, *J* = 7.8 Hz, 4H), 7.35 – 7.29 (m, 3H), 7.29 – 7.25 (m, 4H), 7.20 (dd, *J* = 8.9, 6.3 Hz, 1H), 6.69 (dd, *J* = 8.8, 6.2 Hz, 1H); ^{13}C NMR (101 MHz, DMSO-d_6) δ (ppm) 167.5, 160.8, 156.0, 151.7, 137.5, 130.4, 129.8, 128.3, 127.2, 125.8, 119.0, 114.1, 112.9, 82.1; HRMS (EI-TOF): calcd. for $C_{23}H_{15}N_3O_4$ $[M]^+$ 397.1063; found 397.1073.

*4.6.6. 5-(benzo[c]isoxazol-3(1H)-ylidene)-1,3-diphenyl-2-thioxodihydropyrimidine-4,6(1H,5H)-dione (**4f**)*

From **3f** (1.0 mmol, 429.5 mg); yellow solid (301.8 mg, 73 %); mp 255-256 ºC; ^{1}H NMR and ^{13}C NMR spectral data of the product were compared to those of authentic sample [4a].

*4.6.7. 5-(benzo[c]isoxazol-3(1H)-ylidene)-1-(3-chlorophenyl)-3-phenyl-2-thioxodihydropyrimidine-4,6(1H,5H)-dione (**4g**)*

From **3g** (1.0 mmol, 463.9 mg); yellow solid (180.0 mg, 40 %); mp 250-252 ºC; ^{1}H NMR (400 MHz, DMSO-d_6) δ (ppm) 7.78 (dd, *J* = 8.8, 1.2 Hz, 1H), 7.46 – 7.32 (m, 6H), 7.29 (tt, *J* = 7.3, 1.8, 1.4 Hz, 1H), 7.25 – 7.17 (m, 4H), 6.71 (dd, *J* = 8.9, 6.2 Hz, 1H); ^{13}C NMR (101 MHz, DMSO-d_6) δ (ppm) 178.3, 166.0, 159.5, 159.4, 156.2, 143.2, 141.7, 132.5, 130.2, 129.9, 129.8, 129.5, 128.7, 128.4, 127.1, 127.0, 125.3, 119.3, 114.3, 113.1, 85.3; HRMS (EI-TOF): calcd. for $C_{23}H_{14}ClN_3O_3S_4$ $[M]^+$ 447.0444; found 447.0447.

*4.6.8. 5-(benzo[c]isoxazol-3(1H)-ylidene)-1-(4-chlorophenyl)-3-phenyl-2-thioxodihydropyrimidine-4,6(1H,5H)-dione (**4h**)*

From **3h** (1.0 mmol, 463.9 mg); yellow solid (300.1 mg, 67 %); mp 248-249 ºC; ^{1}H NMR (400 MHz, DMSO-d_6) δ (ppm) 7.78 (dt, *J* = 8.8, 1.1 Hz, 1H), 7.48 – 7.36 (m, 4H), 7.34 (d, *J* = 9.0 Hz, 1H), 7.32 – 7.24 (m, 3H), 7.24 – 7.17 (m, 3H), 6.71 (dd, *J* = 8.9, 6.2 Hz, 1H); ^{13}C NMR (101 MHz, DMSO-d_6) δ (ppm) 178.4, 166.1, 159.5, 159.4, 156.1, 141.7, 140.8, 131.6, 131.5, 130.3, 129.5, 128.5, 128.4, 127.0, 125.3, 119.4, 114.3, 113.1, 85.3; HRMS (EI-TOF): calcd. for $C_{23}H_{14}ClN_3O_3S_4$ $[M]^+$ 447.0444; found 447.0447.

*4.6.9. 5-(benzo[c]isoxazol-3(1H)-ylidene)-1-(4-fluorophenyl)-3-phenyl-2-thioxodihydropyrimidine-4,6(1H,5H)-dione (**4i**)*

From **3i** (1.0 mmol, 447.5 mg); yellow solid (280.4 mg, 65 %); mp 249-250 ºC; ^{1}H NMR (400 MHz, DMSO-d_6) δ (ppm) 7.78 (d, *J* = 8.8 Hz, 1H), 7.39 (t, *J* = 7.6 Hz, 2H), 7.37 – 7.15 (m, 9H), 6.71 (dd, *J* = 8.9, 6.3 Hz, 1H); ^{13}C NMR (101 MHz, DMSO-

d_6) δ (ppm) 178.8, 166.3, 162.2, 159.8, 159.6, 156.1, 141.8, 138.1, 138.1, 131.6, 131.5, 130.4, 129.6, 128.5, 127.0, 125.4, 119.5, 115.4, 115.1, 114.4, 113.1, 85.5; HRMS (EI-TOF): calcd. for $C_{23}H_{14}FN_3O_3S$ $[M]^+$ 431.0740; found 431.0751.

*4.6.10. 5-(benzo[c]isoxazol-3(1H)-ylidene)-1-(4-iodophenyl)-3-phenyl-2-thioxodihydropyrimidine-4,6(1H,5H)-dione (**4j**)*

From **3j** (1.0 mmol, 555.4 mg); yellow solid (323.6 mg, 60 %); mp 258-259 ºC; ^{1}H NMR (400 MHz, DMSO-d_6) δ (ppm) 7.75 (t, J = 9.4 Hz, 3H), 7.39 (t, J = 7.5 Hz, 2H), 7.32 (dd, J = 15.8, 8.1 Hz, 2H), 7.21 (d, J = 7.5 Hz, 3H), 7.05 (d, J = 8.0 Hz, 2H), 6.71 (t, J = 7.5 Hz, 1H); ^{13}C NMR (101 MHz, DMSO-d_6) δ (ppm) 178.3, 166.1, 159.5, 159.3, 156.1, 141.8, 141.7, 137.3, 132.1, 130.2, 129.5, 128.4, 127.0, 125.3, 119.3, 114.3, 113.1, 92.9, 85.3; HRMS (EI-TOF): calcd. for $C_{23}H_{14}IN_3O_3S$ $[M]^+$ 538.9801; found 538.9818.

Acknowledgements

This work is supported by FEDER funds through the POCI - COMPETE 2020 - Operational Programme Competitiveness and Internationalization in Axis I - Strengthening research, technological development and innovation (Project No. 007491) and National Funds by FCT - Foundation for Science and Technology (Project UID/Multi /00709). J. L. Serrano and J. Figueiredo acknowledge a fellowship from Santander-Totta/UBI (BID/ICI-UID FC/Santander Universidades-UBI/2017).

References

[1] Banerjee, B., Recent developments on ultrasound-assisted one-pot multicomponent synthesis of biologically relevant heterocycles. *Ultrasonics Sonochemistry,* 35 (2017), 15-35.

[2] (a) Shaker Raafat, M.; Ishak Esam, A., Barbituric Acid Utility in Multi-Component Reactions. In *Zeitschrift für Naturforschung B*, 2011; Vol. 66, p 1189; (b) Mohammadi Ziarani, G.; Aleali, F.; Lashgari, N., Recent applications of barbituric acid in multicomponent reactions. *RSC Advances,* 6 (2016), 50895-50922; (c) Lopez-Munoz, F.; Ucha-Udabe, R.; Alamo, C., The history of barbiturates a century after their clinical introduction. *Neuropsychiatric disease and treatment,* 1 (2005), 329-43; (d) Figueiredo, J.; Serrano, J. L.; Cavalheiro, E.; Keurulainen, L.; Yli-Kauhaluoma, J.; Moreira, V. M.; Ferreira, S.; Domingues, F. C.; Silvestre, S.; Almeida, P., Trisubstituted barbiturates and thiobarbiturates: Synthesis and biological evaluation as xanthine oxidase inhibitors, antioxidants, antibacterial and anti-proliferative agents. *European Journal of Medicinal Chemistry,* 143 (2018), 829-842.

[3] (a) Yoshikazu, U., 1, 2-Benzisoxazole: A Privileged Structure with a Potential for Polypharmacology. *Current Pharmaceutical Design,* 22 (2016), 3201-3211; (b) Rakesh, K. P.; Shantharam, C. S.; Sridhara, M. B.; Manukumar, H. M.; Qin, H.-L., Benzisoxazole: a privileged scaffold for medicinal chemistry. *MedChemComm,* 8 (2017), 2023-2039.

[4] (a) Serrano, J. L.; Cavalheiro, E.; Barroso, S.; Romão, M. J.; Silvestre, S.; Almeida, P., A synthetic route to novel 3-substituted-2,1-benzisoxazoles from 5-(2-nitrobenzylidene)(thio)barbiturates. *Comptes Rendus Chimie,* 20 (2017), 990-995; (b) Więcław, M.; Bobin, M.; Kwast, A.; Bujok, R.; Wróbel, Z.; Wojciechowski, K., General synthesis of 2,1-benzisoxazoles (anthranils) from nitroarenes and benzylic C–H acids in aprotic media promoted by combination of strong bases and silylating agents. *Molecular Diversity,* 19 (2015), 807-816.

[5] Friedländer, P.; Henriques, R., Zur Reduktion des Orthonitrobenzaldehyds. *Berichte der deutschen chemischen Gesellschaft,* 15 (1882), 2105-2110.

[6] (a) Budruev, A. V.; Dzhons, D. Y., Synthesis of 2,1-benzisoxazoles (microreview). *Chemistry of Heterocyclic Compounds,* 52 (2016), 441-443; (b) Kotov, A. D.; Prokaznikov, M. A.; Antonova, E. A.; Rusakov, A. I., Synthesis of Nitrogen-Containing Heterocycles from Nitroarenes (Minireview). *Chemistry of Heterocyclic Compounds,* 50 (2014), 647-657.

[7] (a) Krüger, S.; Meier, C., Synthesis of Site-Specific Damaged DNA Strands by 8-(Acetylarylamino)-2′-deoxyguanosine Adducts and Effects on Various DNA Polymerases. *European Journal of Organic Chemistry,* 2013 (2013), 1158-1169; (b) Ren, P.-D.; Pan, X.-W.; Jin, Q.-H.; Yao, Z.-P., Reduction of Nitroarenes to N-Arylhydroxylamines with KBH4/BiCl3 System. *Synthetic Communications,* 27 (1997), 3497-3503; (c) Bordwell, F. G.; Liu, W.-Z., Equilibrium Acidities and Homolytic Bond Dissociation Energies of N−H and/or O−H Bonds in N-Phenylhydroxylamine and Its Derivatives. *Journal of the American Chemical Society,* 118 (1996), 8777-8781; (d) Wurz, R. P.; Charette, A. B., An Expedient and Practical Method for the Synthesis of a Diverse Series of Cyclopropane α-Amino Acids and Amines. *The Journal of Organic Chemistry,* 69 (2004), 1262-1269; (e) Lin, Y.-I.; Lang, S. A., Selective reduction of nitro-heterocycles with sodium sulfide in aqueous p-dioxane. *Journal of Heterocyclic Chemistry,* 17 (1980), 1273-1275.

[8] Padiya, K. J.; Gavade, S.; Kardile, B.; Tiwari, M.; Bajare, S.; Mane, M.; Gaware, V.; Varghese, S.; Harel, D.; Kurhade, S., Unprecedented "In Water" Imidazole Carbonylation: Paradigm Shift for Preparation of Urea and Carbamate. *Organic Letters,* 14 (2012), 2814-2817.

[9] Whiteley, M. A., CXXIII.—Studies in the barbituric acid series. I. 1: 3-Diphenylbarbituric acid and some coloured derivatives. *Journal of the Chemical Society, Transactions,* 91 (1907), 1330-1350.

[10] Wang, F.; Zhao, P.; Xi, C., Copper-catalyzed one-pot synthesis of 2-thioxo-2, 3-dihydroquinazolin-4 (1H)-ones from ortho-bromobenzamides and isothiocyanates. *Tetrahedron letters,* 52 (2011), 231-235.

[11] Singh, K.; Sharma, S., An isocyanide based multi-component reaction under catalyst- and solvent-free conditions for the synthesis of unsymmetrical thioureas. *Tetrahedron Letters,* 58 (2017), 197-201.

[12] Koshti, V. S.; Thorat, S. H.; Gote, R. P.; Chikkali, S. H.; Gonnade, R. G., The impact of modular substitution on crystal packing: the tale of two ureas. *CrystEngComm,* 18 (2016), 7078-7094.

[13] Mohammadi, L.; Zolfigol, M. A.; Khazaei, A.; Yarie, M.; Ansari, S.; Azizian, S.; Khosravi, M., Synthesis of nanomagnetic supported thiourea–copper(I) catalyst and its application in the synthesis of triazoles and benzamides. *Applied Organometallic Chemistry,* 32 (2018), e3933.

[14] Manick, A.-D.; Berhal, F.; Prestat, G., Development of a One-Pot Four C–C Bond-Forming Sequence Based on Palladium/Ruthenium Tandem Catalysis. *Organic Letters,* 20 (2018), 194-197.

[15] Botsi, S.; Tsolomitis, A., One or two step acid mediated cyclocondensation process for the preparation of 5-carbethoxy-2-thiouracils from diethyl ethoxymethylenemalonate and thioureas. *Heterocyclic Communications,* 13 (2007), 229-234.

Graphical Abstract

The synthesis and process optimization of symmetric and asymmetric 3-substituted 2,1-benzisoxazoles from 5-(2-nitrobenzylidene)(thio)barbiturates

Leave this area blank for abstract info.

João L. Serrano, Pedro F. Soeiro, Melani A. Reis, Samuel Silvestre, Renato E. F. Boto and Paulo Almeida

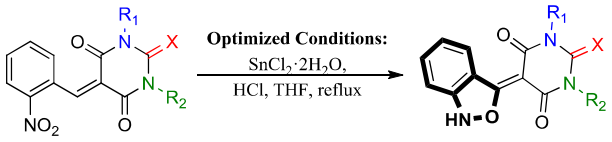

X = O or S; R_1 = H, Me, Ph; R_2 = H, Me, Ph, 3-ClC_6H_4, 4-ClC_6H_4, 4-FC_6H_4, 4-IC_6H_4.

Supplementary Material

Click here to download Supplementary Material: 2,1-Benzisoxazoles Tetrahedron Suplementary Material.docx